The Dissertation Committee for Adam Till Garland Certifies that this is the approved version of the following dissertation:

The Behavior of Proteins at Solid-Liquid Interfaces

Committee:

Eric Anslyn, Supervisor

Xiaoyang Zhu

Christopher Bielawski

Guangbin Dong

Ning Jiang

Stephen Martin

David Hoffman

The Behavior of Proteins at Solid-Liquid Interfaces

by

Adam Till Garland, B.S.

Dissertation

Presented to the Faculty of the Graduate School of

The University of Texas at Austin

in Partial Fulfillment

of the Requirements

for the Degree of

Doctor of Philosophy

The University of Texas at Austin

May 2014

Dedication

This work is dedicated to Frank and Christine Garland who made me the man I am today, and to my wonderful wife Diana Zamora Olivares who keeps me the man I am today.

Acknowledgements

I would like to thank my original principal advisor, Xiaoyang Zhu, for his critical support and guidance. Xiaoyang has been my inspiration for diversification of my skills and excellence in all elements of my multidisciplinary studies. He has encouraged me to get out of my comfort zone and push myself to accomplish the work that needs to be done. I would also like to thank Lei Shen, my partner in research without whom much of this work would not have been possible.

I would also like to thank my supervisor, Eric Anslyn, for all of his help and support over the years. Eric is widely known for his hospitality and kindness and never turns someone away when they are in need. Without his help and facilities I could never have accomplished this work.

My graduate research would not have been possible without the help and advice from the all members past and present of the Zhu group and the Anslyn group. I would like to thank former Zhu group members Josh Morris and Raluca Gearba for their advice and help. I would like to thank Anslyn group members Helen Seifert, Hannah Jo, Erik Hernandez, and Igor Kolesnichenko for their support and help.

I would specifically like to thank my wonderful wife and Anslyn group member Diana Zamora-Olivares. In addition to teaching me to use HPLC, she has always been there for both professional and emotional support. I would not gotten this far without her.

Lastly, I would like my wonderful family for supporting me and giving me the courage to continue on with my work. I never would have been prepared to the extent that I am today had my mind and soul not been crafted by my family and loved ones since the day I was born. I love you all so much.

The Behavior of Proteins at Solid-Liquid Interfaces

Adam Till Garland, Ph.D.

The University of Texas at Austin, 2014

Supervisor: Eric Anslyn

The behavior of a protein molecule at the solid-liquid interface is a worthy scientific problem for at least three reasons. The main driving force for studying this problem is a practical one, as many areas of bio-related technologies, such as medical implants, biosensing, and drug delivery, require the understanding of protein-surface interactions. In this dissertation, the nature of the precursive weakly adsorbed state of proteins during binding is reviewed. From this perspective, the adsorption and binding of proteins to a solid block copolymer thin film was achieved with regular spacing. Further efforts produced a monolayer of green fluorescent protein (GFP) covalently bound with regular spacing and orientation to a diblock copolymer thin film. This protein could be folded and refolded by changing solvent characteristics. We also explored the binding of DC-SIGN to mannose and mannotriose bearing lipid membranes. While no binding was observed, the usefulness of the lipid-based glycan microarray was proven using the well-studied CTB-GM1 binding motif.

Table of Contents

List of Tables

List of Figures

List of Schemes

Chapter 1. Mobile Precursor Mediated Protein Adsorption and Specific Binding to Surfaces[a]

1.1. INTRODUCTION

The adsorption of a protein molecule on a solid surface is a worthy scientific problem for at least three reasons.[1,,3] The main driving force for studying this problem is a practical one, as many areas of bio-related technologies, such as medical implants, biosensing, and drug delivery, require the understanding of protein-surface interactions. From the point-of-view of pure biological science, it is now well recognized that a large number of functional interactions happen at surfaces, e.g., cell membrane surfaces. The field of surface and interfacial surface science also inevitably evolves from the treatment of small gas molecules and surfactants to more complex systems. While these three fields have developed independently, they share many common physical concepts albeit often with different names. It is the purpose of this tutorial to discuss one particularly simple concept: a mobile precursor state to adsorption.

[a] Garland, A.; Shen, L.; Zhu, X., Mobile precursor mediated protein adsorption on solid surfaces. *Prog. Surf. Sci.* **2012,** *87* (1–4), 1-22. Section 1.1 was written by Xiaoyang Zhu. Section 1.2 was written by Lei Shen.

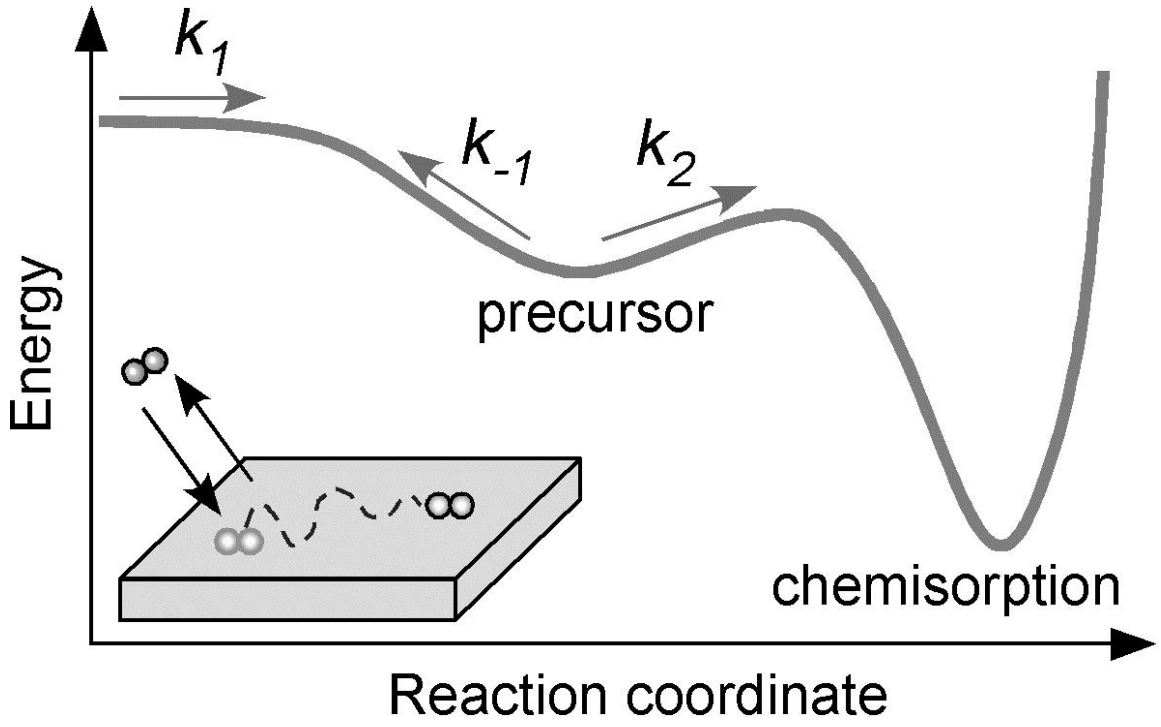

Figure 1.1. *Schematic potential energy surface for the chemisorption of small molecule on a solid surface*.

Let us start with the simplest model system: the chemisorption of a small molecule (*M*) on a clean metal single crystal surface (*S*), cartoon in **Figure 1.1**. It is well established in the field of ultrahigh vacuum (UHV) surface science that going from a gas molecule to a chemisorption species most often cannot be described by a single step. Instead, the molecule first falls into a weak interaction well to form a "mobile precursor state" on the surface as described by Kisliuk et al.[4] The molecule in the precursor state can desorb back into the gas phase or find a favorable site and irreversibly fall into the chemisorption well. The energetics of the interaction between the small molecule and the surface are represented by the fraction of molecules which successfully form the weakly adsorbed state upon collision with the surface. This fraction is termed the "sticking probability." The final product in this dynamic process is an immobilized molecule with changes in

intra-molecular structure and the formation of new chemical bond(s) to the surface. Such a precursor-mediated chemisorption reaction can be described by:

$$M(g)+S \underset{k_{-1}}{\overset{k_1}{\rightleftharpoons}} M^*(a) \underset{k_{-2}}{\overset{k_2}{\rightleftharpoons}} M(a) \qquad \text{(Eq. 1.1)}$$

where (g) & (a) represent gas and adsorbed states, respectively; M^* is the mobile precursor state. The potential energy surface in **Figure 1.1** effectively describes the kinetics of such a process. Under stead-state approximate (for M^*), the rate of chemisorption in this model is:

$$\frac{d[M_a]}{dt} = \frac{k_1[M_g][S]}{1 + k_{-1}/k_2} \qquad \text{(Eq. 1.2)}$$

A feature of the precursor-mediated adorption mechanism is the kinetic competition between the two channels for the precursor state: k_{-1}/k_2. Note that, for more complex molecules, this simple kinetic model can be extended to include multiple precursor states depending on molecular conformation and/or orientation, as well as multiple chemisorption states with varying degree of adsorption strength.

Now we consider the adsorption of a protein molecule from an aqueous solution to a solid surface. *Is the dynamic process conceptually different than what is depicted in* ***Figure 1.1****?* The answer is "no", but we can certainly expect that the adsorption of a protein molecule onto a surface is a much richer process than that of a small gas phase molecule.

The diffusion of macromolecules to a surface is the first step towards adsorption. Macromolecules diffuse at different rates towards the surface depending on their size and chemical/physical identity. Unlike that for gas adsorption depicted in **Figure 1.1**, the

local environment in the near surface region for protein adsorption is not uniform. This non-uniformity is reflected in a concentration depletion zone in the near surface region due to adsorption and, if the surface is charged, the presence of an electrical double layer. When the surface of interest is hydrophilic, there is a hydration layer on the surface[5]. This hydration layer is a fundamental factor in determining adsorption characteristics because it must be disrupted before irreversible protein adsorption can proceed. On highly hydrophilic solid surfaces such as SiO_2, the hydration layer is believed to be of nanometer thickness and the viscosity of this water film can be many orders of magnitude higher than that of bulk water.[6-8] The thickness of such a hydration layer can be greatly extended when one grafts a thin film of a hydrophilic polymer, such as poly(ethyleneglycol) (PEG), to the surface. The free energy cost of disrupting the extended hydration layer is likely one of the main reasons for the resistance of a PEG film to protein adsorption.[9]

For a surface in contact with a biological solution, besides the hydration layer, a protein molecule approaching the surface is expected to encounter various adsorbed small and macromolecules. Thus the initial dynamic steps in the adsorption of a protein molecule involve the interaction and displacement of other more weakly adsorbed molecules. When the pre-adsorbed molecules are difficult to replace, the surface becomes resistant to protein adsorption, as is the case for Tween surfactants adsorption[10] or bovine serum albumin (BSA) blocking.[11] For a real biological surface-the cell membrane, the surface is intrinsically heterogeneous. The cell membrane surface is covered with or consists of a high-density of macromolecules, particularly glycans, peptides, and proteins. Thus, for an approaching protein, the adsorption process is like parachuting into a tropical jungle.

The protein itself is also much more complex than the simple diatomic molecule illustrated in **Figure 1.1**. A protein molecule is a self-organized polymer, with primary (sequence), secondary (α-helix and β-sheet), and tertiary (folding) structures. Both secondary and tertiary structures are environment sensitive. The surface presents a chemical/physical environment very different than that of a protein molecule in the native state. As a result, a protein molecule must reorganize to various extents as it evolves from the native state to the adsorbed state. Thus, instead of one or a few precursor states for a small molecule, one should expect a spectrum of precursor states for protein adsorption.

This account will start from the conceptual framework illustrated in **Figure 1.1** to develop a fundamental understanding of protein adsorption. We begin with an introduction to macromolecular adsorption in general and move on to a summary of experimental and theoretical studies on protein adsorption in particular. We attempt to synthesize from this database the central concept of mobile precursor state in protein adsorption. Finally, we discuss the importance the precursor state plays in a quantitative description of protein adsorption kinetics and in guiding the design of rational surfaces for biosensors, biomaterials, and nanomedicine.

1.2. ADSORPTION OF MACROMOLECULES

1.2.1. Normal Polymers

The adsorption of polymers on surfaces is a well-researched subject and treated extensively in textbooks. **Figure 1.2** illustrates the dynamics of the polymer adsorption process, which is very similar to the precursor-mediated mechanism for the chemisorption of a small molecule. At the initial stage, a polymer chain in solution comes

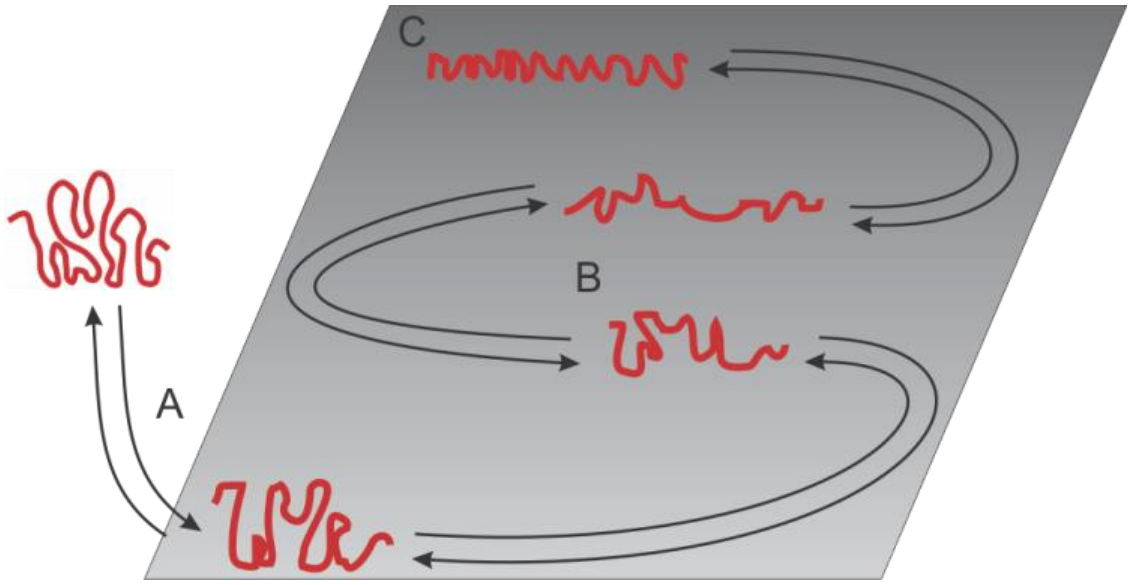

Figure 1.2. *Schematics of polymer adsorption onto a surface*: (A) initial contact; (B) diffusion in the the weakly adsorbed precursor state; and (C) the final immobilized state.

into contact with the surface and can become weakly adsorbed into a mobile precursor state. In the precursor state, the polymer diffuses along the surface while reorganizing (along with the solvent molecules). The reorganization process increases the adsorption strength and decreases the 2D surface diffusion coefficient of the polymer molecule until it finally stops. The final state is reached when the macromolecule's adsorption strength no longer continues to increase appreciably. The exact timing of the formation of the strongly adsorbed state can be difficult to define. Adsorption energies greater than 6kT are representative of irreversible adsorption.[12] There are two contributions to adsorption free energy: entropic (conformational relaxation and

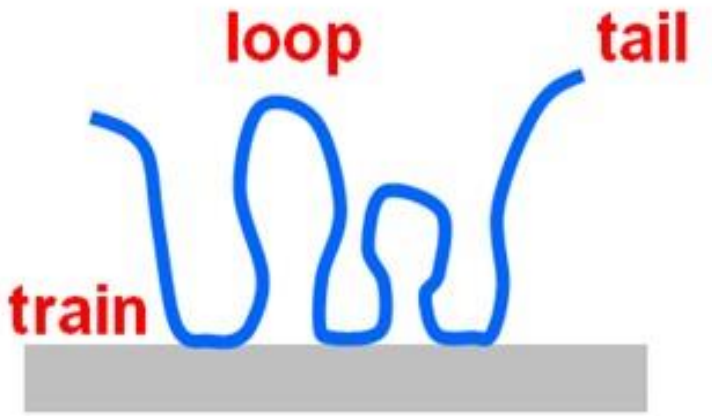

Figure 1.3. *The train-loop-tail structures of an adsorbed polymer molecule*.

hydrophobic dehydration) and enthalpic (hydrogen bonding, van der Waals interactions, and electrostatic attraction).[13] Whether or not the adsorption process leads to a tightly bound and relatively immobile state is system specific and depends on the solution/surface conditions. The structure of adsorbed polymer molecules is dynamic and coverage dependent. A weakly adsorbed polymer molecule tends to form train-loop-tail structures (**Figure 1.3**). The term "train" refers to the units along the polymer backbone in direct physical contact with the surface. As the dynamic process progresses, a polymer molecule increases its contact area and adsorption energy with the surface. This process can be succinctly called a "brush-to-pancake" transition. The reverse process also happens in the immobilized state at high coverage as inter-adsorbate interaction forces a "pancake-to-brush" transition: loops and tails in solvent swollen polymer coils are elongated normal to the surface. These elongated chains can be thought of as a polymer brush. The presence of a train segment increases the enthalpic gain upon adsorption, and

the loops and tails reduce the entropic penalties. Note that, in the presence of heterogeneity, longer polymer chains with higher binding enthalpy and lower Brownian motion kinetic energy can displace shorter ones from the surface. Chemically distinct polymer molecules with higher affinity to the surface can also displace ones with lower affinity.

Despite the much larger size of a polymer molecule, the kinetics of the polymer adsorption process depicted in **Figure 1.3** can be described by the precursor-mediated adsorption mechanism in equations (1.2) & (1.3), originally developed for the chemisorption of small molecules. Interested readers are referred to the review of Stuart & Fleer.[14]

1.2.2. Polyelectrolytes

Polyelectrolytes are one special class of polymers with charged macro-ions and small counter ions in aqueous solution. DNA and most proteins are all polyelectrolytes. In the adsorption of polyelectrolytes, Coulombic interactions between polymer segments and the surface, as well as between charges in polymer chains, play crucial roles. In general, polyelectrolyte adsorption is most strongly controlled by the surface charge density σ_s, polymer chain charge density σ_p, polyelectrolyte concentration C, salt concentration C_s, and pH value. The adsorption energy of polyelectrolytes to charged surfaces is usually higher than those of nonionic polymers.[15] Because of the strong intra- and inter-chain Coulombic interactions, it takes polyelectrolytes more time than nonionic polymers to rearrange into the final adsorbed state and reach equilibrium.

Small ions in solution screen the Coulombic interaction. Thus, the salt concentration C_s can strongly influence the polyelectrolyte adsorption process. At a neutral surface without charge, the adsorbed amount of polyelectrolyte increases with an increase in C_s. At a charged surface, the effect of C_s on polyelectrolyte adsorption

depends on the structure of the polyelectrolyte layer on the surface. When the polyelectrolyte forms a 2D adsorbed layer with low surface coverage, the increase of C_s results in an increase in adsorbed amount. If the polyelectrolyte forms a 3D adsorbed multilayer with high surface coverage, the amount of adsorption decreases with an increase in C_s.[16]

The amount of adsorbed polyelectrolyte increases with an increase of the polymer chain charge density σ_p. When the charge on the polymer chain is equal to that on the surface, the adsorbed amount reaches the maximum and then decreases with further increase in σ_p. The maximum is called charge compensation point.[17] This phenomenon is general and occurs for many polyelectrolytes.

1.3 PROTEIN ADSORPTION

1.3.1. A comparison between proteins and polymers

The mechanism of protein adsorption is not far removed from that of polymer adsorption. The thermodynamic driving forces are the same and the kinetic equations 1 and 2 are still applicable. There are quantitative differences. The configurational entropy of a protein in solution is low while in the native state, compared with high configurational entropy of a homopolymer chain in a good solvent. Both systems undergo a loss of configurational entropy going from the solvated state to the adsorbed state, but $|\Delta S|$ for protein adsorption is much smaller than that for homopolymer adsorption. From an enthalpic point of view, disruption of intra-chain interactions is necessary before adsorption can proceed, and thus strong intrachain interactions present a thermodynamic barrier to adsorption. Van Eijk and Stuart concluded that most polymers unfold much easier than proteins.[18] Polymers in good solvent have little in the way of intrachain binding strength and van der Waals forces holding the random coil together are easily

overcome. Polyelectrolytes are capable of stronger intrachain electrostatic interactions, but these interactions are largely random and weak. Conversely, proteins have quite strong intramolecular interactions due to concerted hydrophobic, electrostatic, and hydrogen bonding interactions. For this reason, it is more difficult for a protein molecule to unfold and irreversibly adsorb onto the surface.

The quantitative difference between the energetics in unfolding/re-arrangement of protein and polymer molecules gives rise to a fundamental difference in adsorption kinetics. In both cases, approach toward the surface occurs through diffusion limited mass transfer. Upon interaction with the surface, both begin to unfold and re-arrange to increase contact with the surface. The unfolding/re-arrangement process may occur in a mobile state as the macromolecule samples the surface before reaching a strongly adsorbed state. The high-energy barrier to unfolding for a protein molecule prevents it from doing this as rapidly as a polymer. Therefore, proteins take much longer than polymers to complete the irreversible adsorption process. In addition, the unfolding of a protein likely occurs in steps. The unstable regions will unfold first followed by more stable regions. A polymer molecule has no regular order to its folded forms, so its unfolding pathway can be considered continuous. The dynamic processes discussed above for both polymers and proteins should depend sensitively on chemical and morphological details of the surface.

The presence of weakly adsorbed protein molecules as precursors to strongly adsorbed states suggests a dynamically changing reversibility in the adsorption process. At early stages of the adsorption process when the relatively weak adsorption free energy is of the order kT or lower, the adsorption process is reversible, i.e., desorption from the precursor state is possible. This is similar to the first step in equation (1.1). As the dynamic process of adsorption proceeds, the adsorption energy increases and desorption

becomes increasingly unlikely. The reversibility in the adsorption process is essential to the replacement of adsorbed protein molecules by ones with higher adsorption energy, as detailed later.

In addition, many proteins exhibit the potential for binding to substrates in biological environments (either in vitro or in vivo) through specific binding sites. This pathway may proceed directly from the well natured solution state or it may pass through the weakly adsorbed precursor state. The characteristics of the surface will determine whether the specific or non-specific adsorption pathway will dominate. While a weakly adsorbed protein may still retain sufficient tertiary structure to allow for the specific binding event to occur, at some point in the progression towards the strong non-specifically adsorbed state the protein will have lost too much of its binding site configuration to bind specifically. A surface conducive to the formation of this state will not permit significant specific binding. In addition, presenting the possibility of specific binding sites does not prevent the strong non-specifically adsorbed state from being reached. A specifically bound protein in such an environment is not necessarily hindered from denaturation and non-specific adsorption. Maintenance of proteins in the well natured state when specifically bound to a surface requires proper understanding of the non-specific pathways which would prohibit or impede the formation of the well natured specifically bound state.

1.3.2. Adsorption Isotherms

An adsorption isotherm relates the surface coverage of adsorbed molecules to the concentration (or pressure). In the simplest form, the precursor state is neglected and Equation (1.1) reduces to:

$$M(l)+S \underset{k_{-1}}{\overset{k_1}{\rightleftharpoons}} M(a) \qquad \text{(Eq. 1.3)}$$

where the solution (l) phase molecule is in direct equilibrium with the adsorbed state (a). If one defines a relative coverage of adsorbed molecules as θ, the available surface sites for molecular adsorption is $[S] = 1-\theta$. Under equilibrium conditions, the coverage of adsorbed molecules is:

$$\theta = \frac{K[M]}{1 + K[M]} \qquad \text{(Eq. 1.4)}$$

where $K = k_1/k_{-1}$ is the equilibrium constant (in appropriate unit) and $[M]$ is molecular concentration in the solution phase. While equation (1.4) has been commonly used to fit experimental adsorption isotherms, one must remember that it is a very crude approximation which neglects the essential physics of adsorption dynamics. A number of improved albeit empirical isotherms such as random sequential adsorption (RSA) and scaled particle theory (SPT) are used to better describe experimental data.[19] Regardless of its inability to quantitatively predict protein adsorption, Langmuir type isotherms have proven useful in very simple adsorption systems when the protein molecules do not reach the irreversibly adsorbed state in significant amounts and can be approximated as hard spheres and modeled by RSA according to the principle of Brownian motion.[20] However, the use of Langmuir based isotherms to describe adsorption for an irreversible system is inherently erroneous.[21]

The full protein binding equation permitting for specific as well as non-specific binding will cause the following modifications to equation (1.3) to yield equation (1.5):

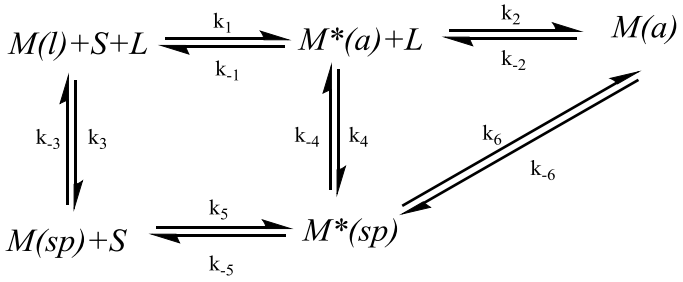

(Eq. 1.5)

where *L* represents a specifically binding ligand on the surface and (*sp*) represents a specifically bound state. While this equation is extremely complicated, most systems will show a number of these steps to be essentially irreversible as well as that some of these pathways are very rarely taken. Furthermore, the previously discussed empirical binding isotherms often describe a system in sufficient detail such that consideration of all reactions in this equation is not necessary. However, this equation reveals multiple conditions which can be modified in the interest of controlling the amount of protein which forms the strong non-specifically adsorbed state. Since most routes go through a weakly adsorbed precursor state, study of the nature of this state will reveal essential information about controlling it and subsequently the behavior of proteins at the liquid/solid interface.

1.3.3. Experimental determination of adsorbed proteins

A number of experimental techniques have been applied to the quantification of protein adsorption on surfaces. Radio-isotopic Labeling involves the covalent binding of a radioactive isotope, typically an isotope of iodine, into the protein in question. The protein's presence may then be detected by measuring the emitted radiation.[22]

Ellipsometry measures changes in the polarization of light reflected off a sample and relates the changes to the thickness of the adsorbed protein layer, provided the refractive index of the bulk solution and that of the substrate surface are known.[23] Directly measuring small increases in mass during adsorption is possible with a quartz crystal microbalance (QCM).[24] An improvement is QCM with dissipation monitoring (QCM-D) which measures mass and "softness" of the adsorbed material.[25] Note that QCM measures the total mass of all adsorbed molecules at the solid/liquid interface and care must be taken to isolate the mass of adsorbed proteins. One can determine surface protein coverage from changes in refractive index using optical biosensors.[19] Surface plasmon resonance (SPR) is a label-free technique which quantifies the amount of mass adsorbed to a surface based on refractive index changes.[26] It has proven very useful for the determination of biomolecular binding kinetics as well[27]. Another technique based on refractive index is optical waveguide light-mode spectroscopy (OWLS).[28] Other surface analytical techniques, such as X-ray photoelectron spectroscopy (XPS) and second ion mass spectroscopy (SIMS), has also been used to probe adsorbed protein molecules, but the analysis is done in the dried state in an ultrahigh vacuum environment.[29] Unfolding of a protein molecule in the adsorbed state changes secondary and tertiary structures and these changes can lead to shift in vibrational frequencies of the amide bonds as determined by Fourier transform infrared (FTIR) spectroscopy.[30] The absorbance of the amide peaks can also be used to determine the relative coverage of adsorbed protein molecules. Direct imaging of adsorbed protein molecules at the aquesous/solid interface is possible with the Atomic force microscopy (AFM).[31] The AFM can also be operated in the force mode to probe protein-receptor interactions.[32,33]

1.3.4. Surface properties

Whether a protein molecule strongly adsorbs on a solid surface is determined primarily by the surface properties, e.g., hydrophobic, hydrophilic, or charged. These properties may work in a concerted fashion in protein adsorption. We discuss each property below.

1.3.4.1. Hydrophobic Surfaces

A hydrophobic surface repels water, as indicated by a relatively high water contact angle (around 90^{o}). The inner hydrophobic core of a protein can interact very favorably with a hydrophobic surface, but the outer face of the protein is more hydrophilic and prefers to remain hydrated. Interaction with a hydrophobic surface may start with small hydrophobic domains on the protein, but significant rearrangement of the protein structure is necessary to permit the exposure of inner hydrophobic domains for stronger interaction with the surface. This results in a substantial loss of the protein's native tertiary structure. The presence of the adsorbed protein with its hydrophilic groups pointing away from the surface may lower the surface energy, an effect similar to that of a surfactant. At an early stage of the adsorption process, the moderately denatured form may have adsorption energy $\leq$ 6 kT and desorption can occur.[12,34] Once the inner core has been exposed, the protein proceeds rapidly towards the strongly adsorbed state (adsorption strengths greater than 6kT). Hydrophobic surfaces give rise to relatively high adsorption energies in the range of 30-200 kT for the final adsorbed state.[35]

In general, proteins adsorbed on hydrophobic surfaces are tightly bound and in many cases cannot be easily separated from the surface without the aid of chemical reagents such as surfactants.[36-38] Chen et al. used AFM to directly measure the adsorption strength of proteins on polymer surfaces.[31] They placed a polystyrene-coated AFM tip in

a BSA solution, allowing protein to adsorb on to the tip. Afterwards, the protein-coated tip was brought into contact with a polymer surface and pulled away. The force required to remove the tip from the surface was then correlated to the strength of the interaction between BSA and the surface. The authors found that the interaction with the BSA coated tip was strongest on bare polystyrene and weakest on areas of the surface that had already been exposed to protein.

1.3.4.2. Hydrophilic Surfaces

A hydrophilic surface interacts favorably with water and is usually covered with a hydration layer when in contact with an aqueous solution. This creates a barrier through which adsorbing protein molecules must break through before interacting with the underlying surface.[36] The additional energy requirement to push the ordered water layer out of the way limits the overall thermodynamic energy gain of adsorption. Thus, protein molecules adsorb more weakly on hydrophilic surfaces than they do on hydrophobic surfaces. Unlike the situation on hydrophobic surfaces where extensive structural reorganization is expected for adsorbed protein molecules, the inner hydrophobic domains of protein have little to gain energetically through interaction with a hydrophilic surface. The maintenance of the tertiary structure leads to weak and reversible protein adsorption on hydrophilic surfaces.

A PEG coating presents a hydrophilic surface which is particularly repulsive to protein adsorption. Sigal et al. noted that while there are surfaces more hydrophilic than PEG, PEG seems to resist protein adsorption better than any other hydrophilic surfaces.[36]A PEG coated surface presents a three-dimensional hydration layer, thus making dehydration more costly in free energy than a typical two-dimensional hydrophilic surface. Herrwerth et al. found that self-assembled monolayers (SAMs) with

oligoethylene glycol (OEG) termination are repulsive to protein adsorption when there are more than two ethylene glycol repeat units.[39] If the packing density of the SAM becomes too high, as is the case on Ag(111), the OEG terminal groups adopt the less hydrated all-trans configuration and protein adsorption can occur.[40] Latour analyzed in detail the thermodynamic and entropic penalties associated with protein adsorption to a long chain OEG SAM and concluded that the primary reason for protein resistance is entropic.[41]

1.3.4.3. Charged Surfaces

A charged surface may promote strong protein adsorption.[42-44] Many of the outer hydrophilic domains of a protein are either positively or negatively charged. Hydrophilic surfaces with a significant portion of charged groups are capable of strong electrostatic interaction with those on the protein groups. At the initial stage, both favorable and unfavorable electrostatic interactions between charged domains on a protein molecule and those on the solid surface serve to reorient and guide the approach of a protein molecule.[45] Brusatori et al. found that the transport limited adsorption rate of negatively charged albumin onto a quartz surface increases when a voltage is applied to the surface, but remains almost unchanged for the positively charged cytochrome C.[28] However, the rate of adsorption after the surface has been significantly populated is greatly increased with bias voltage for both proteins. The authors suggest that the role of the voltage in the surface limited regime is mainly to reorient adsorbed proteins to allow for more efficient packing, although multilayer formation should not be ruled out. Ngankam et al. demonstrated the ability of a charged surface to direct the orientation of adsorbed protein.[46] They used AFM to show that fibronectin adsorbs perpendicularly to a polyallylamine hydrochloride surface (positively charged) and parallel to a polystyrene

sulfonic acid surface (negatively charged). Fibronectin is an elongated protein with negatively charged ends. Antibody binding to the terminal groups was also observed to be greater in the case of the perpendicularly oriented proteins versus those parallel to the surface.

Electrostatic interaction also contributes to the adsorption energy in the strongly adsorbed state. Jeyachandran et al. showed that BSA adsorbs on a GeOH surface with higher adsorption energy and higher surface coverage than those on a polystyrene surface.[38] The outer surface of a protein molecule is heterogeneously charged at neutral pH, depending on the peptide sequences in a given region. For a surface with homogeneous charge, certain regions of the protein will react favorably with the surface while others will not. Nakanishi et al. examined the adsorption of peptide segments of β-lactoglobulin onto stainless steel in acidic media (a positively charged surface). They found that peptides containing amino acids with carboxylic acid side groups adsorbed most strongly onto this positively charged surface.[47]

Though charged surfaces tend to exhibit strong protein adsorption characteristics, the cellular membrane, which has a charged outer surface, does not exhibit significant non-specific protein adsorption. The zwitter-ionic head groups of the cellular membrane lipids, while charged, are largely repulsive to non-specific adsorption. Feng et al. showed that a silicon surface grafted with poly(2-methacryloyloxyethyl phosphorylcholine), which presents zwitter-ionic groups, showed much reduced protein adsorption as compared with the unmodified surface or with a polymer brush lacking phosphorylcholine groups.[37]

1.3.4.4. Chemical or Physical Heterogeneity

While homogeneous surfaces are simple to create in the laboratory, proteins rarely encounter a true homogeneous surface in nature. When the surface heterogeneity is on a dimension scale much longer than the dynamic path sampled by a protein in the precursor state leading to strong binding, one can simply treat the problem as adsorption onto multiple surfaces or domains. If the heterogeneity of the surface is on a nano-meso scale compatible with the sampling distances of precursor states, or on nano-scale matching the inter-domain distances on a protein molecule, the surface heterogeneity will affect both kinetics and thermodynamics of protein adsorption.

A protein interacts with a chemically heterogeneous surface very differently than with a homogeneous surface. When presented with a surface of chemical heterogeneity of a size scale similar to the protein's own structural features, the reorganization of the protein becomes complicated. The ideal situation for strong interaction would require pattern matching, but this is usually an unlikely event. Thus, one may expect weaker protein adsorption on a chemically heterogeneous surface than that to homogeneous surfaces of the separate constituents.

Ostuni et al. examined the effect of surface heterogeneity using a SAM of mixed functionalities.[48] A SAM of carboxylic acid terminated carbon chains was first converted to pairs of anhydride groups that were subsequently opened with various functionalized amines. This created a chemically heterogeneous surface with randomly interspersed carboxylate groups and arbitrary functionalities. The authors found that when positively charged groups were used as the introduced functionalities, overall protein adsorption was significantly reduced as compared to either carboxylate or positively terminated SAMs alone. In general, mixed SAMs containing positively charged groups which were incapable of hydrogen bonding, such as quaternary amines, showed the greatest levels of

resistance to non-specific adsorption. Baxamusa et al. examined the adsorption of BSA onto random copolymer films formed by chemical vapor deposition of varying compositions of hydrophilic (HEMA) and hydrophobic (PFA) monomers.[49] Copolymers of this type have heterogeneities on the molecular scale, smaller than the dimensions of the protein itself. They found that BSA adsorbed the least amount on an intermediate surface concentration of hydrophilic and hydrophobic functionalities and attributed this to the protein behaving as a "surface probe" which samples the surface as it is re-organizes itself in searching for the strong adsorption sites. When the hydrophobic and hydrophilic domains phase separate into larger domains, the size scale begins to approach that of the protein itself. Hobara et al. examined the adsorption of horse heart cytochrome C onto phase separated heterogeneous SAMs (mercaptopropionic acid and hexadecanethiol).[50] They found that proteins could only adsorb to the surface once the charged hydrophilic domains reached a certain percentage of the surface area. The amount of adsorbed protein increased exponentially with increasing surface concentration of mercaptopropionic acid, indicating a dependence on the size of the domains.

Shen et al. studied the kinetics of protein adsorption using nm – μm scale patterns involving hydrophobic polymer domains (polystyrene) in a hydrophilic polymer (poly-2-hydroxyethyl methacrylate) matrix. They discovered a critical requirement on the sizes of thehydrophobic/adhesive pads for appreciable protein adsorption. The area of each adhesive pad must be a few hundred times larger than the footprint of a protein molecule before irreversible adsorption occurs. They attributed this finding to the minimal surface area sampled by a protein molecule in the mobile precursor state. When the area of a hydrophobic adhesive domain is smaller than the critical size, the protein molecule in the precursor state on the hydrophobic pad has not gone through sufficient reorganization before encountering the hydrophilic matrix and desorbs, **Figure 1.4.**[51]

Surfaces may also contain physical heterogeneities on the length scale of the dimensions of a protein molecule. Proteins adsorbing to a roughened, curved, or patterned surface behave very differently compared to on a smooth surface. Surface curvature plays an important role in the protein adsorption mechanism. Convex surfaces with a tight radius of curvature require more distortion of the protein in order to maximize its interaction with the surface. This additional energy barrier slows the adsorption process and weakens the overall interaction between the protein and the surface. Research by Lundqvist et al. details the adsorption characteristics of human carbonic anhydrase variants onto silica nanoparticles . These researchers found that the size of the silica nanoparticles played a strong role in the development of the molten globule state. Larger particles were shown to induce stronger changes to the secondary

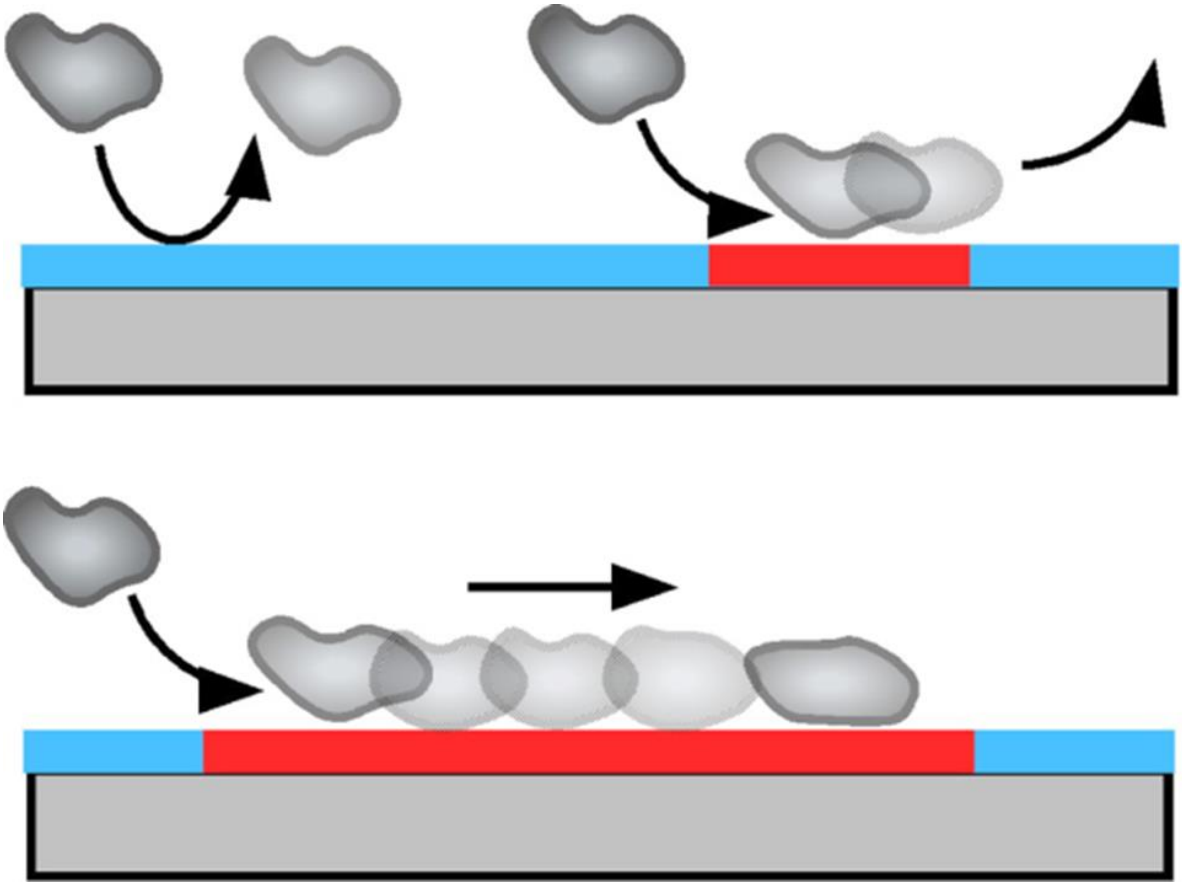

Figure 1.4. *Schematic illustration of protein adsorption on hydrophobic domains (red) in a hydrophilic matrix (blue)*. Figure reproduced with permission.[51]

and tertiary structure of the protein molecule. They suggest that the tight radius of curvature on the smaller particles prevent higher levels of contact between the protein and the surface, thus limiting the amount of deformation in the protein's native structure and weakens the overall interaction. The size of the protein molecule also plays a strong role in adsorption to curved surfaces. Roach et al. compared the adsorption of BSA and fibrinogen onto SiO_2 nanoparticles of various radii.[52] **Figure 1.5** shows the results obtained for these two proteins. These authors found that BSA exhibited behavior similar

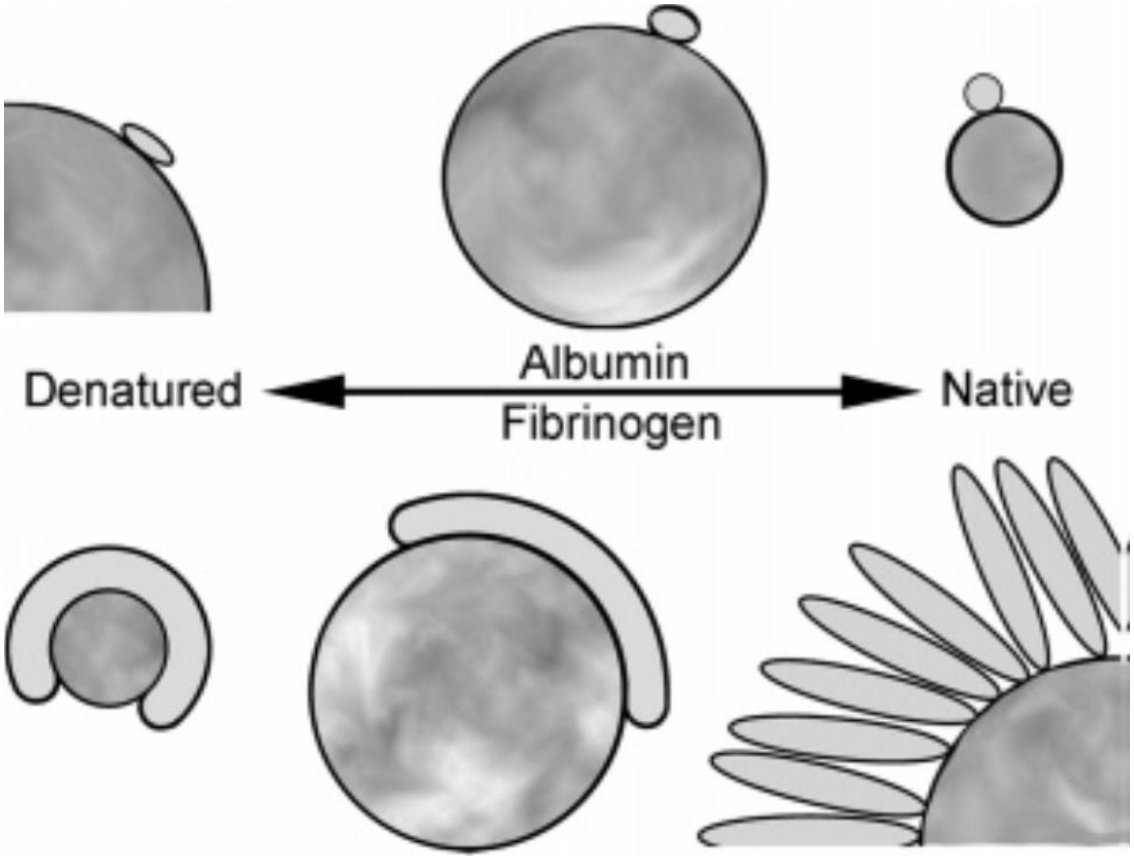

Figure 1.5. *Schematics showing the relationship between surface curvature and protein deformation following adsorption*. Figure reproduced with permission.[52]

to that observed by Lundqvist et al. concerning human carbonic anhydrase. These are both relatively small proteins and have significant structural stability. Conversely, fibrinogen is very large and soft. The amount of fibrinogen adsorbed to particles of small radii was found to be similar to that of a monolayer of fibrinogen lying parallel on flat surfaces. This is due to the ability of fibrinogen to significantly distort its tertiary structure during adsorption. However, the amount adsorbed to the larger particles was found to be more than a monolayer coverage of flat-lying molecules, suggesting a significant amount of protein in the perpendicular orientation. Tan et al. generated two-

dimensional ordered patterns using self-assembled monolayers and AFM based lithography (nano-shaving). Using patterns of antigen with different lateral dimensions, these authors found that antibody binding was most efficient when the surface dimensions match those of the Fab sites on the antibody.[53]

Kumar et al. studied the adsorption of various proteins onto nano-structured surfaces formed from diblock copolymer, polystyrene-polymethylmethacrylate (PS-PMMA). PS-PMMA thin films can be tailored to form nanoscopic lamellar structures parallel to the solid surface. The lamellar phase consists of convex PMMA hills and concave PS valleys. Although both phases are hydrophobic, Kumar et al. found that the amount of protein adsorption on the diblock copolymer surface was 3-4 times higher than that on either homopolymer (much higher than the increase in surface area caused by induced curvature). The adsorbed proteins were found almost completely in the lower valleys formed by the PS phase of the diblock. These authors also studied blends of the two homopolymers that gave PMMA islands and toroids surrounded by a PS matrix. Protein adsorbed to this surface was found to be concentrated at the boundary between the PS and PMMA regimes. In both cases, proteins preferred to adsorb to areas of significant concavity. Matsusaki et al. performed similar measurements on lamellar PS-PMMA films.[54] They found that fibronectin and γ-globulin adsorbed almost exclusively into the PS valleys. Fibrinogen was somewhat less discriminate, adsorbing in some cases across the PMMA hills. Collagen was found to be entirely indiscriminate. The trend shown here is that elongated proteins tend to show little preference for surface features on this scale, whereas smaller, more spherical proteins can easily reach the PS valleys. On concave surfaces with curvature comparable to the shape of a protein molecule, the protein does not need to spread as much as on a flat surface in order to achieve significant contact with the surface to irreversibly adsorb. This provides thermodynamic and kinetic

driving forces in favor of adsorption. Similar arguments may account for enhanced adsorption on roughened surfaces.[55]

1.3.5. Protein properties

1.3.5.1. Protein Structure

Proteins are heterogeneous in structure. The inside of the protein consists of a relatively high concentration of hydrophobic groups and the surface is high in concentration of charged and neutral hydrophilic groups. This difference in organization is what gives the protein its structural stability. The more hydrophobic the core and the more hydrophilic its surface, the more stable the native state of the protein is. Proteins with a relatively high level of structural stability are designated as being "hard" proteins, such as lysozyme and ribonuclease. Conversely, those with a low level of stability are designated "soft", such as fibrinogen and fibronectin. The ability of a protein to unfold and reorganize in order to maximize energetically favorable interactions with a solid surface decreases with increasing internal stability. As a result, hard proteins tend to adsorb more slowly and less strongly than soft proteins. This also means that hard proteins tend to maintain more of their tertiary structures after adsorption than soft proteins do.

Billsten et al. studied the effects of mutation on the adsorption of human carbonic anhydrase onto silica nanoparticles (diameter = 9 nm).[56] The mutation in the protein reduces its internal stability, causing the mutated protein to unfold and adsorb much more readily than the wild type. This finding was corroborated by Karlsson et al., who showed that the location of the mutation played a strong role in the overall change in internal stability.[57] They found that mutations in the interior of human carbonic anhydrase (position 56) could cause significant destabilization of the internal structure without

significantly altering the protein's activity. The more destabilized protein molecule enters the molten globule state much more rapidly upon exposure to silica nanoparticles than the more stable native protein does.

1.3.5.2. Protein Size

Soft proteins tend to be large while hard proteins are usually smaller. A soft protein possesses a larger contact area with the surface than hard proteins do, resulting in higher adsorption strength for the former. This enables large and soft proteins to adhere to many surfaces, such as uncharged hydrophilic surfaces that are repulsive to smaller proteins. While binding to an uncharged hydrophilic surface is weak compared to a hydrophobic surface, the number of contacts made by larger proteins is enough to result in irreversible adsorption to the surface.[12] Sigal et al. studied the relationship between surface hydrophilicity and protein adsorption as well as the ability of adsorbed proteins to be removed from a surface by detergent molecules[36]. While large and soft proteins like fibrinogen were found to adsorb on hydrophilic surfaces, hard proteins (such as lysozyme and pyruvate kinase) do not. Noh et al. showed more overall adsorbed mass from larger proteins than those from smaller ones.[34]

1.3.6. Other Factors

Many factors contribute to the internal stability of a protein. While many proteins are constructed to withstand extreme environmental conditions, deviation from these conditions causes destabilization of the protein's structure. This speeds up the unfolding process and makes it easier for the protein to proceed from the weak precursor state to the strongly adsorbed state.

1.3.6.1. Temperature

The stability of a protein depends strongly on temperature. Upon heating, entropic contributions become significant. At sufficiently high temperature, the entropic instabilities will outweigh the enthalpic free energy gained from folding and the protein will become denatured. Arnebrant et al. showed that the amount of α-lactalbumin and β-lactalbumin that could adsorb to a hydrophilic chromium surface increased with increasing temperature. It was also found that temperature based denaturation of β-lactalbumin was reversible owing to its structural integrity versus the irreversible denaturation of α-lactalbumin.[58]

1.3.6.2. pH

Protein folding prevents the access of non-structural water to the interior, but most proteins possess some water molecules as part of their internal structure. Though bulk water does not diffuse into the interior, the miniscule size of protons make them capable of diffusing deep into the interior of a protein, leading to structural change or denaturation. Therefore, changes in pH can affect not only the kinetics and thermodynamics of protein adsorption, but also the structure of a protein molecule in the adsorbed state.[59] At very extreme pH values, hydrolysis of the amide bonds can even occur, as in the form of acid based digestion in the stomach and intestines.

With respect to adsorption to charged surfaces, pH can have a much more pronounced effect. Aside from the aforementioned effects of pH on protein stability, the pH of the solution also affects the charge on both the protein and the surface. Protonation or deprotonation of functional groups on the protein and/or on the surface can determine whether or not the electrostatic interaction between the two will be favorable or unfavorable. However, quantifying this effect can be dauntingly convoluted. The

contributions of pH to the thermodynamic stabilization of the protein as well as the electrostatic interactions with the surface can simultaneously promote and hinder protein adsorption, making analysis of the role of pH on one system difficult to apply to a general adsorption model.

1.3.6.3. Ionic Strength

Ions other than protons in a solution are capable of dramatically changing the adsorption behavior of proteins. Dissolved ions screen charges on a protein's outer surface and decrease electrostatic interaction between charge groups on protein molecules and those on a solid surface. This raises the activation energy required for denaturation, slows the rate of adsorption, and increases the rate of desorption from a surface. The response of adsorption characteristics to ionic strength depends on many factors including the concentration of charged groups on the protein's surface and the ability of the protein to adsorb through the formation of aggregates. Buijs et al. showed that human growth hormone, which has a net negative charge at neutral pH, exhibits increased adsorption on SiO_2 (also negatively charged) under increased ionic strength (from 10mM to 150mM).[60] This is due to screening by dissolved ions of the unfavorable charge interaction. In contrast, the adsorption of lysozyme, which is net positively charged, decreased strongly with increasing ionic strength due to the screening of a favorable interaction.

1.3.6.4. Bulk and surface Concentration

Besides the mundane effect of increasing the reaction rate, as per equation (1.2), increasing the bulk concentration of protein can affect the protein adsorption mechanism in more fundamental ways.[34] Surfaces that are normally resistive to protein adsorption

can become protein adhesive if the bulk concentration is high enough. Holmberg et al. showed that protein resistant SAMs with terminal short OEG groups could experience protein adsorption when the solution protein concentration was high enough.[61] This may be understood from the precursor mediated adsorption model. The concentration of protein molecules in the weakly adsorbed precursor state increases with solution concentration. When the precursor concentration is high enough, the probability of weakly adsorbed protein molecules undergoing sufficient rearrangement to become strongly adsorbed also increases. The surface concentration also plays an important role in protein adsorption.[62] A surface with strongly adsorbed protein molecules is usually resistant to the adsorption of more proteins. This is the basis for the commonly used technique of BSA blocking to render available surface sites resistant to further protein adsorption in protein microarrays[63] or enzyme linked immunosorption assay (ELISA).[11]

1.3.6.5. History dependence

One of the most intriguing features of protein adsorption is the way that proteins change their adsorption strength based on the time that they have been present on a surface. It is well documented that the quantity of protein molecules adsorbed on a surface depends strongly on the timing of the introduction of the protein species. This history dependence would not have been observed if proteins were static on the surface. The history dependence of proteins can be explained through protein mobility on the surface as well as the spreading of proteins once adsorbed to the surface.[21]

1.4. DYNAMICS OF THE PRECURSOR STATE

1.4.1. Surface spreading

During non-specific adsorption, the primary way that a protein maximizes its interaction with a solid surface is by increasing its level of contact, or "footprint." As the footprint grows larger, the fraction of the solid surface's area in direct contact with the interfacial water becomes reduced. In cases where the interaction between the solid surface and water is of particularly high energy, the spreading of the protein's footprint can significantly reduce the surface energy of the system. It is this reduction in surface tension which drives the spreading process. Differentiating between the reduction in surface tension due to adsorption versus a protein's tendency to increase interaction energy with the surface can be difficult.

The spreading of proteins on the surface also makes their adsorption energies difficult to determine. Desorption rates of gases are commonly related to their adsorption strength. However, in the case of proteins, desorption frees up surface area for remaining proteins to spread. The effect of desorption on the adsorption strength of remaining proteins makes the use of this technique for the determination of protein adsorption strength very difficult.

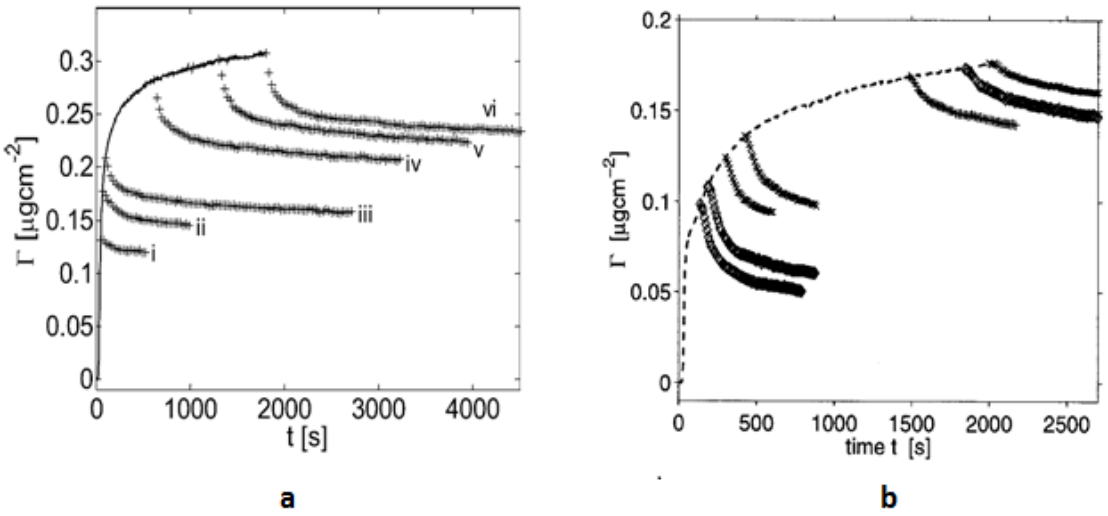

Figure 1.6. *Adsorption and desorption plots for a) cytochrome c and b) fibronectin*. Figures reproduced with permission.[66,67]

Most proteins have oblong shapes and possess the ability to adsorb in various conformations, which makes examination of the spreading footprint difficult. The so called "growing disk model", put forward by Pefferkorn et al.[64], simplifies this issue by modeling the spreading footprint as a disk whose radius steadily increases with time. The footprint eventually reaches a maximum size at which the interaction between the protein and the surface is strongest and further spreading is not energetically favorable. This simplification is quite useful for modeling the initial adsorption rate and the saturation amount, but does not take into account the irreversible adsorption of proteins. The model assumes spreading proteins will readily displace other ones, which is not the case in systems permitting irreversible adsorption. This prevents the model from displaying history dependence[12]

Once the weakly adsorbed state forms, the protein begins spreading its footprint. Agnihotri et al. demonstrated the changing height profile of proteins adsorbed to a surface.[65] Using AFM, these authors found that the height of fibrinogen adsorbed on

HOPG decreased over a period of about 2 hours before stopping. This decrease in height suggested a spreading of the outer domains of the protein over the same time span.

The structural stability of a protein is a critical factor in determining the rate at which it spreads on the surface. Small and hard proteins must overcome significant energy barriers in order to lose tertiary structure so that spreading can occur. These barriers are not as high for larger, softer proteins. Therefore, hard proteins have a tendency to spread much slower than soft proteins. This is demonstrated in research performed by Tie et al.[66] and by Calonder et al.[67] **Figure 1.6** shows desorption curves of cytochrome c and fibronectin respectively. Solutions of the proteins at 100μg/mL were passed over a $Si(Ti)O_2$ and desorption was initiated by switching to buffer solution at various times along the adsorption curve. The desorption rate for cytochrome c, a small and hard protein, decreased with increasing time. However, the desorption rate for fibronectin, a large and soft protein, increased with time. Fibronectin is capable of spreading and forming the strongly adsorbed state quickly upon adsorption to this surface. At short times, the surface coverage is low and most of the fibronectin is strongly adsorbed as evidenced by the slow desorption rate. As time increases, surface crowding causes a large fraction of the adsorbed fibronectin to be in the weakly adsorbed state, resulting in an increased desorption rate. Cytochrome c, however, cannot spread as rapidly as fibronectin. Therefore, at short times the amount of cytochrome c in the strongly adsorbed state is relatively low, resulting in a high desorption rate. As the barriers to spreading are gradually overcome with time, cytochrome c can adopt the strongly adsorbed state. The decreasing adsorption rate shows that at high surface concentrations the strongly adsorbed proteins prevent other proteins from forming the weakly adsorbed state on the surface. It is possible that a spreading cytochrome c

molecule displaces neighboring proteins, an effect which is not observed to a significant extent for fibronectin in this case.

The hydrophilicity of the surface can determine the maximum extent of spreading for a given protein. A protein adsorbing to a hydrophobic surfaces causes a large change in the surface tension. This change gives thermodynamic impetus for further spreading to occur. Conversely, on a hydrophilic surface, the change in surface tension is not so great and the protein will spread to a lesser extent. Santore and Wertz used successive adsorption of fibrinogen to determine the long term spreading kinetics and final footprint size of fibrinogen on hydrophobic and hydrophilic surfaces[68]. The final footprint size on hydrophobic C16 SAMs was found to be ~500 nm^2, whereas on the hydrophilic OH SAMs the final footprint was only ~160 nm^2.

The bulk and surface concentrations have a strong effect on the ability of a protein to spread on the surface. If the rate of protein adsorption is significantly higher than the rate of spreading, then proteins can cover the surface before they have spread significantly. If the rate of adsorption is lower than the rate of spreading, the protein molecule which arrives first will have time to spread and block the adsorption of additional proteins. This is shown in the effect of changing bulk concentration on the final surface loading of protein. Experiments performed by van der Veen et al. showed that proteins adsorbed from low bulk concentration solutions were not capable of reaching the level of surface loading mass achieved at higher bulk concentration solutions.[69]

1.4.2. Surface Mobility

The ability of a protein to move while it is adsorbed to a surface provides a critical pathway for the protein to maximize its interaction with the surface. A mobile

protein can sample the surface landscape for stronger interaction sites. All proteins exhibit some form of surface diffusion, whether strongly adsorbed or weakly adsorbed. Tie et al. demonstrated the interesting history dependence on protein re-adsorption experiments due to surface mobility[66]. The authors used OWLS to study fibronectin adsorption kinetics. A solution of fibronectin was passed over a SiO_2 surface, rinsed with buffer solution, and then re-exposed to fibronectin solution. It was found that the re-adsorption rate reached after rinsing was faster than that at the same level of surface coverage during the first adsorption step. The authors attribute this increase in rate to aggregation of the strongly adsorbed protein during the rinse. Surface diffusion coefficients of proteins have been reported in a wide range ($\sim 10^{-8}$ to $\sim 10^{-11}$ cm^2/s).[70-73]

Surface chemistry plays an essential role in determining the mechanism of surface mobility. Wertz et al. suggested two different mechanisms of adsorption depending on the hydrophilicity of the surface[12]. They used -OH and -CH_3 terminated SAMs and found the dynamics of fibrinogen adsorption to be distinctively different on these two surfaces. On the hydrophilic –OH terminated surface, the protein tends to achieve stronger contact with the surface primarily through reorientation rather than spreading. The protein molecule "rolls" along the hydrophilic surface until the best interaction is found. This was determined through the observation that old contacts with the surface were likely sacrificed in favor of new and stronger ones. In contrast, on the hydrophobic –CH_3 terminated SAM, a protein molecule tended to keep old contacts and simply make new contacts around them by spreading. Here surface mobility of the fibrinogen on the hydrophobic surface is manifested in "sliding" rather than rolling.

The surface protein coverage also has a dramatic effect on surface mobility. Initially arriving proteins are free to diffuse over the local surface area, but proteins arriving later do not experience a clean surface. They diffuse along the surface through an

archipelago of other diffusing proteins. Models depicting such diffusion were first described by Saxton.[74] It is more difficult for the protein to navigate through crowded two-dimensional environment, and so the diffusion coefficient tends to decrease as surface protein coverage increases. Tilton et al. examined the surface diffusion coefficient with varying surface concentration.[75] The researchers found that the experimental data could be well described by the model of Saxton. The diffusion coefficient of BSA on PMMA at infinite surface dilution was around $5.6 \times 10^{-8} cm^2/s$, whereas at 50% coverage the value had decreased by ~90%.

Protein structure is critical to the mechanism of surface mobility. It's well known that larger molecules tend to have smaller diffusion coefficients in solution. The same principle applies to proteins on surfaces with the addition of the effect of size on adsorption strength. More strongly adsorbed proteins need to overcome a higher activation barrier during laterally diffuse.

A number of techniques have been used to quantify protein diffusion coefficient. Total internal reflectance fluorescence (TIRF) utilizes fluorescence excited by an evanescent wave which penetrates to a distance on the order of a fraction of the light wavelength into the bulk solution. This causes the majority of the resulting fluorescent signal to be produced by proteins near the solid/liquid interface. Tilton et al. used TIRF combined with fluorescence recovery after photobleaching (FRAP) to determine the surface diffusion coefficient of adsorbed BSA on several surfaces.[70] Care must be taken in situations where the surface can change the fluorescent characteristics of the tag. Daly et al. used this effect to their advantage by using two fluorescent signals, one which was changed by surface interaction and one which was not, to quantify adsorption amount as well as surface induced denaturation.[62]

Recently, Shen et al. directly measured surface diffusion coefficient using TIRF microscope in the single molecule tracking mode.[76] **Figure 1.7** compares the single molecule trajectories of a fluorescence tagged amyloid-β peptide on polystyrene-block-poly(2-hydroxyethyl methacrylate) (PS-b-PHEMA) diblock copolymer surfaces. The single molecule trajectory on the hydrophobic PS_{200}-b-$PHEMA_{50}$ surface (PHEMA cylinders in PS matrix) shows clearly shorter diffusion distances (for fixed time intervals) than those on the more hydrophilic PS_{140}-b-$PHEMA_{150}$ surface (PS and PHEMA lamellae). Quantitative analysis gave diffusion constants of 0.21 $\mu m^2/s$ and 2.90 $\mu m^2/s$ on the PS_{200}-b-$PHEMA_{50}$ and PS_{140}-b-$PHEMA_{150}$ surfaces, respectively.

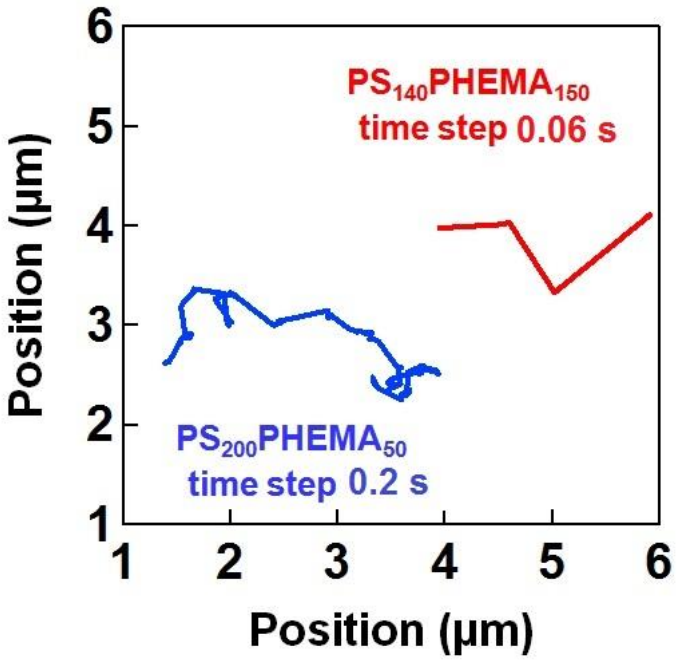

Figure 1.7: *Single molecule trajectories of amyloid-β peptide on polystyrene (PS)-block-poly(2-hydroxyethyl methacrylate) (PS-b-PHEMA) diblock copolymer surfaces.*[76]

1.4.3. Multi-conformation adsorption

While many proteins have somewhat globular shapes, no protein molecule has a completely uniform surface. Proteins are capable of adsorbing to surfaces in a myriad of

configurations. One of the clearest examples of the ability of a protein to adsorb with multiple conformations is that of lysozyme. Adsorption data of lysozyme performed at high bulk concentrations (~1 mg/mL) is known to exhibit unique behavior during the transition from a transport limited regime to a surface coverage limited regime. A so-called "overshoot" of lysozyme adsorption occurs quite sharply at the end of the transport limited regime. Daly et al. observed several structural reorganizations of lysozyme after initial adsorption to SiO_2 and suggested that dimers could be forming on the surface.[62] Wahlgren et al. suggested that the surface catalyzed the formation of protein dimers as an explanation for the adsorption overshoot.[77] The dimers could form until the lysozyme has denatured to the point where the dimer was unstable, causing it to collapse and the surface loading to decrease, but simulation based on this model did not fit experimental data well. Daly et al. suggested that reorganization from end-on to side-on adsorbed states could explain the discrepancy between experimental data and simulation results.[62] Lysozyme has a slightly oblong shape. Wertz et al. suggested that lysozyme initially adsorbed in the end-on configuration, which was capable of more efficient packing on the surface, and changed to a strongly adsorbed side-on configuration.[35] They used TIRF to quantify fluorescently labeled lysozyme adsorption. It was found that high bulk concentration (>5 mg/mL) and/or high flow rate (>5.0 s^{-1}) would produce the observed effect. The so-called "roll over" model led to satisfactory agreement with experimental data.

Fibrinogen is much longer and has a more elongated shape than lysozyme does. Many researchers have found that the amount of fibrinogen which can adsorb to a hydrophobic surface significantly exceeds the amount that would be produced by a monolayer of protein laying flat on the surface. Roach et al. described the orientations which fibrinogen can assume on a surface.[30] Based on QCM measurements, the authors

suggested that fibrinogen could assume a primarily side-on configuration at low surface concentration and re-orient to the end-on configuration as surface coverage increases. This correlates well with the observation that the fraction of reversibly adsorbed fibrinogen increases with time on such surfaces.

1.4.4. Multi-protein adsorption

While studies on the adsorption of individual proteins to surfaces are paramount to understanding the basic adsorption mechanism, they cannot reveal the true nature of protein adsorption in vivo. In the blood plasma, there are a large number of proteins at concentrations varying over many orders of magnitude. The sum of the adsorption behaviors of individual proteins will not be the same as the adsorption behavior of these proteins in the same solution. Multiple proteins in solution will interact with each other while attempting to adsorb, producing unique adsorption profiles not observable with individual proteins.

The most complicated element of multi-protein adsorption is the presence of a variety of adsorption characteristics. If one protein is capable of stronger interaction with the surface than another, the more strongly interacting protein will dominate the surface population. This often results in surface populations whose composition is very different from the bulk composition. The so-called "Vroman Effect" was first described by Vroman and Adam, **Figure 1.8.**[78] They noted that after several different surfaces had been exposed to blood plasma for a certain amount of time, fibrinogen seemed to dominate the surface even though it was not the dominate protein in blood plasma. They suggested that small proteins that could diffuse to the surface the fastest would be the

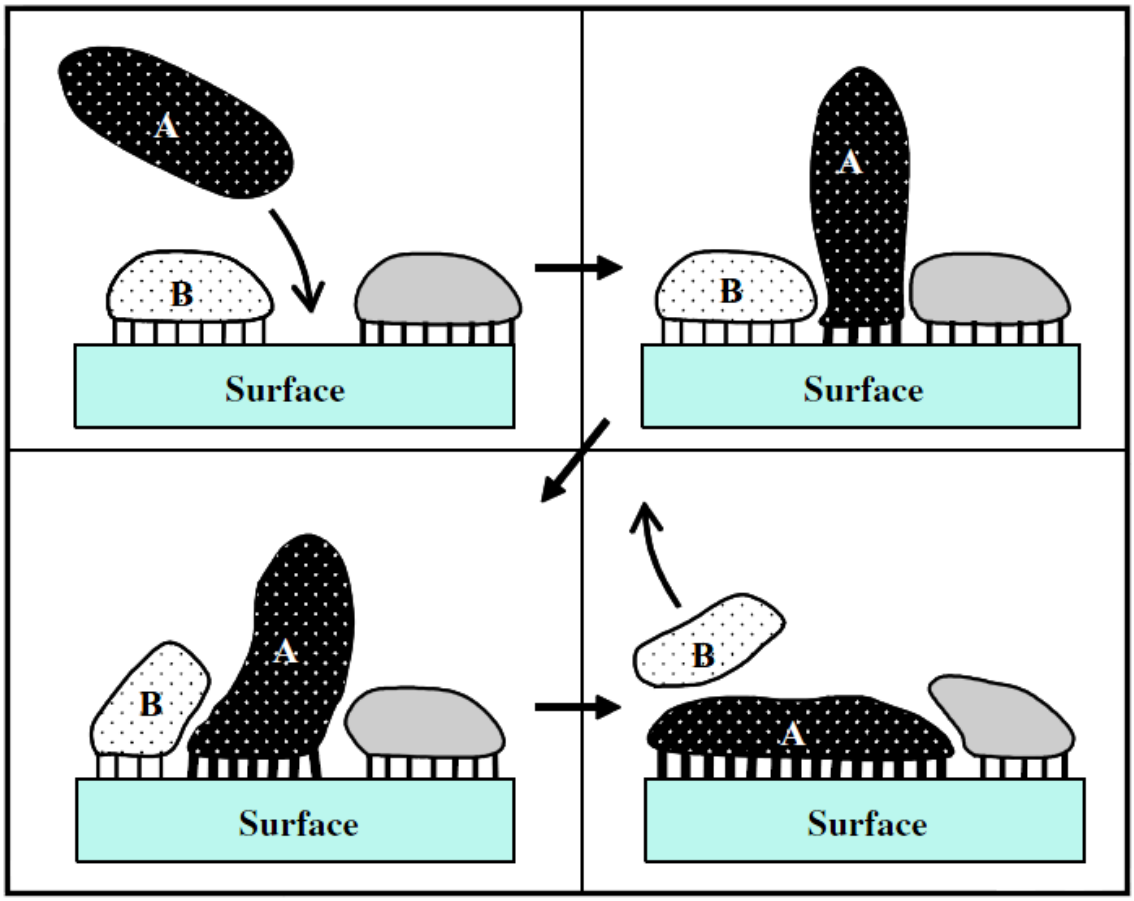

Figure 1.8. *Displacement of adsorbed proteins via the Vroman Effect*. The free energy gained from increasing the level of contact of protein A with the surface is enough to pay the free energy cost of the desorption of protein B. Protein A must also have room to form the weakly adsorbed state on the surface so that spreading can occur. Figure reproduced with permission.[21]

dominant species on the surface at short times, but these proteins would eventually be displaced at longer times by larger proteins that adsorb stronger on the surface.

During displacement, one protein increases its level of contact with the surface while the displaced protein loses contact with the surface. This process may occur either through surface spreading or through reorientation. If the free energy gained from the adsorption of one protein is more than the free energy cost of desorbing another from the

surface, then displacement can occur. However, the protein doing the displacing need to at least adsorb, albeit weakly, near a protein molecule already adsorbed. If there is no available room on the surface to form the weakly adsorbed state, displacement will not be able to proceed. Wertz et al. studied the displacement of albumin by fibrinogen on a hydrophobic SAM surface.[79] They found that once a monolayer of albumin had formed on the SAM, displacement by fibrinogen became minimal.

The ability of proteins to displace one another on a surface plays an important role in adsorption driven biological processes, such as the coagulation cascade. Jung et al. demonstrated that fibrinogen adsorbed to SiO_2 at pH 8 could be displaced when exposed to human plasma solution.[80] However, once the solution had been cycled from pH 8 down to pH 3.5 and then back to pH 8, the displacement became ~170x less. The authors attribute this to the rearrangement of αC domains on fibrinogen, weakening the adsorption strength at neutral pH. This change could potentially be brought about via alternate means in response to a biological stimulus and could be a major contributor to the formation of blood clots.

The Vroman effect was established based on protein adsorption to hydrophilic charged surfaces. On hydrophobic surfaces, the effect is somewhat different. Noh et al. observed what they termed a "Vroman-like effect" on hydrophobic surfaces whereby the surface was dominated in terms of number population by smaller proteins.[81] Larger proteins still tend to dominate the mass of adsorbed protein on the surface. This is likely due to the much higher strength of adsorption for protein molecules, including small ones, on the hydrophobic surface than on the hydrophilic surfaces. Smaller proteins strongly discriminate against hydrophilic surfaces whereas larger proteins are not nearly as discriminating. As a result, small changes in surface characteristics can have great

impacts to the adsorption characteristics of small proteins while causing minimal alterations to those of larger one.

The issue of biofouling of artificial implants in the human body has been a particularly difficult problem to many investigators over the past a few decades. The formation of blood clots within mechanical artificial organs is one of the leading causes of failure in such devices. Convention holds that the formation of blood clots within these devices is surface initiated. However, the way in which the surface initiates the blood coagulation cascade has yet to be determined. Perhaps the most puzzling element is the fact that, while more proteins are capable of adsorbing to hydrophobic materials, artificial organs constructed from hydrophilic materials fail due to coagulation even faster. It must be the case that something other than the mere presence of adsorbed protein initiates coagulation. Vogler et al. suggested that the rapid formation of a monolayer of small proteins on a hydrophobic surface prohibits contact with blood coagulation factors and hinders the initiation of the cascade.[82] This is similar to the description provided above of the "Vroman-like Effect" observed by Noh et al. However, the strong activation by hydrophilic surfaces, with which there is minimal interaction with protein, remains a mystery. With specific chemical interactions with the surface ruled out, it is possible that surface mobility of adsorbed protein plays a strong role in the blood coagulation cascade. Mobile proteins weakly adsorbed to the surface can reorient themselves rapidly, enabling them to sample the surrounding environment easily. This increased sampling rate may improve the speed of the initiation of the coagulation cascade.

While the competitiveness of protein adsorption is commonly discussed, there exists the potential for cooperative effects. It is well accepted that a mixture of proteins can result in an overall higher surface loading than either of the two proteins alone due simply to higher packing efficiency.[34] Rabe et al. discussed the possibility that protein

surface aggregates could guide adsorbing proteins towards available adsorption sites.[83] This cooperative protein adsorption effect must be studied in greater detail if a clearer understanding of multi-protein adsorption is to be achieved. A potential experiment to quantify this behavior would involve a surface which was conducive to the non-specific adsorption of one protein, but repulsive to the non-specific adsorption of another.

1.5. ACTIVITY OF IMMOBILIZED PROTEINS

The ability of a protein to maintain its activity while adsorbed to a surface is of fundamental importance to several technologies including protein microarrays, drug delivery systems, and biomimetics. Non-specific adsorption in most cases causes perturbation of the tertiary structure to some degree, which in turn will alter the ability of proteins to perform their intended function. Surface chemistry will determine both the strength of the protein-surface interaction as well as the activity of the adsorbed protein. Specific adsorption (via a particular functional group) and precise control of the chemical environment surrounding an adsorbed protein are often needed to maintain the activity of an immobilized protein molecule.[63]

Most proteins must maintain their secondary and tertiary structure in order to perform their intended functions. For example, there must be little disturbance of the binding pocket of an enzyme to interact with its substrate. Unfortunately, predicting the change in activity of a protein adsorbed to a surface cannot be easily obtained from knowledge of activity and denaturation in the solution phase. Karlsson et al. demonstrated that when human carbonic anhydrase was adsorbed onto a SiO_2 nanoparticle, the active site conformation was lost before the majority of the tertiary structure was disrupted.[57] In contrast, the tertiary structure was normally lost before the active site structure was disrupted during denaturation in the solution phase. This

suggests that the mechanism of denaturation in solution is different from the mechanism of denaturation on a surface. In the case of human carbonic anhydrase, it is likely that the binding site or areas near the binding site has an affinity for the SiO_2 surface. This causes the binding site to be oriented towards the surface, which disrupts the binding sites structure as well as blocking its access by intended substrate.

The activity of an adsorbed protein is dynamic. Proteins that adsorb to the surface first tend to have different activities than those adsorbed later in the adsorption process. Lee et al. studied the activity of ribonuclease A during adsorption to mica.[84] These researchers noticed that the activity per mole of adsorbed protein on the surface actually increased as the surface concentration increased. The authors attribute this observation to packing induced reorientation of adsorbed proteins. In this case, nearby adsorbed proteins aid each other in maintaining the native state with the active site facing outward into solution.

Proteins typically lose their active site conformation when the interaction between the protein and the surface is strong. A successful strategy to prevent denaturation is to immobilize proteins to a surface which does not interact strongly with the protein. Such techniques involve the binding of a protein to a chemical moiety engineered into the protein and a non-interacting surface to allow for immobilization. The most desirable binding motifs are those which can provide the desired interaction strength, whether reversible or irreversible, in a chemical environment which does not significantly disrupt the protein's structure, and with chemical bonding which allows maximum control over the protein's orientation and configuration. Such binding motifs include (among others) the streptavidin-biotin interaction, various "Click" reactions, DNA base pair interactions, and nitrilotriacetic acid-6x histidine tag binding.[85-91] One part of the binding motif is

engineered into the protein's primary structure, typically either the N or C terminus, while the other part is grafted onto a repulsive surface, such as PEG brush.

1.6. CONCLUDING REMARKS

This tutorial attempts to apply simple concepts of physisorption and chemisorption to the understanding of protein interaction with surfaces. The complex problem of protein adsorption may be reduced to a set of simple principles not too different than those developed for the adsorption of a simple gas phase molecule on a single crystal metal surface. We focus on the dynamic aspects of protein adsorption, particular the presence of a spectrum of mobile and weakly adsorbed precursor states as a protein evolves from the natured state in the solution phase to a denatured and strongly adsorbed state. The presence of the precursor states is essential to the kinetics and thermodynamics of protein adsorption. How to interrogate and control the precursor states can be an effective strategy in designing surfaces for various applications, such as biosensors, drug delivery systems, and medical implants. In this regard, there are a number of knobs one can turn. Examples include, among others, surface chemistry, surface topology, chemical or physical patterns, and solution conditions. These factors, when combined with smart materials, e.g., polymers sensitive to external stimuli (light, pH, temperature, etc.), may allow us to design optimal and intelligent interfaces for protein-surface interactions.

Acknowledgement. This work was supported by the US Army Research Office (W911NF-08-1-0287) and the University of Texas at Austin.

Chapter 2: Two Dimensional Nanoarrays of Individual Protein Molecules[b]

2.1. INTRODUCTION

Immobilizing protein molecules at solid surfaces with nanometer dimensional control is of interest to increasing miniaturization in biosensing and high throughput bioassaying.[92,93] Micro- to nano-scale protein patterns may also be used in interrogating protein-cell interactions at the molecular level.[94,95] Most physical or chemical methods for immobilization can also lead to the clustering or aggregation of immobilized protein molecules, leading to reduced activity or accessibility. This also necessitates spatial control on molecular dimensions. While scanning probe lithography techniques have been used to generate nano-scale protein patterns on solid surfaces,[96,97] these approaches usually do not control inter-protein arrangements at the individual protein level. Only when the lithographical feature, such as individual gold nanoparticles written by dip-pen nanolithography, approaches that of protein molecules can the immobilization of single protein become possible.[98] However, scanning probe lithography techniques are inherently serial (even with multiple tips) and are limited to small areas and model surfaces. For large-scale immobilization of protein molecules with spatial control on the single molecule scale, one would ideally need a self-assembly technique. Such a technique should satisfy at least two conditions: 1) it should present well-ordered patterns of chemical contrast on the length scale of protein molecules; 2) it should resist non-

[b] Shen, L.; Garland, A.; Wang, Y.; Li, Z.; Bielawski, C. W.; Guo, A.; Zhu, X. Y., Two Dimensional Nanoarrays of Individual Protein Molecules. *Small* **2012,** *8* (20), 3169-3174. Results shown in section 2.4. were obtained by Lei Shen. Azide functionalized proteins were prepared by Yini Wang. Alkyne functionalized diblock copolymer was prepared by Christopher Bielawski's research group. Histidine tagged proteins were prepared by Athena Guo.

specific protein adsorption but allow only immobilization with specific chemical functionality.

Here we make use of block copolymer thin films to satisfy the above conditions for the self-assembly of protein nano-patterns. Block-copolymer thin films are known to phase separate into well-ordered structures, such as the hexagonally packed vertical cylinder phase or vertical lamellar phase.[99,100] The dimensions of these structures are of the order of a few tens of nanomaters, the exact length scale of individual protein molecules, thus satisfying the first condition. A number of research groups have explored the use of block-copolymers thin film nano-patterns, such as those of poly(styrene)-*block*-poly(methyl methacrylate) (PS-*b*-PMMA) diblock copolymers, for the adsorption of proteins.[101-106] However, most of these block-copolymers consist of only hydrophobic blocks that do not resist the non-specific adsorption of protein molecules and, thus, do not satisfy the second condition. To circumvent the non-specific adsorption problem, we explore the use of block-copolymers containing protein resistant blocks. While poly-ethylene-glycol (PEG) is perhaps most resistant to protein adsorption and PS-*b*-PEG is known to form well-ordered nano-patterns,[100] the PEG containing block-copolymer thin film is unstable in aqueous solution due to the extensive swelling of the PEG block. Another hydrophilic and biocompatible polymer is poly(2-hydroxyethyl methacrylate (PHEMA), which is known to resist nonspecific protein adsorption.[107] Recently, we found that thin films formed from PS-*block*-poly(2-hydroxyethyl methacrylate) (PS-*b*-PHEMA) diblock copolymer, with PS as cylinders in the majority PHEMA matrix, were stable in aqueous environment and resisted non-specific protein adsorption.[108] Thus, the PS-*b*-PHEMA diblock copolymer thin film in the vertical (PS) cylinder phase can satisfy both

conditions for the immobilization of protein molecules with spatial control on the single molecule scale.

To cause the proteins to become bound to the cylindrical PS domains, a handle for binding needed to be installed in some fashion into the PS domains. Several strategies were pursued to this end. The simplest methods involved modification of the phase separated diblock copolymer thin film after it had already been cast. In addition to maintaining the requirements previously stated, more conditions needed to be met for this method to be viable. 1) The modification must be selective for the PS domains over the PHEMA domains, and 2) the modification of the surface must cause no significant change to the morphology of the polymer. In addition to these, the method for the covalent attachment of protein to the copolymer surface also required restraints. 1) The attachment must not cause permanent change to the structure of the protein, and 2) the attachment must be strong enough to irreversibly bind the protein to the surface.

Once immobilization is achieved, investigation into the effects that the surface has on protein function may be investigated. Proteins that are in an environment that they are not suited for are susceptible to denaturation. The process of protein denaturation is illustrated in **Figure 2.1**.[109] While a denatured protein is capable of refolding itself when placed in the proper environment, neighboring proteins and other molecules can interfere with the process. This causes the protein to mis-fold into a stable aggregate state that is usually incapable of performing its proper function. Partially denatured proteins with a significant amount of beta sheet formation can form so called "amyloid" structures with nearby denatured proteins. Amyloid structures have been implicated in major diseases such as Alzheimer's and Creutzfeldt-Jakob disease.[110,111] The exact role of protein spacing and arrangement during the refolding process remains largely unknown. Gaining a better

understanding of the way that proteins refold in the presence of other proteins will give critical insight into the development of these diseases.

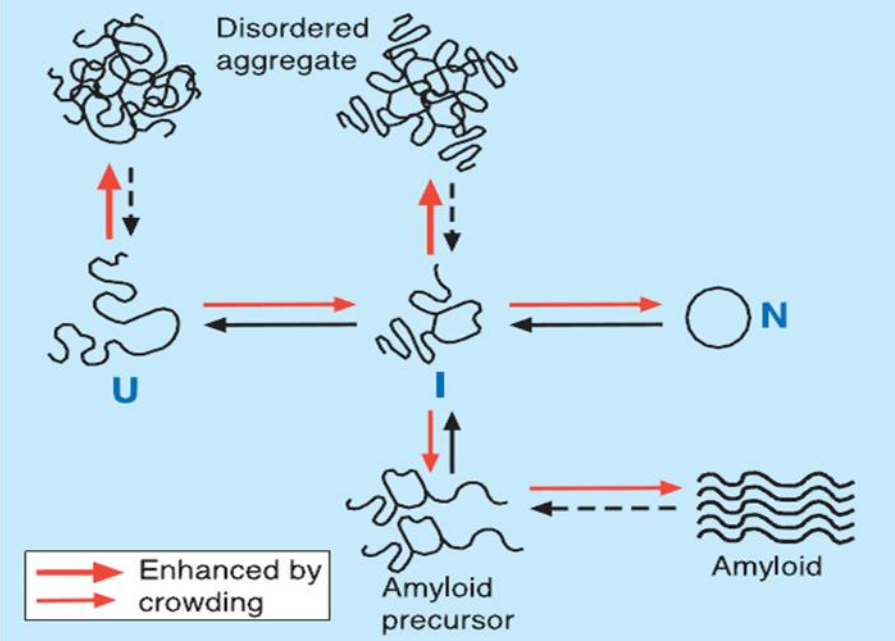

Figure 2.1. *Protein denaturation and mis-folding process*.

Inside the human body, so called "chaperone" proteins are produced when homeostasis is disrupted and proteins begin losing their tertiary structure.[112] Chaperones encapsulate denaturing proteins and protect them from the environment. Once homeostasis is restored, the proteins are released from the chaperones in their folded state. The local environment inside the chaperone is critical to maintaining the protein in the well natured state. The inside surface of the chaperone is not merely resistant to nonspecific adsorption. It is a heterogeneous surface with regions of hydrophilicity, hydrophobicity, and positive and negative charge. Understanding the interplay between a heterogeneous surface and the ability of a protein to unfold and refold will give insight

not only into the function of chaperones but also into controlling protein function at interfaces.

2.2. BENZOPHENONE-BASED LINKERS

Our first strategy is illustrated in **Figure 2.2**. We use PS-*b*-PHEMA diblock copolymer with the repeating unit in the PHEMA block ~3x that of the PS block to form thin films on gold substrates with vertical cylinders of PS in PHEMA matrix. Modifying the PS domain while leaving the PHEMA domain unmodified would require a method which was unreactive towards hydroxyl groups and esters while being reactive with some element of the PS chain. The simplest route to install functionality into PS without reaction with PHEMA was determined to be through radical chemistry utilizing the stable tertiary benzyl position in the PS chain. Such a stable radical position does not exist on PHEMA, giving the selectivity required.

It has been shown that UV light is capable of crosslinking PS in the presence of a photoinitiator such as benzophenone.[113] A synthetic linker containing a benzophenone moiety at one end and a covalent attachment motif at the other could be used to connect the attachment motif to the PS domains via UV initiated radical chemistry. The copolymer thin film was found to be unstable in the presence of most organic solvents. Only methanol/water containing less than 20% w/v methanol would not damage the morphology of the film. Finding a linker which is soluble in aqueous mixtures of this type would be necessary.

The attachment motif chosen was the Cu(I) catalyzed 1,3-Huisgen cycloaddition "click" reaction. This reaction is capable of forming a covalent linkage between a

terminal alkyne and an organic azide under mild conditions at room temperature. Such conditions have been used to link alkyne-functionalized proteins with organic azides as well as azide-functionalized proteins with alkyne bearing substrates with little deformation to the overall structure of the protein.[114]

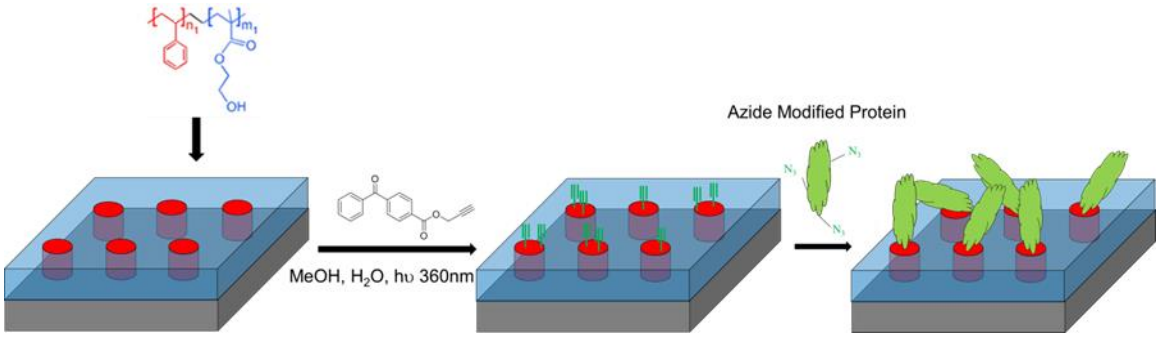

Figure 2.2 . *Schematic illustration of the generation of PS-b-PHEMA block-copolymer thin film with PS cylinders (red) in the PHEMA (blue) matrix*. The PS domains are modified to present alkyne functionality for the specific immobilization of azide-tagged protein molecules via click chemistry.

Before synthesis of a linker, the ability of benzophenone to selectively bind to the PS domains needed to be determined. By attaching a fluorinated derivative of benzophenone to the PS-PHEMA thin film, XPS could be used to determine the intensity of the fluorine signal on the surface compared to pure PS and pure PHEMA. In addition, films cast from mixtures of PS-PHEMA and PS homopolymer were used to produce surfaces of intermediate PS surface area. Commercially available 2-amino-2',5'-bis(trifluoromethyl)benzophenone (ATB) was used to determine the selectivity. This compound forms a suspension in methanol/water solvent at concentrations below 20% w/v. The suspension was found to form at concentrations as low as 1% methanol. This is preferable to a solution as it allows the ATB to adsorb to the PS domains for immobilization. This was shown to be the case via SPR (**Figure 2.3**). The ATB solution shows little to no adsorption onto PHEMA, mild adsorption onto PS-PHEMA, and the strongest adsorption on PS. Exposure of ATB solution to PHEMA surface was alternated

several times showing no significant change in the SPR response. It is notable that the final PS adsorption intensity is ~2x the intensity on PS-PHEMA, which corresponds well to the ~2.5x more surface area covered by PS in pure a film of PS vs PS-PHEMA.

Gold substrates were coated with PS-PHEMA and PS-PHEMA that had been mixed with various concentrations of PS (additional 20, 40, and 80% PS). A pure PHEMA surface was used as a control. The substrates were placed in a 2 inch petri dish and immersed in 10mL of 375μM ATB in 1% methanol/water. While submerged, the substrates were exposed to 100W of 365nm UV light for 2 hours. Substrates were then rinsed with 10% methanol to remove unlinked ATB and dried with nitrogen. XPS showed a linear relationship between PS content and fluorine signal (**Figure 2.4**). There was no discernable fluorine signal on the pure PHEMA film outside of the noise. These observations indicate a strong selectivity for PS by benzophenone-based linkers. The pure PS-PHEMA diblock appears as an aberration due to its higher fluorine signal versus a PS-PHEMA film doped with 20% pure PS. This is likely due to the discrepancy between total PS content and the accessible surface area of PS in the film. Shen et al. showed that thin films cast from mixtures of PS-PHEMA and PS form large globular nanoscale features.110 These features have a larger volume to surface area ratio than the features in pure PS-PHEMA. This potentially accounts for a reduction in PS surface area for the 20% doped film which is recovered by the addition of higher concentrations of PS.

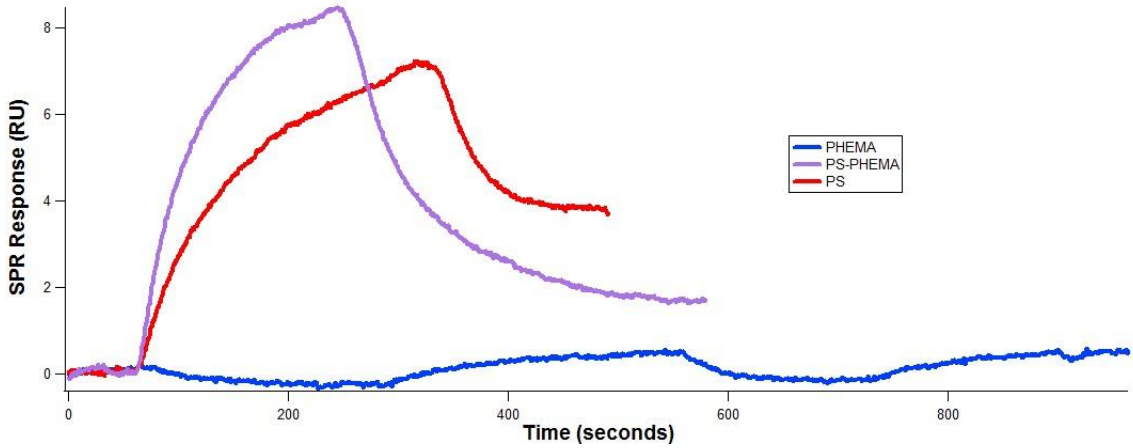

Figure 2.3. *Adsorption of ATB suspension onto PHEMA, PS-PHEMA, and PS.* ATB concentration was 50μM in 1% MeOH.

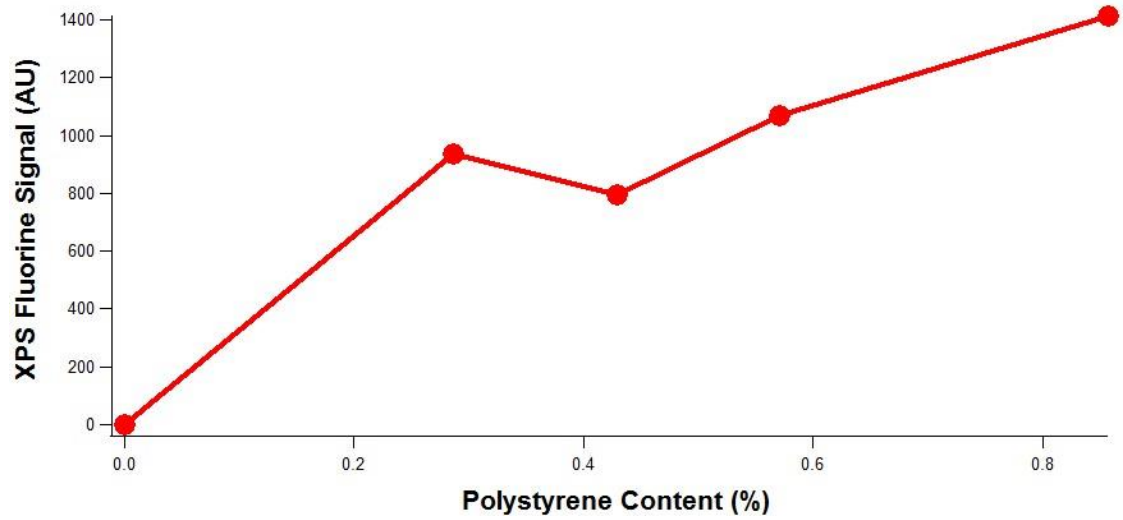

Figure 2.4. *Fluorine intensity as measured by XPS vs. polystyrene content*.

Having satisfied the condition for specificity for PS, linker **1** was synthesized via Steglich esterification of 4-benzoyl benzoic acid and propargyl alcohol. Unfortunately, it was not possible to form a stable suspension of the synthesized linker in methanol/water. Mixed aqueous solvents using small percentages of acetone, ethanol, or isopropanol were attempted, but all mixtures damaged the morphology of the copolymer thin film. A new method for the modification of the PS domains would be required.

2.3. ALKYNE FUNCTIONALIZED PS-PHEMA (PSA-PHEMA)

A novel copolymer was synthesized by Li Zicheng of the Bielawski group to meet our requirements. The structure of the polymer can be seen in **Figure 2.5**. This polymer is of similar structure to normal PS-PHEMA except that the styrene monomers of the PS domain are functionalized with a propargyl group para to the polymer backbone. The polymer contained 40 repeat units of the alkyne functionalized PS (PSA) and 240 repeat units of PHEMA. Unfortunately, this polymer alone was found to be incapable of forming the proper nanoscale morphology for protein binding. To provide the proper morphology, mixtures of this polymer with unmodified PS-PHEMA were spin casted onto gold substrates, solvent annealed, and checked for nanoscale structures via AFM. Films cast from a mixture of 4:1 PS_{60}-*b*-$PHEMA_{150}$/PSA_{40}-*b*-$PHEMA_{240}$ were found to have a nanoscale morphology largely identical to that of unmodified PS-PHEMA. The resulting polymer thin film presents alkyne functional groups on the PS domains for the specific attachment of azide tagged protein molecules via "Click" chemistry.[115] The new route for attachment of proteins to the polymer surface is shown in **Figure 2.5**.

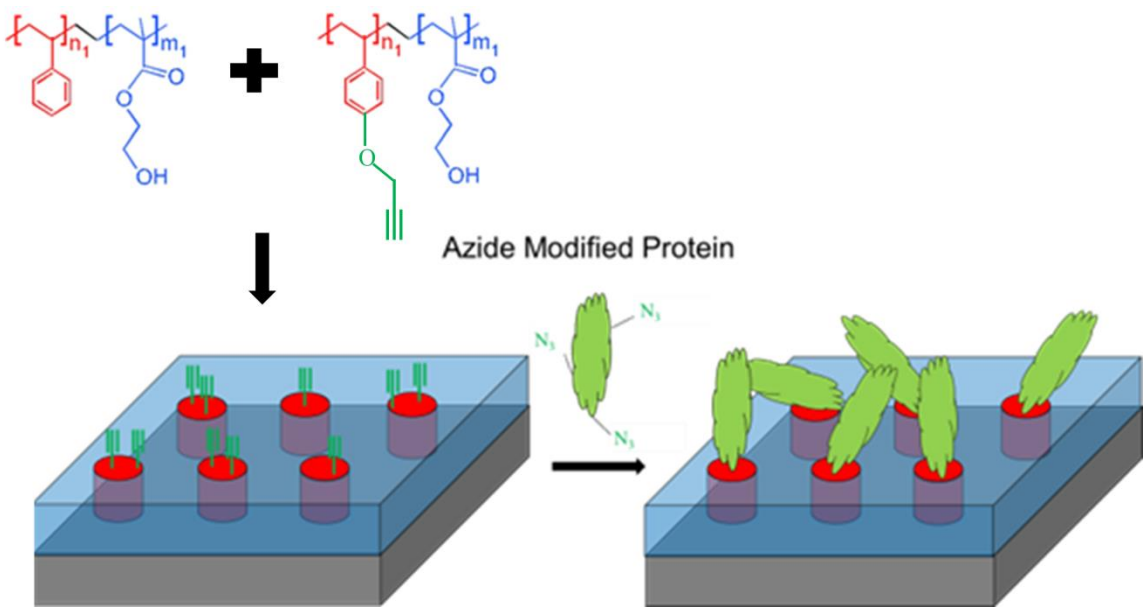

Figure 2.5. *Alkyne functionalized PS-PHEMA (PSA-PHEMA) where n_1=40 and m_1=240 is used in conjunction with normal PS-PHEMA to form alkyne bearing thin films*. The attachment of azide functionalized proteins is shown.

2.4. PROTEIN IMMOBILIZATION

As we show below, the limited size of the PS domains, along with the repulsive nature of the PHEMA matrix results in the immobilization of single molecule per domain. **Figure 2.6** shows atomic force microscopy (AFM) images taken under aqueous solution for the polymer film from spin-coating of PS_{60}-*b*-$PHEMA_{150}$/PSA_{40}-*b*-$PHEMA_{240}$ mixtures (4:1 wt). Micro phase-separated domains are observed with the minor PS cylindrical domains (~hexagonal packing) appearing higher in topography and brighter in phase. A cross sectional profile (Fig. 2.5 C) of the topography shows the PS domains are higher than the surrounding PHEMA by ~2 nm. We estimate that the diameter of each PS domain (from phase image) of 15 ± 3 nm, with inter-domain distance of ~28 ± 3 nm. We verify the resistance of the block-copolymer surface to nonspecific protein adsorption using surface plasmon resonance (SPR) spectroscopy to quantify the amounts of irreversibly adsorbed protein.

Figure 2.6 D shows SPR responses of the surface upon exposure to solutions (50 mg/ml) of three model proteins: fibrinogen (FBN), myoglobin (MYO), and lysozome (LYS). The SPR responses show rise in signal upon exposure to protein solution due mainly to changes in refractive index. In each case, the signal returns to the baseline when the surface is exposed to washing buffer, indicating negligible adsorption of protein molecules.[108] Note that both liquid phase AFM and SPR spectroscopy show the stability of the polymer thin film under aqueous solution. We chose three azide-tagged protein molecules, LYS (13.7 kDa, 2×3×3 nm^3), MYO (17 kDa, 2×3.5×4 nm^3), and FBN (340 kDa, 50×7×7 nm^3) to demonstrate the immobilization of individual protein molecules to the alkyne functionalized PS domains via highly specific and facile click chemistry. While all dimensions of LYS and MYO molecules are smaller than the diameter of the PS domains, one of the dimensions of FBN is larger than the diameter of each PS domain or the inter-domain distance on the block-copolymer surface. To unambiguously demonstrate the specificity of the "Click" reaction for protein attachment we show in **Figure 2.7 E**, X-ray photoelectron spectra (XPS) for PS-*b*-PHEMA thin film samples that have been immersed in the azide-FBN solution for six hours with (red) and without (black) the Cu(I) catalyst. As expected, the azide containing proteins only attaches to the alkyne functional groups on the surface in the presence of the Cu(I) catalyst.

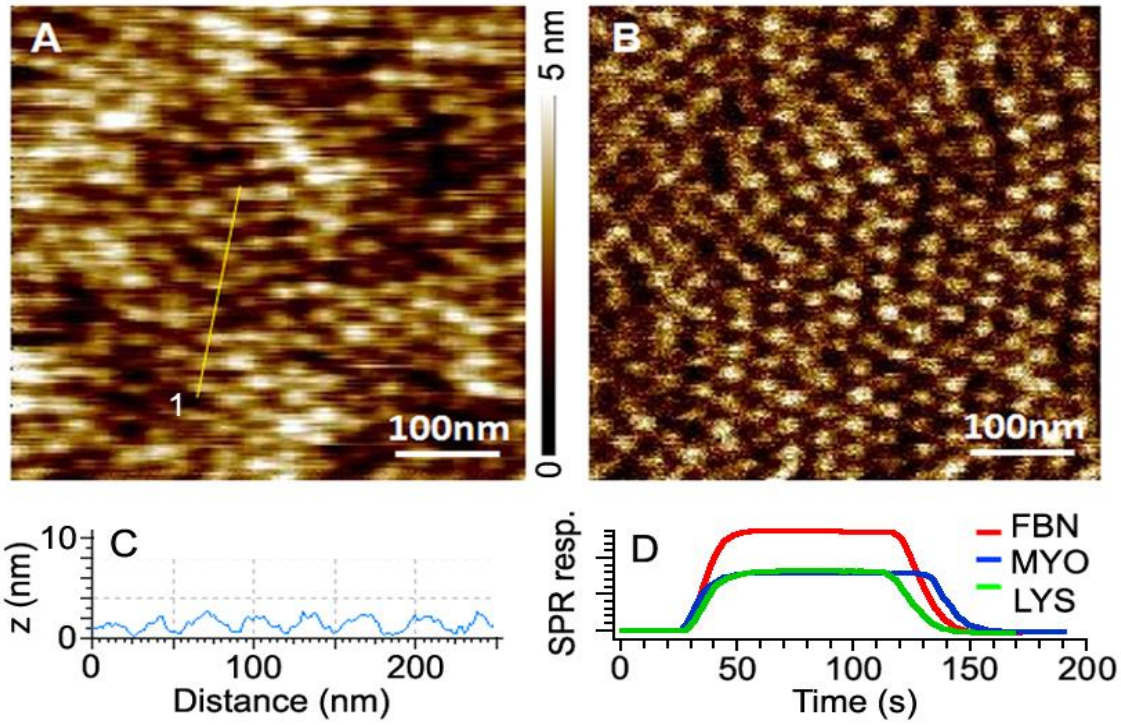

Figure 2.6. *AFM images for PS-b-PHEMA thin film in water*: A) topography, B) phase, and C) cross sectional profile. Panel D shows SPR responses of the PS-b-PHEMA surface upon exposure to three protein solutions (50 μg/ml), fibrinogen (FBN), myoglobin (MYO), and lysozome (LYS). Here the rise and decay in SPR signal correspond to the injection of protein and buffer solutions, respectively.

We image the immobilized protein molecules on the PS-*b*-PHEMA surface under aqueous solution using AFM, **Figure 2.7 A-C**. In each case, the adsorbed protein molecules appear as nearly uniform and individual features. As expected, the size of each feature scales with the size of the protein molecules (LYS < MYO < FBN). This is most obvious in cross sectional profiles (**Figure 2.7 D**), where the apparent height variations are 3 ± 1 nm, 4 ± 1 nm, and 7 ± 2 nm for LYO, MYO, and FBN, respectively. For LYO and MYO, the apparent heights are in excellent agreement with the sizes of the protein molecules. For the elongated FBN, the 7 ± 2 nm height corresponds to an adsorbed fibrinogen molecule with the long molecular axis parallel to the surface. For the smallest LYO molecule, AFM image (**Figure 2.7 C**) shows that the adsorbed protein layer adopts

the same ordered structure and periodicity as the underlying hexagonal PS-*b*-PHEMA structure. Thus, there is one LYO molecule on each PS domain. For the slightly larger MYO, there is clearly less long range order than that of LYO and the inter-MYO distance is on average 20-30% larger than the inter-PS domain distance, indicating that not every PS domain is occupied by an adsorbed protein. This is surprising as the lateral size of each MYO molecular is ~4x smaller than the diameter of each PS island. We attribute this less than one-to-one immobilization efficiency to a kinetic effect. As we discovered recently,[108] the adsorption of a protein molecule undergoes a mobile precursor state, which reorganizes and samples the surface before irreversible adsorption (covalent bonding via click chemistry in the present case).

The sampling distance in the mobile precursor state can be more than one order of magnitude larger than the dimension of a protein molecule. As a result, the presence of an adsorbed MYO on one PS domain not only prohibits the adsorption of a second MYO molecule, but also affects the kinetics of adsorption on neighboring PS domains. In the case of FBN, the long molecular dimension can bridge two PS domains (separated by the PHEMA matrix). There is again a lack of long-range order in the image, but we can clearly identify each individual fibrinogen molecule which is elongated, consistent with the highly anisotropic fibrinogen molecule. The average inter-molecular distance is ~50 nm, which is the same as the long molecular dimension in the native state, but much longer than the short molecular dimension (7 nm). The less than close-packing can also be explained by a kinetic effect and the space requirement of precursor state before irreversible adsorption. The immobilization of individual protein molecules on this nano-patterned surface is in stark contrast to that on a hydrophobic surface, such as PS, where adsorbed protein forms clustered and featureless islands (**Figure 2.8**).

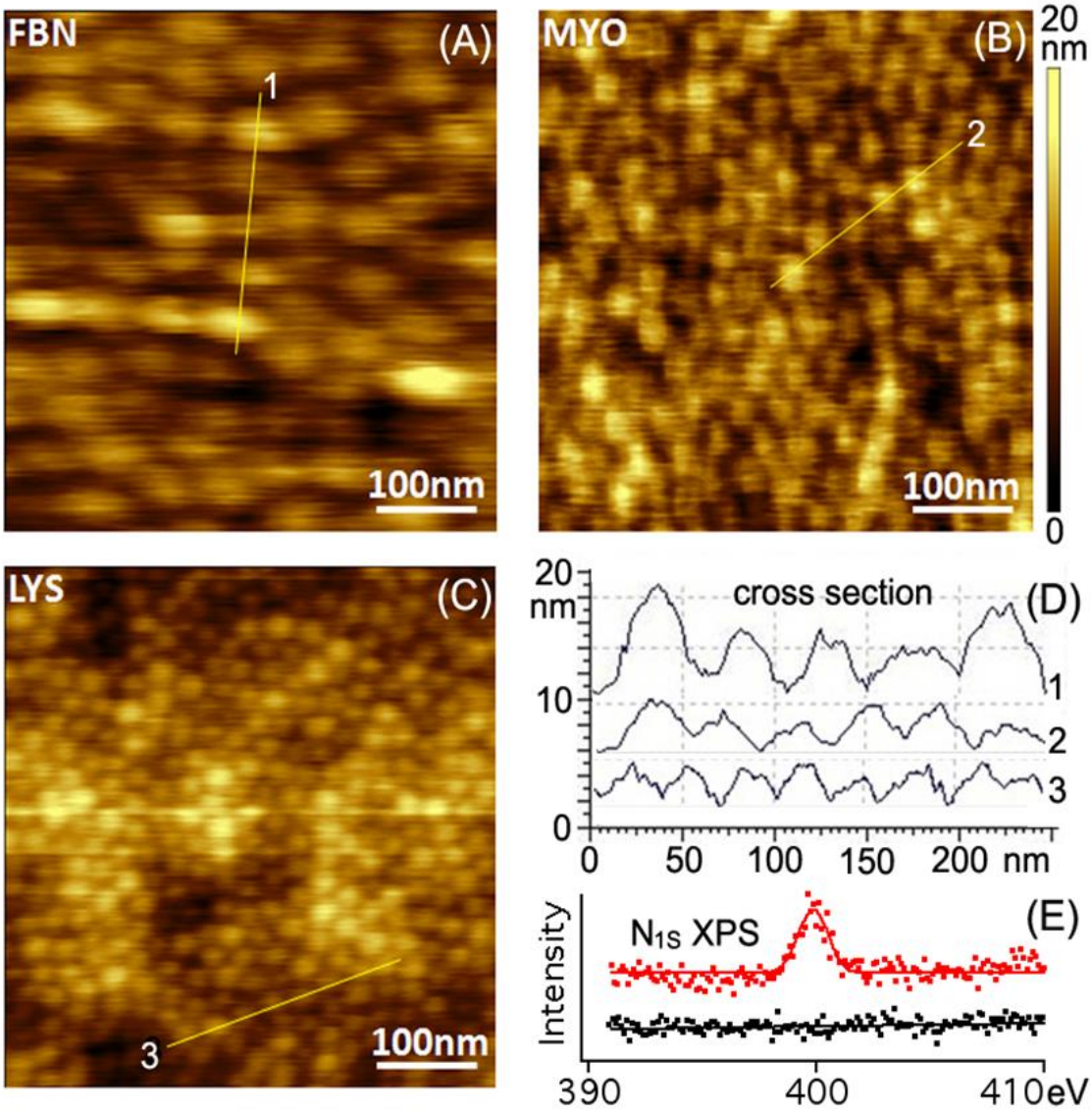

Figure 2.7. *AFM height images taken under aqueous solution of (A) FBN, (B) MYO, and (C) LYO immobilized on the PS-b-PHEMA block-copolymer thin film surface.* Panel (D) shows three cross sectional profiles (height vs. lateral distance) of the three images. Panel (E) compares XPS spectra (intensity vs. binding energy) in the N1s region of the PS-b-PHEMA block-copolymer thin film surface after reaction with azide tagged FBN in the presence (red) or absence (black) of Cu(I) catalyst for click chemistry.

The percentage of nitrogen element for the protein nanoarray is less than that for protein clusters and islands on PS (**Table 2.1**).

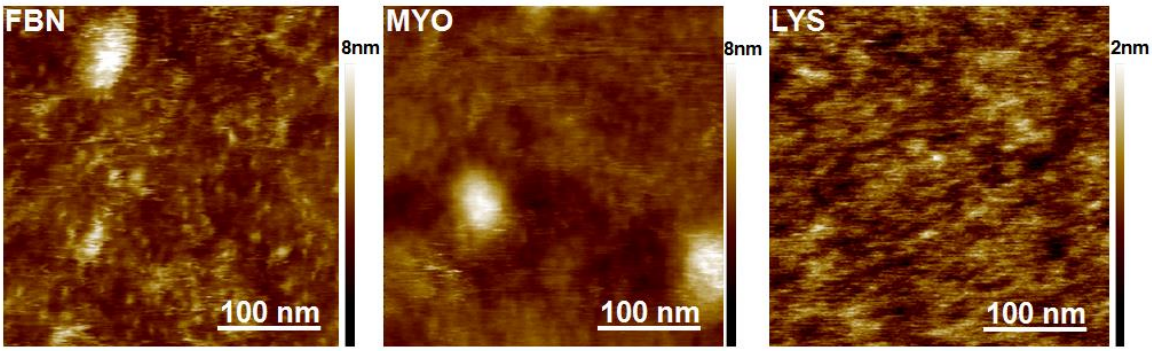

Figure 2.8. *AFM height images taken under aqueous solution of FBN, MYO, and LYO immobilized on the hydrophobic PS thin film surface*.

	Fibrinogen	**Myoglobin**	**Lysozyme**
Polystyrene	8.1%	5.0%	5.0%
PS-b-PHEMA	6.0%	2.0%	1.3%

Table 2.1. *The percentage of nitrogen signal of XPS data for fibrinogen (FBN), myoglobin (MYO) and lysozome (LYS) protein nanoarrays on PS-b-PHEMA and clusters of these proteins on PS surface*.

We use the well-known antigen/antibody pairs, i.e., FBN/anti-FBN, MYO/anti-MYO, and LYS/anti-LYS, to test the biological activity of the resulted protein nanoarray. **Figure 2.9** shows the SPR spectrum of the antibody binding process. It is clearly seen that the protein nanoarrays could capture their corresponding antibodies, which indicates that the immobilized antigen proteins keep their activity and interact with antibodies directed against their epitopes. The next step will be the quantitative analysis of antibody detection using such protein nanoarray. To summarize, we demonstrate the formation of two-dimensional nanoarrays of individual protein molecules using an ordered nano-pattern of a PS-*b*-PHEMA diblock copolymer thin film. The polymer surface is repulsive to nonspecific protein and stable in an aqueous environment. We show the specific

immobilization of azide-tagged protein molecules only to the alkyne-functionalized PS cylinder domain in repulsive PHEMA matrix. The self-assembly strategy allows the easy formation of nanoarrays of individual protein molecules on a large scale and may find wide ranging applications, such as biosensing and assaying, biomaterials, and mechanistic cell biochemistry studies.

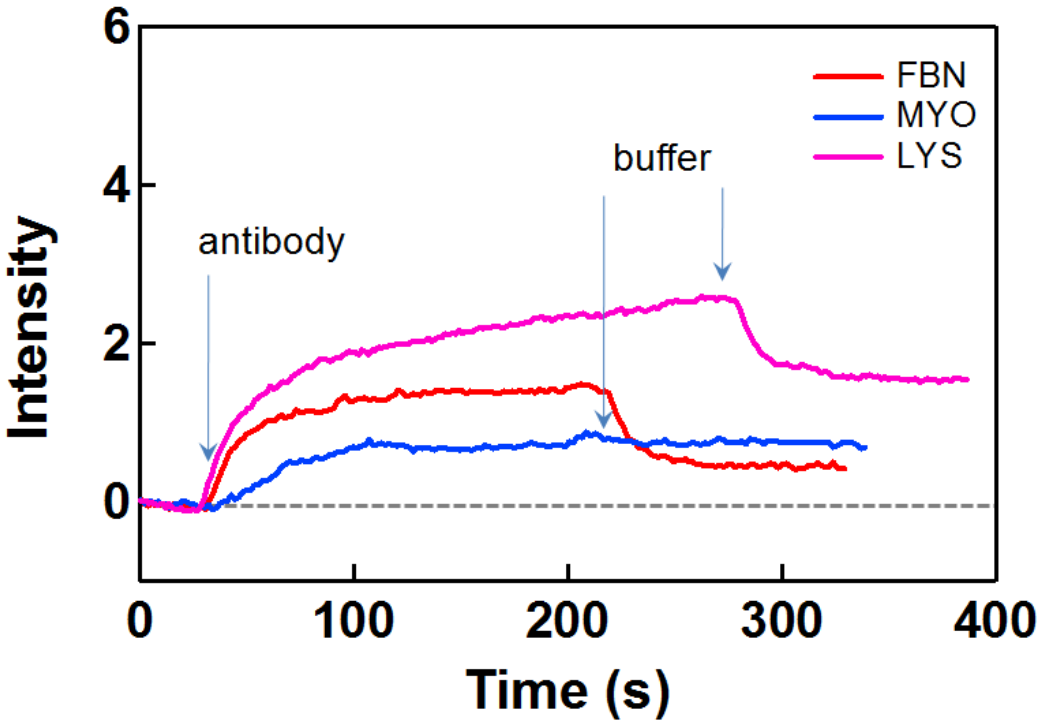

Figure 2.9. *The SPR spectrum of the FBN/anti-FBN, MYO/anti-MYO, and LYS/anti-LYS antigen/antibody binding process*.

2.5. HIS-GFP DENATURATION AND REFOLDING

2.5.1. Linker Synthesis

Based on these results, a system which permits more control over protein conformation was designed. While the azide functionalized proteins are capable of being immobilized onto specific areas, their orientation on the surface is random depending on where the azide moiety is. To control the orientation of the immobilized protein, a specific single attachment site must be present. One such commonly used binding moiety is the six histidine tag (6xHis) binding with copper/iminodiacetate (Cu-IDA) system.[116] For this process, the protein is usually functionalized during the recombinant synthesis. A nucleotide sequence representing a series of six histidine units is inserted into the mRNA code for the protein. The 6xHis tag is typically placed at either the C or N terminus of the protein to provide accessibility and to minimize disruption of tertiary structure. These histidine residues are capable of forming a complex with a Cu(II) ion bound to the nitrilotriacetate ion. This complex is quite stable and is capable of immobilizing the modified protein to the Cu-IDA group and whatever the Cu-IDA group is attached to.

An ideal candidate for monitoring protein folding is the green fluorescent protein (GFP). GFP fluoresces green when exposed to blue light, but only if it is in the well natured state. When the internal fluorophore is exposed to water due to the denaturation of the protein the fluorescence becomes quenched. The fluorescence of the protein provides a clear signal as to whether the protein is natured or denatured. In addition, GFP can be easily synthesized via recombinant synthesis to contain the 6xHis tag at the N-terminus. This 6xHis functionalized GFP (His-GFP) is commercially available.

To complete the setup a means of functionalizing the diblock copolymer with Cu-IDA groups is required. A linker was chosen containing an azide moiety at one end and an iminodiacetic acid (IDA) group at the other linked by 9 repeat units of ethylene glycol.

An azide terminated OEG with 9 repeat units of ethylene glycol was found to be commercially available. From this starting material it is only a single step esterification with the acyl chloride derivative of nitrilotriacetic acid to form the final azide-IDA linker. The synthesis is shown in Scheme 2.1.

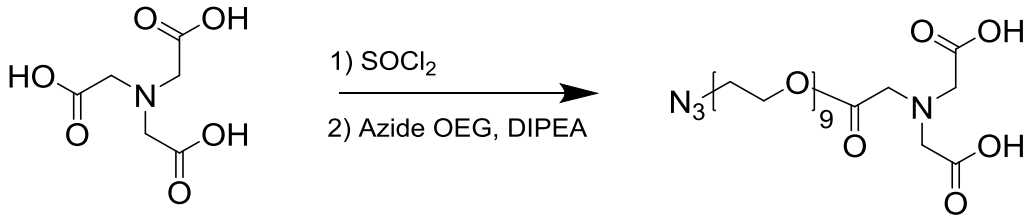

Scheme 2.1. *Synthesis of azide-IDA linker.*

2.5.2. Immobilization of His-GFP

A similar method to the protocol for attaching the azide functionalized proteins was used to attach the Cu-IDA linker to the surface. The method for immobilization of the His-GFP onto the modified PSA-PHEMA surface is shown in **Figure 2.10 A**. Binding of the His-GFP to the modified surface was monitored by SPR as shown in **Figure 2.10 B**. The high final SPR response shows the strong coverage of the protein on the modified surface. Control experiments without the linker present show no adsorption of His-GFP. This shows not only that the presence of the linker is critical, but also that the film is resistant to non-specific adsorption of His-GFP over these timescales.

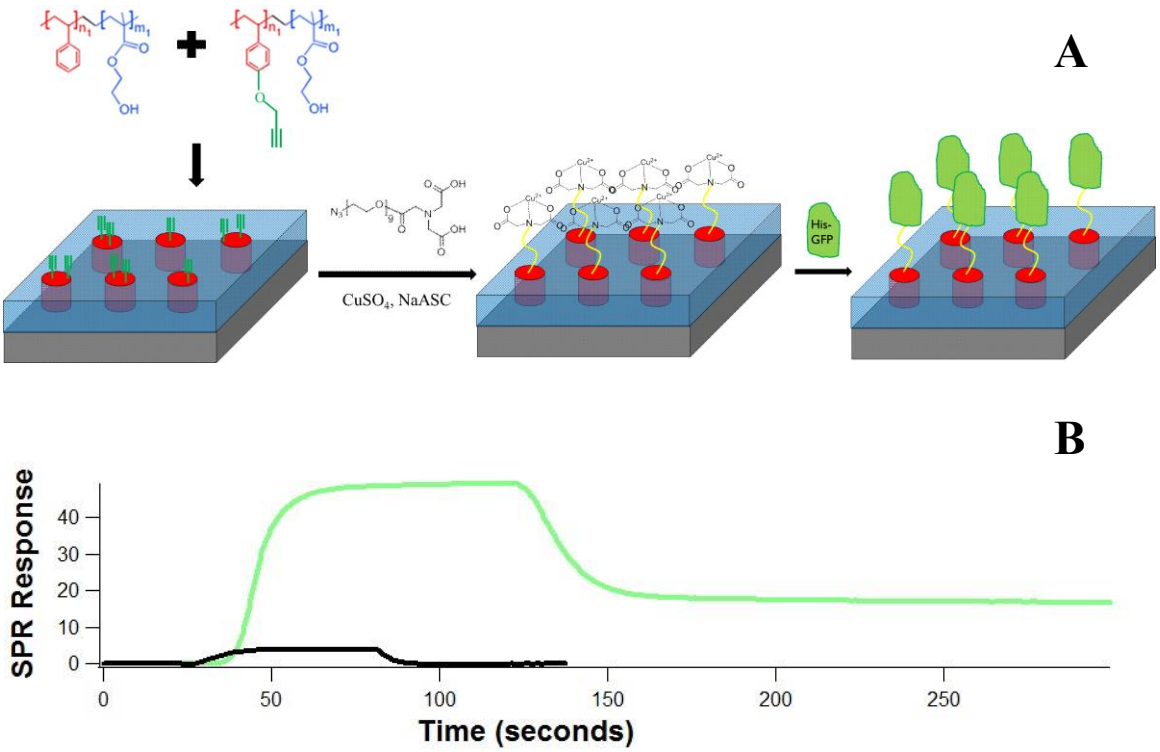

Figure 2.10. *Immobilization of His-GFP.* A) Modification of the alkyne copolymer thin film and subsequent immobilization of His-GFP. B) SPR showing the binding of His-GFP to the modified surface (green) and the control on the film without the linker present (black).

2.5.3. Denaturation and Refolding of His-GFP

After showing that the His-GFP could be immobilized on the surface, experiments were begun to show its ability to unfold and refold while immobilized. A drop of His-GFP in PBS buffer solution was spotted onto the Cu-IDA diblock to allow for binding to take place. If the spot was simply rinsed away with buffer afterwards, the observed fluorescence was found to be concentrated heavily on the periphery of the spot with very weak fluorescence in the center. This is due to the so called "coffee ring effect" whereby the protein concentration along the periphery of the droplet is increased by capillary flow as the solvent evaporates.[117] To produce a more uniform spot of fluorescent protein, the droplet was drained after spotting with a micropipette. The fluorescence experiments are shown in **Figure 2.11**. The protein is kept under a meniscus of solvent at all times. To

denature the protein, the meniscus (originally PBS buffer solution) is exchanged with DI water. The lack of salts and mild acidity of DI water causes the protein to unfold and the fluorescence of the interior structure to be quenched. Exchanging the DI water meniscus with PBS buffer solution causes the protein to refold and fluorescence to be restored. This was cycled several times with no significant loss in fluorescence intensity. This in and of itself suggests two possibilities: the close proximity of the proteins to one another at this size scale does little to harm the proteins' ability to refold, or that the DI water solution only denatures the protein enough to quench the fluorescence. Further experimentation will be required under more stringent denaturing solutions to determine an explanation for these results.

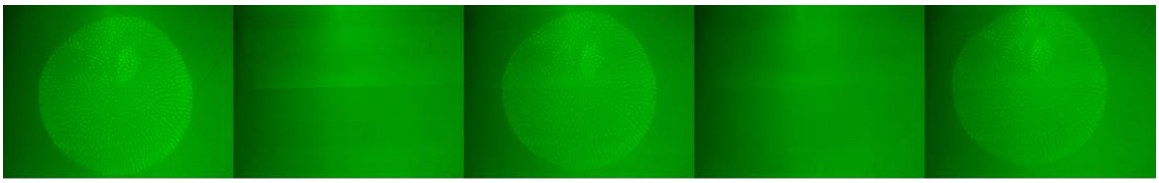

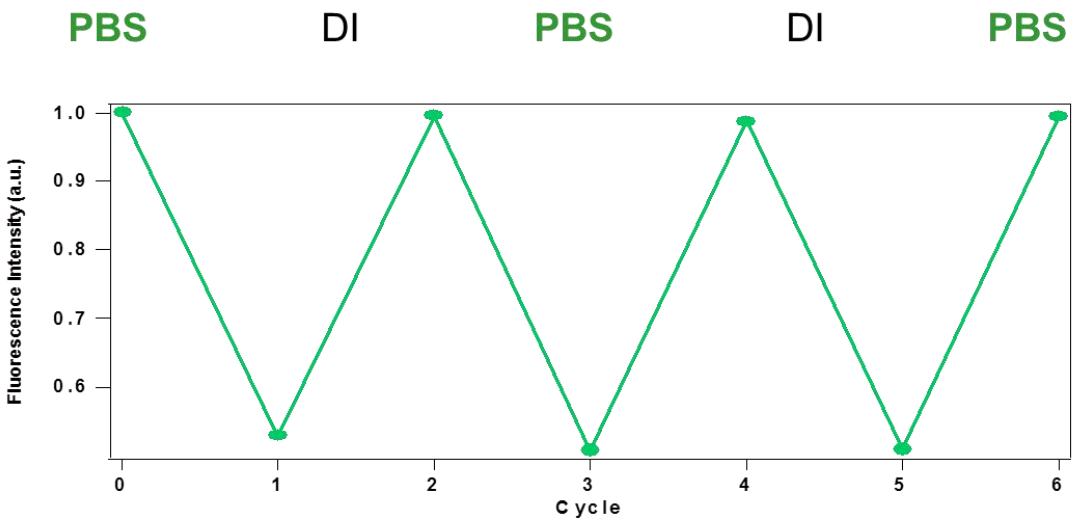

Figure 2.11. *Fluorescence loss and recovery for His-GFP immobilized on the modified IDA-PSA-PHEMA surface*.

2.5.4. Non-Covalent Linker Immobilization

Control experiments on the nature of this setup revealed an unfortunate and unexpected scenario. First, it was shown that the presence of the IDA groups is critical to the binding of the protein. Two samples in which the linker was attached to the surfaces were treated identically except that one film was treated with the azide-OEG starting material while the other was treated with the azide-OEG-IDA linker. After exposure to His-GFP solution, fluorescence was only visible on the film with the IDA groups present indicating that the 6xHis tag is was binding to the Cu-IDA group. However, when a PS-PHEMA film with no surface alkyne groups was treated with the azide-OEG-IDA linker, fluorescence was observable and recoverable. This suggests strongly that the linker is not attaching only to the PS domains, but also inserting into the PHEMA matrix.

The method of attachment to the PHEMA domains is uncertain, since it must be strong enough to tether a protein to the surface. It is unlikely that the linkage is covalent since the only linkage point capable of doing this would be the carboxylate groups of the Cu-IDA. If this were to happen, the Cu-IDA group would no longer be available for protein binding and no fluorescence would be observed. If some linkers are covalently bound while others are not then it may be possible to remove the weakly attached linker either before or after the exposure of His-GFP to the surface. Surfactants such as TWEEN have been shown to be capable of removing non-specifically adsorbed protein from a surface.[118] Following binding, a surfactant of this type could be used to remove any proteins that are not attached strongly to the surface. Alternatively, it may be possible to connect the linker to the protein before the click chemistry. This may hinder the linker's ability to imbed itself into the PHEMA domains.

2.6 CONCLUSIONS AND FUTURE DIRECTIONS

To the best of our knowledge, this work demonstrates the first time that whole proteins have been immobilized to diblock copolymer films of this type. It has been clearly demonstrated that the proteins are covalently bound to the surface and retain enough of their tertiary structure to be recognized by their respective antibodies. It has also been shown that fluorescent protein can be used to signal the state of the protein in the folded or unfolded state while immobilized to such a diblock copolymer film.

The non-covalent immobilization of the His-GFP to the PSA-PHEMA may be hindered or prevented by washing of the surface with a surfactant such as TWEEN following His-GFP binding. This will likely remove weakly bound proteins and their linkers from the surface. Afterwards, studies may be undertaken to understand the role of the spacing of the proteins between each and their ability to refold following denaturation. This may be accomplished by adjusting the sizes of the blocks of the copolymer to create domains that are spaced further apart. Care must be taken during this process to ensure that only one protein is immobilized per domain. If this is an issue it may be corrected by shrinking the size of the PSA domains by once again tuning the size and ratio of the blocks of the copolymer. This may provide valuable information into the formation of amyloid plaques.

Furthermore, studies may be performed to examine the role of the distance from the proteins to the surface in their ability to refold after denaturation. The closer the proteins are to the surface the more they will interact with it during denaturation and refolding. By shortening the length of the linker, interaction with the amphiphilic surface can be increased. This may yield insight into the ability of the heterogeneous inner surface of chaperone proteins to assist proteins in the refolding process.

Acknowledgement. This work was supported by the US Army Research Office (W911NF-08-1-0287 to XYZ) and the Robert A. Welch Foundation (F-1621 to CWB).

2.7 EXPERIMENTAL METHODS

Polymer thin film preparation

The PS_{60}-*b*-$PHEMA_{150}$ (M_{PS} = 6200, M_{PHEMA} = 20500, and M_w/M_n = 1.18) diblock copolymer was obtained from Polymer Source, Inc, and used as received. PSA_{40}-*b*-$PHEMA_{240}$ (M_w/M_n = 1.3), which contains alkyne-functionalized polystyrene (PSA), was synthesized by atom-transfer radical polymerization (ATRP) from 1-((prop-2-yn-1-yloxy)methyl)-4-vinylbenzene and 2-hydroxyethyl methacrylate.. PS_{60}-*b*-$PHEMA_{150}$/PSA_{40}-*b*-$PHEMA_{240}$ mixtures (4:1 wt) were dissolved in THF with concentration of 1.0 wt%, over 1 day at least to reach completely dissolution before use. The polymer thin films were obtained by spin-coating the polymer solutions (1.0 wt%) onto gold substrate at 3000 rmp for 60s, followed by solvent annealing in $CHCl_3$/methanol (1:1 v:v) vapor for 4 h. In the following, we refer this mix thin film as PS-b-PHEMA for short.

Proteins

Fibrinogen from human plasma (FBN), myoglobin from equine skeletal muscle (MYO), and white egg lysozome (LYS) were purchased from Sigma-Aldrich with purity ≥ 98%. The sizes of their native state in solution are 50×7×7, 4×3.5×2, and 3×3×2, respectively. Phosphate buffer saline (PBS) was freshly prepared using sodium and potassium salts (NaCl, KCl, Na_2HPO_4 and KH_2PO_4) to give pH 7.4 at 25 °C. Protein solutions were prepared in such PBS buffer at a concentration of 50 μg/mL immediately

before use. Imidazole-I-sulfonyl azide hydrochloride was synthesized according to the procedure of Goddard-Borger et al..[119] Azide functionalized proteins were prepared according to the procedure of van Dongen et al..[120] His-GFP with modification at the N-terminus was made by recombinant expression in E. Coli by Athena Guo and was used as received.

Click chemistry

Azide-protein was linked to the PS-*b*-PHEMA surface as the following protocol: fresh CuSO4 (6 mg/mL) and sodium ascorbate (6 mg/mL) solutions were mixed (10 µL: 10 µL); 25 µL N3-protein solution (2 mg/mL) was added into the mixture and the yellow precipitates were spun down (~8000rmp); the remaining clear solution was spotted on PS-b-PHEMA surface and incubated in a humidified chamber for 6 h. Finally, the samples were rinsed with PBS buffer.

Azide-OEG-OH (product P6741-EGOHN3, M_n=480 Da, M_w/M_n=1.35) was purchased from polymersource.com and used as received. MW Azide/Cu-IDA linker was attached to the PS-*b*-PHEMA surface according to the following protocol: fresh CuSO4 (6 mg/mL) and sodium ascorbate (6 mg/mL) solutions were mixed (10 µL: 10µL); 25µL of 5µg/mL linker solution was added into the mixture and the yellow precipitates were spun down (~8000rmp); the remaining clear solution was spotted on PS-b-PHEMA surface and incubated in a humidified chamber for 6 h. Finally, the samples were rinsed with DI water.

Liquid Atomic Force Microscopy (L-AFM)

The surface morphology of film was imaged by scanning force microscope (SFM) using a commercial AFM (Agilent Technologies 5500) in the MAC mode. The sample in a water cell was three-dimensionally moved by a scanner. A silicon cantiliver (spring

constant 42 N/m and resonance frequency 50 kHz) was applied for the scan at a scan rate of 1.5 Hz. The A/A_{free} value was set to 0.95, where A is the set point amplitude and A_{free} is the free oscillation amplitude, sometimes lower to obtain high contrast images.

X-ray photoelectron spectroscopy (XPS)

All XPS measurements were carried out on a Kratos AXIS Ultra DLD model with an Al K_α X-ray anode at an analyzer path energy of 80 eV. The total average time for each spectrum (N_{1s} region) was approximately 5 min.

Surface Plasmon Resonance (SPR)

All SPR spectra were recorded on a SPRimagerII (GWC Technologies Inc.) spectrometer at room temperature (23 ^{o}C). Initially, the sample substrate was equilibrated in the PBS buffer (pH 7.4) at a flow rate of 3 μL/s. Once a stable background was obtained, protein PBS buffer solution was injected into the cell at the same flow rate. The SPR signals for 16 parts (0.5 × 0.5 mm^2 each) on the sample substrate (18 × 18 mm^2) were measured and averaged as a function of time until they reached a plateau. Then, the original PBS buffer solution was injected to replace the protein solution and to wash away the weakly bound proteins. From the value change of the SPR baseline, the absorption amount of objects can be calculated.

2.7.1. Synthesis of Cu-IDA Linker

Azide-OEG-CuIDA linker (**1**)

Nitrilotriacetic acid (510 mg, 2.67 mmol) was placed in a roundbottom flask with stirbar. $SOCl_2$ (10 mL) was added. A condenser was attached. Solution was kept at reflux with stirring overnight. $SOCl_2$ was removed in vacuo. A deep red waxy solid resulted. Solid was dissolved in $CHCl_3$ (10 mL) and added to a roundbottom flask. DIPEA (1 mL)

was added. Azide-OEG-OH (0.5 mL at 1 mg/mL in $CHCl_3$) was added to the solution dropwise. Solutions were stirred at room temperature for 24 h. Solvents were removed in vacuo. TLC shows absence of starting material and the formation of a new material as well as unreacted NTA (Rf values, 1:1 Hexanes/EtOAc: SM@0.3, Product@0.5, NTA@0.0)

H^1 NMR (300 MHz, $CDCl_3$) δ: 0.82 (t, 2H, J_1=J_2=6.6) 1.22 (s, 6H), 2.29 (t, 2H, J_1=J_2=7.6), 3.34-3.38 (m, 2H), 3.61 (s, 36H), 4.17-4.21 (m, 2H)

MALDI-MS (m/z): [M+Na^+] calcd. for $C_{28}H_{52}N_4O_{16}$ 723; Found 723. [M+H2O+Na^+] calcd. for $C_{28}H_{54}N_4O_{17}$ 741; Found 741.

Chapter 3. Protein Binding to Functionalized Lipid Bilayers

3.1. INTRODUCTION

The interplay between lectins and their sugar substrates is involved in several essential biological processes, including cellular communication, immune system response, and reproduction.[121] Unfortunately, studying this type of binding has proven quite difficult. Unlike protein-protein binding, where the sequences of both proteins are directly templated by the DNA, glycolipid synthesis is not templated by the cell. Instead, cells produce a wide class of various glycolipids. Cells change the composition of this vast array of glycolipids on their surfaces to accomplish a wide variety of goals, including indication of cell type, internal processes, and intercellular communication.[121] Proteins known as lectins are used by cells as the typical transduction route for interpreting information presented by another cell's surface glycan composition. Compared with protein-protein binding strength, most individual protein-sugar binding interactions are quite weak. One on one binding interactions between a lectin and monomeric sugars usually involve K_d's in the millimolar range.[122,123] For this reason, multiple lectins on the surface of a cell are recruited to a lectin in order to initiate a strong binding interaction (K_d<$1x10^{-8}$M). The result is an extremely complex system of interactions based not on the presentation of a single binding motif, but on a recipe of various glycolipids and glycoproteins. Small changes to the glycolipid composition of the cell membrane can mean drastic changes for the types of cells, antigens, and pathogens it interact with.

One of the most important biological pathways which depend heavily on interpreting a cell's surface glycan composition is that of the immune system. The immune response begins with the dendritic cells. The dendritic cells are responsible for

locating pathogens and bringing them to the bone marrow for T-cell identification and replication. Dendtritic cell specific ICAM-3 grabbing non-integrin (DC-SIGN) is a membrane protein found in high concentrations in dendritic cells. It is the primary lectin by which dendritic cells recognize pathogens. This protein has recently gained attention for its role in the proliferation of HIV. HIV contains a membrane protein known as gp-120 which is covered with various high-mannose residues. DC-SIGN binds to these high-mannose residues and transports the virus to T-cells bearing the CD4 membrane protein. This interaction facilitates transmission of the virus into the T-cells where viral replication can take place. The virus is capable of both direct infection of the dendritic cell and of infecting T-cells once the infected dendritic cell arrives. Understanding the exact mechanism of the initial binding to DC-SIGN will aid in our understanding of the life cycle of the virus as well as the development of new AIDS treatments.

Much research has been done to uncover the way in which DC-SIGN interacts with HIV glycoprotein. The hope is that there may be a way to disable DC-SIGN in an HIV positive patient without compromising the patient's immune system. Hijazi et al. showed that the presence of DC-SIGN greatly increases the binding strength between HIV glycoprotein and CD4.[124] Langerin, another lectin present in dendritic cell membranes, did not show this affect although its overall roll in the immune system response is very similar to DC-SIGN. Understanding the way in which DC-SIGN interacts with high mannose residues can reveal much about what differentiates it from other lectins. In addition, understanding the way in which several weakly binding glycans interact with DC-SIGN may give insight into the synthesis of new tightly binding ligands which deactivate DC-SIGN and yet leave Langerin active. This would theoretically disable the route by which HIV replicates while leaving the body's ability to recognize other pathogens largely intact.

The study of proteins' interactions with sugars has historically been performed using glycan microarrays.[125] A typical example of such an array would involve the irreversible immobilization of the sugar in question onto a solid surface after which a solution of protein could be flowed across the surface and binding can be quantified. While this is generally sufficient for a qualitative analysis of binding kinetics, solid-phase assays do not accurately represent the *in vivo* environment. Solid surfaces are quite foreign to the body and are rarely involved in *in vivo* protein binding. Sugars immobilized on a solid surface are incapable of long range motion and cannot form the patterns required for tight binding. The local density of the sugars in the binding assay must be very high in order to permit the tight binding interaction in the immobilized state. While the average glycan density may be qualitatively set, the local density of binding sites on the size scale of the binding protein can be very difficult to control using solid-phase microarrays. One of the more common approaches involves the functionalization of a protein (usually BSA)[126] with the intended sugars and then non-specifically adsorbing the protein onto a hydrophobic surface. While the concentration of sugar-functionalized protein in solution can be easily manipulated, the surface concentration of exposed sugars is difficult to precisely determine. Not only that, but the number of sugars per protein is not easy to control is usually held fixed.

A lipid bilayer such as the cell membrane allows for great variation not only in the total concentration of exposed sugars but in the nanoscale surface density of sugars. A glycan microarray constructed from a functionalized lipid bilayer would have several advantages over the solid phase methods common today. First, it allows for improved control over the total glycan density. While it is difficult to control the extent of non-specific protein adsorption in the solid phase array described, lipid bilayers may be formed from controlled mixtures of functionalized and non-functionalized lipids. This

allows for multiple surface concentrations to be tested for a clearer and more complete understanding of the binding interaction. Second, the fluid mosaic nature of the lipid bilayer permits 2D diffusion of the glycans. Unlike the immobilized solid phase system, a fluid substrate allows for the recruitment of multiple sugars in a similar fashion to what occurs naturally in a cell membrane. This allows for stronger surface binding interactions than if the sugars were fixed. Finally, a lipid bilayer is more representative of the *in vivo* environment than a solid phase array. While the solid phase systems are often adequate for a qualitative assessment of binding, the results are difficult to relate to the true *in vivo* mechanics of the interaction. Few if any glycan/protein interactions occur at a solid/liquid interface *in vivo*. A lipid/liquid interface system will provide results that yield additional insight into the nature of these binding interactions that cannot be determined using solid phase systems.

Surface plasmon resonance imaging (SPR) was chosen as the detection method. While several methods exist for the quantification of binding to a surface, most require chemical labeling to either the lectin or the substrate to detect the binding event. One of the primary goals of this study is to replicate the *in vivo* environment as closely as possible. The introduction of foreign transduction moieties further removes the system from *in vivo* and makes our findings less meaningful. For this reason, a label-free method was preferred. Also, unlike most solid state methods such as ELISA which are capable of only quantifying the amount bound protein, SPR enables analysis of binding kinetics in real time. This allows for a much deeper understanding of the binding interaction as it is taking place.

3.2. GLASSIFICATION OF SURFACES

Complete lipid bilayers are only capable of forming on hydrophilic surfaces. Due to the hydrophobic nature of gold and the fact that it is required for SPR, a hydrophilic coating of some sort needed to be formed on top of the gold film. Self-assembled monolayers (SAMs) are commonly used to modify gold surfaces with a variety of functionalities. A SAM formed with a hydrophilic head group of some kind resembles in many ways the outer leaf of a lipid bilayer.[127,128] While so called "hybrid bilayers" are easily formed on gold, they do not accurately represent the behavior of a complete lipid bilayer. The underlying SAM must be formed with very high quality if the overlaid lipid bilayer is to form properly. This limits the use of SAMs for this purpose since the stability of alkanethiol SAMs on gold in oxygenic environments is limited.[129]

Phillips et al. developed a method for the deposition of nanoscale glass films on top of gold thin films for the purpose of forming lipid bilayers for use in SPR experiments.[130] The method is shown in **Figure 3.1**. A layer by layer (LBL) deposition is performed on a SAM modified gold surface by alternating exposure to polyallylamine hydrochloride (PAH) and sodium silicate solution. The positively charged PAH associates favorably with the negatively charged carboxylate groups on the SAM, forming the first layer. On top of the PAH, basic sodium silicate solution favorably interacts with the polymer. This process was repeated until the appropriate thickness was obtained. Baking the films in an oxygenic environment caused the removal of PAH and underlying SAM, leaving behind solid glass.

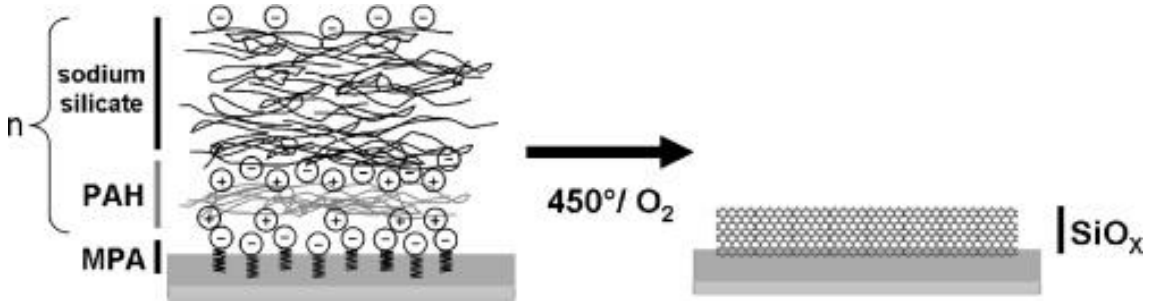

Figure 3.1. *Layer by layer glassification process*.[116]

While this technique was used with limited success, the variability in the quality of the glass surfaces was difficult to control. Chips were made with 5, 10, and 20 layers of PAH/sodium silicate. The 10 layer films seemed to provide the best physical stability and were thick enough to cover all underlying gold while still giving acceptable SPR signal. Formation of the lipid bilayer by exposure to a solution of lipid vesicles can be monitored by SPR. This process is shown in **Figure 3.2.**

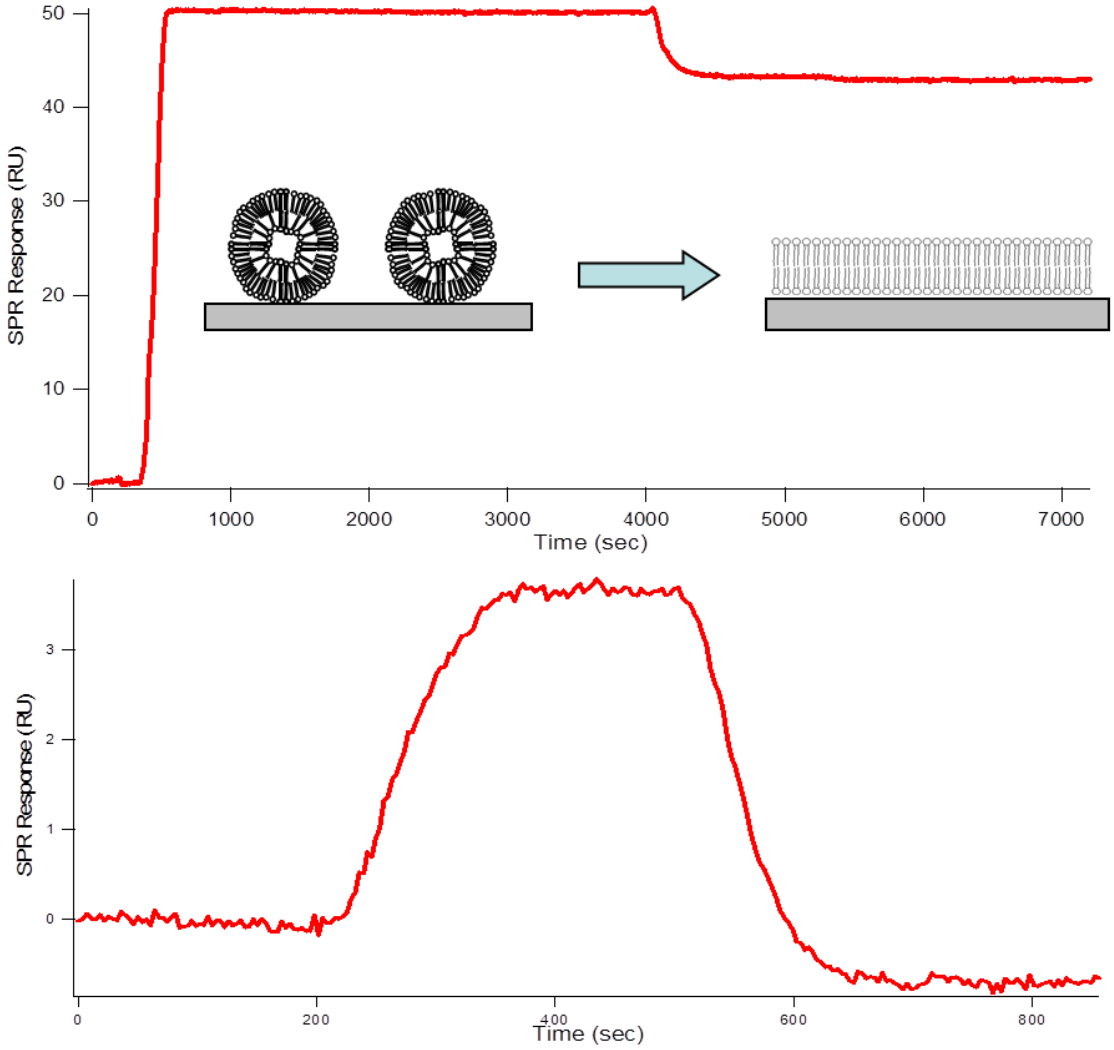

Figure 3.2. *Lipid bilayer formation monitoring via SPR*.

Fluorescence recovery after photobleaching (FRAP) was performed on the films to determine the quality of the supported lipid bilayer on glass. A typical FRAP experiment is shown in **Figure 3.3**. A wide variance in calculated diffusion coefficients was observed. While several showed acceptable diffusion (1-5μm2/s), most had a very large immobile lipid fraction (>60%) or showed no detectable diffusion. Control experiments on glass microscope coverslips consistently showed acceptable diffusion.

Minute changes to the conditions during the LBL deposition (pH, solution concentration, and deposition time) had dramatic effects on the quality of the resulting glass film, resulting in a lack of uniformity between batches. Not only that but the variance within individual batches was observed to be quite high. This may have been due to the positioning of the SAM chips on the ceramic rack used for solution deposition. To obtain highly reproducible results, a new method for glassification was sought.

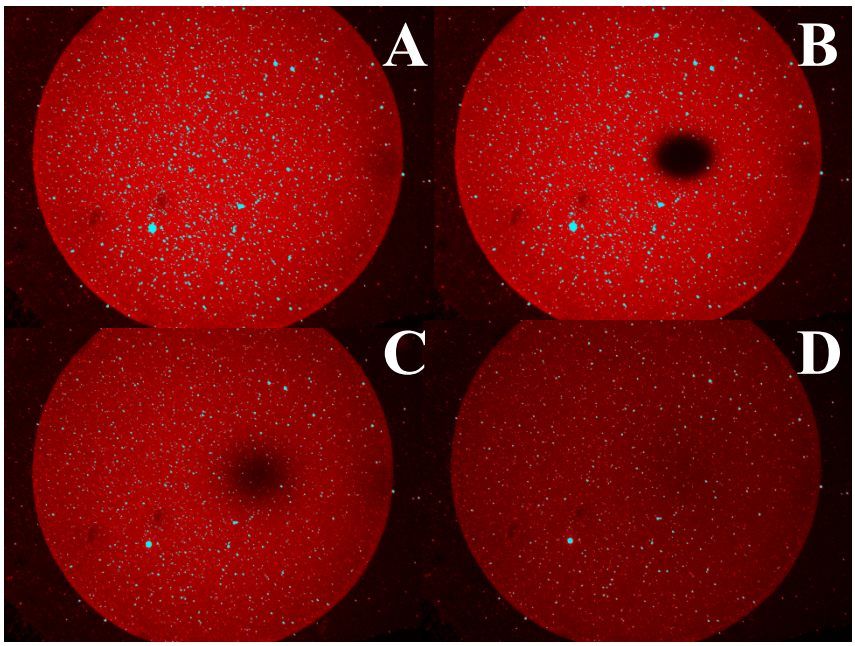

Figure 3.3. *FRAP performed on a fluorescently labeled lipid bilayer*. A) Before bleaching. B) Immediately after bleaching. C) 20 minutes after bleaching. D) 2 hours after bleaching.

Inductively coupled plasma chemical vapor deposition (ICP/CVD) can be used to deposit various materials as high quality thin films of ~2nm roughness.[131,132] Briefly, the technique creates a plasma of a material and then uses charged plates to create a potential which moves the plasma into contact with a substrate. The cool temperature of the substrate compared to the plasma causes it to solidify on the surface of the substrate as a very flat and uniform coating. Silane gas combined with oxygen gas in the presence of an

electric current produces a silicon-oxygen plasma. When this plasma is brought into contact with a gold substrate, a coating of silicon oxide is formed on the surface of the gold. It was found that the silicon oxide had little affinity for the gold surface and was easily damaged by exposure to aqueous environments. A 1nm coating of chromium on top of the gold layer previous to silicon oxide deposition provide sufficient adhesion between the underlying gold and the deposited silicon oxide.

Such a system can be easily used to demonstrate the binding between a lectin and its glycan substrate. However, a higher throughput system can be made using this surface as a starting point. Photolithography is commonly used to make patterns of a wide variety of shapes and sizes on substrates with very high levels of feature control. It was determined that photolithography would be used to change the simple glass surface into an array for monitoring multiple substrates. **Figure 3.4** shows the process of array fabrication. The method produces shallow circular wells with bare glass substrate at the bottom of each. The walls of the wells and remaining surface are made from thermal deposition of chromium, forming a hydrophobic well with a hydrophilic floor. Smaller wells allow for a larger number of samples to be run at the same time. However, there are also issues with stability of the solution spots during bilayer formation which place a minimum on the size of the wells. Experimentation showed that minimum size to be around 2mm in diameter. Though the glass coated chip could be covered with these wells, only around 16 would fit into the 1cm SPR flow cell at a time.

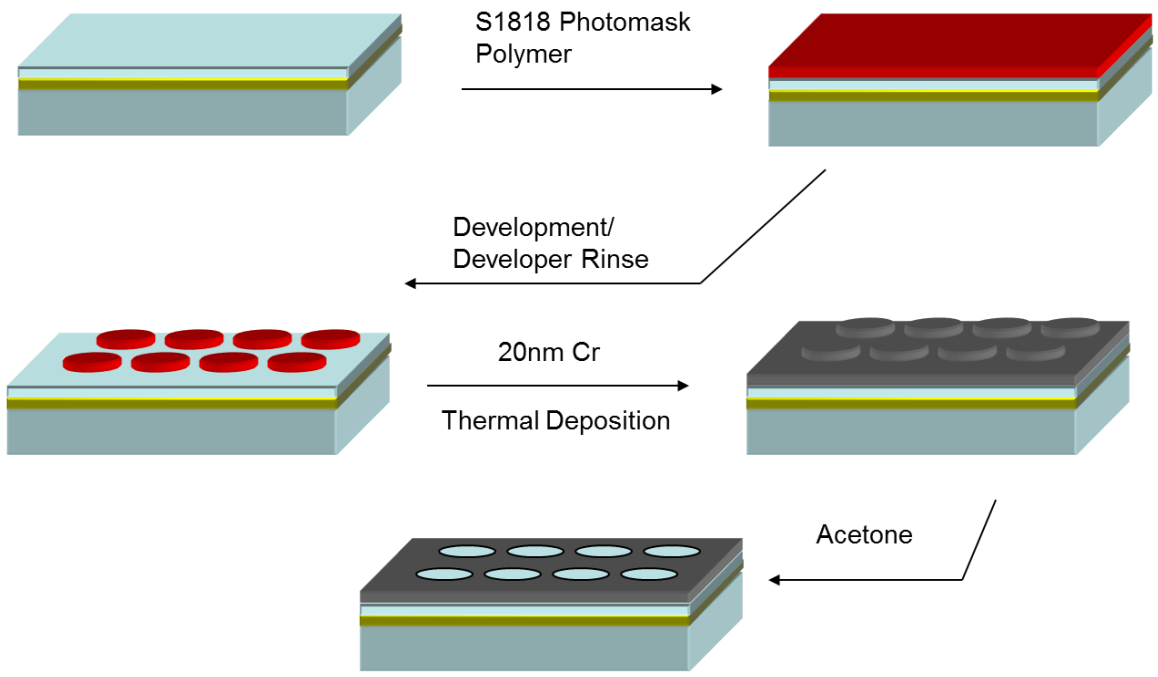

Figure 3.4 *Schematic of the array fabrication.*

3.3. Results and Discussion

3.3.1 CTB/GM1 Binding Assessment

The performance of the array was first tested for efficacy using the cholera toxin subunit B (CTB) and monosialotetrahexosylganglioside (GM1) binding motif. CTB is the recognition unit of cholera toxin which is responsible for binding to glycan GM1 found on the surface of endothelial cells. This binding interaction has been well studied and characterized.[133] It is among the strongest lectin/glycan interactions known, typically showing K_d values in the picomolar to low nanomolar range depending on the setup. This allows for the use of low concentrations of both the lectin and the glycan in the lipid bilayer. Both CTB and GM1 are commercially available at low cost. These factors make the CTB/GM1 system and ideal test platform.

Results from 2 SPR experiments using the array to examine the CTB/GM1 interaction were compiled. For these experiments, lipid vesicle solutions were made using egg phosphatidylcholine and 0.5, 1.0, and 2.5% GM1 functionalized lipids. A control with pure egg phosphatidylcholine was included. These solutions were spotted onto two 16 well arrays with 4 replicates per lipid. A solution of 228nM CTB was passed over the array in the SPR flow cell. The SPR response curves, shown in **Figure 3.5**, show a clear and strong correlation between GM1 content and CTB binding intensity. The final intensity values are shown in **Table 3.1**. The values for intensity per percent of GM1 in the bilayer match each other with a standard deviation of only 0.021.

GM1 Content (%)	**Final Intensity (RU)**	**Intensity per GM1 %**
0.5% GM1	0.54	1.07
1.0% GM1	1.03	1.03
2.5% GM1	2.61	1.04

Table 3.1. *GM1 content and final SPR intensity*.

During the association phase following the introduction of the CTB solution to the system, the SPR response is described by **Equation 2.1**:

$$R = (1 - \exp\{-(k_a C + k_d)t\})k_a C R_{max}/(k_a C + k_d) \qquad \textbf{Eq. 3.1}$$

The SPR response curves during the association phase can be fitted to determine the binding constant (K_d) of the interaction, where $K_d = k_d/k_a$. The data from the 0% lipid bilayer was subtracted from the remaining curves to remove changes in signal due to bulk

refractive index change. The fits are shown in **Figure 3.5**. The K_d values calculated for each curve were 8.8±0.1, 8.1±1.0, and 0.3±1.1 nM for the 0.5, 1.0, and 2.5% GM1 lipid bilayers respectively. The K_d of CTB/GM1 varies greatly depending on the system used to measure it, but the obtained values are well within accepted literature values of the strength of the interaction being in the low nanomolar range.

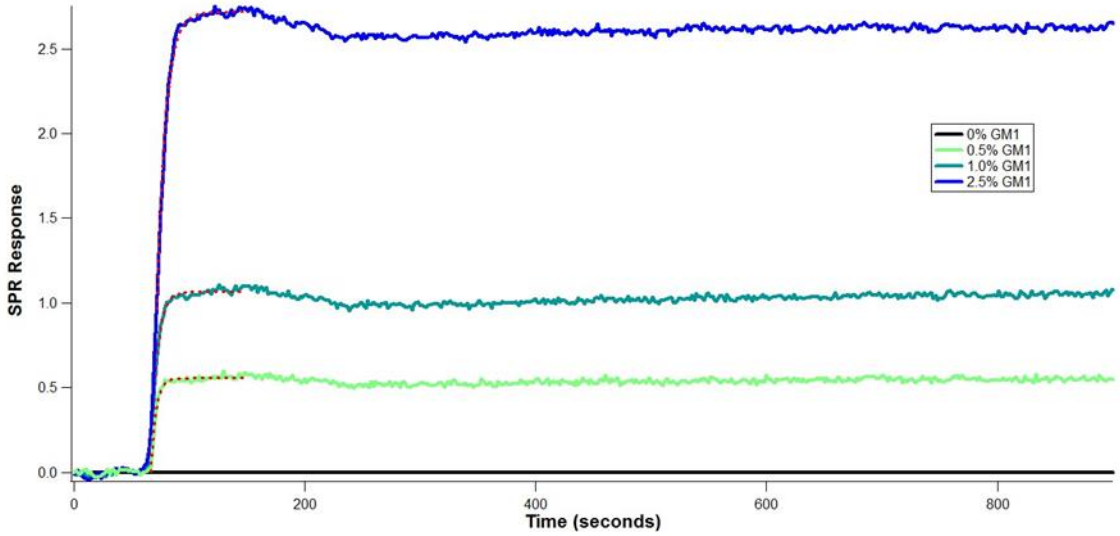

Figure 3.5. *Binding of CTB to GM1-functionalized lipid bilayer at various concentrations of GM1 functionalized lipid*. CTB concentration was set at 228 nM. Curve fits are shown as dotted red lines.

3.3.2. Synthesis and Binding of Mannose Lipid

Having shown that the system is effective with previously studied protein/glycan systems, work began to apply the system towards studying the DC-SIGN/mannose binding interaction. The binding strength between single mannose residues and DC-SIGN is not particularly strong with K_d values reported in the mM range.[134] Strong recruiting will be required for the DC-SIGN to bind well to the surface. To investigate the recruiting ability permitted by the lipid bilayer, a simple mono-mannose lipid was constructed. The

first lipid synthesized was made from amidation of mannosamine and a carboxylic acid-terminated lipid. The resulting lipid **1** was used to form lipid bilayers on the array chip. DC-SIGN solution (655 nM in Tris buffer) was passed over the surface in the SPR flow cell. The results are shown in **Figure 3.6 A**. No binding was detectable even at mono-mannose lipid concentrations as high as 20%. FRAP showed that at concentrations higher than this the 2D diffusion of the lipid bilayer begins to slow and overall bilayer integrity is diminished.

One potential explanation for this is the orientation of the mannose rings in the mono-mannose lipid. Research has shown that for binding to DC-SIGN, mannose groups must present hydroxyls 3 and 4 towards the binding protein.[122] However, in this glycolipid hydroxyls 3 and 4 are not oriented directly outward towards the solution. To correct for this, a new mono-mannose lipid **5** was synthesized. The synthetic route is shown in **Scheme 3.1**. This mono-mannose lipid presents hydroxyls 3 and 4 outward towards solution. In addition, the longer tail connecting the sugar to the lipid provides for increased mobility to allow the sugar to find the proper orientation for stronger binding. The previous SPR experiments were repeated using mono-mannose lipid **5**. The results can be seen in **Figure 3.6 B**. Unfortunately, no binding was seen via the SPR response. The most likely explanation now is the weakness of the binding interaction between mannose and DC-SIGN.

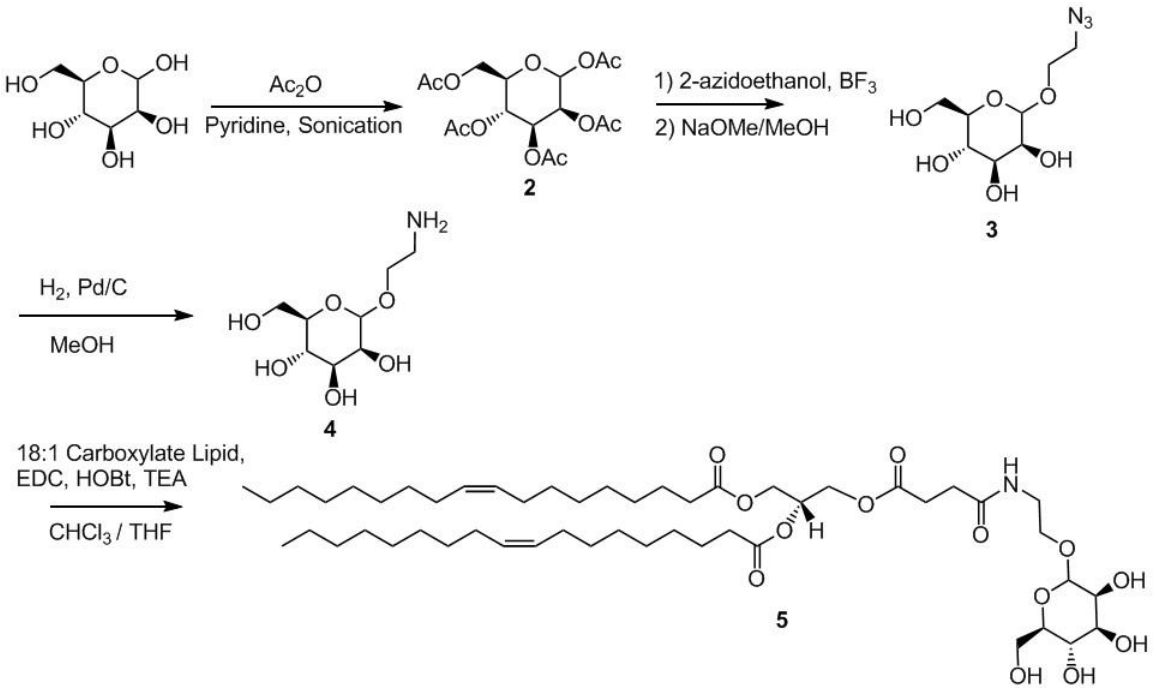

Scheme 3.1. *Synthesis of mannose lipid conjugate*. Carboxylate lipid was purchased from Avanti Polar Lipids and used as received.

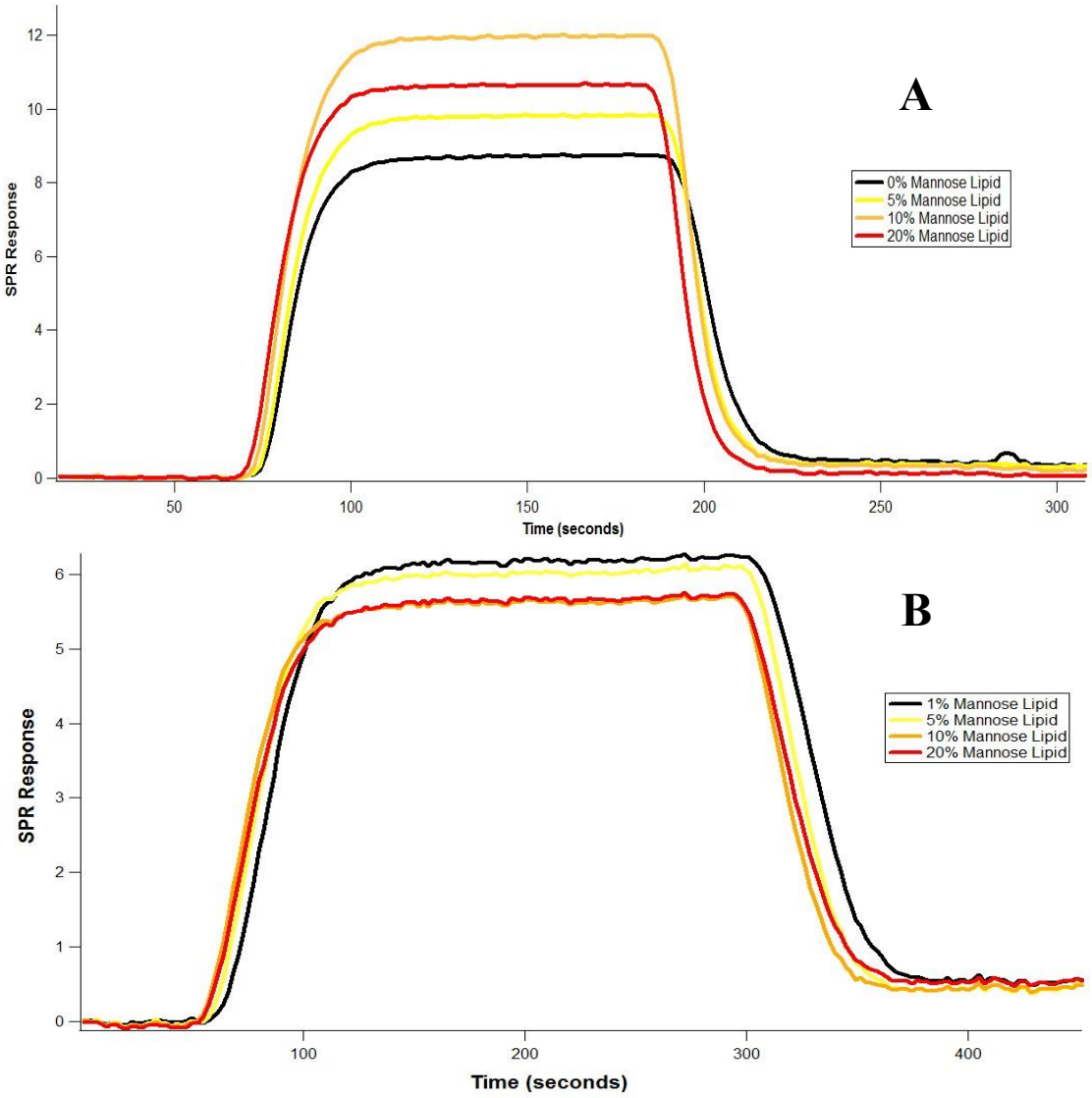

Figure 3.6. *Binding between DC-SIGN and mono-mannose lipids*. A) Binding to lipid **1**. DC-SIGN concentration was 655 nM. B) Binding to lipid **5**. DC-SIGN concentration was 456 nM.

3.3.3. Synthesis and Binding of α-3,6-mannotriose Lipid

To improve the binding strength, a mannotriose based lipid was synthesized. Research has shown that the interaction between DC-SIGN and α-3,6-mannotriose is

stronger than the interaction with mannose.[135] However, it is still only moderate in strength. Recruitment will still be required to show significant binding via SPR.

The synthesis of the mannotriose ligand is shown in **Scheme 3.2**. The Huisgen click reaction binding motif was chosen for the connection of the mannotriose to the lipid. This type of reaction typically proceeds under pH neutral conditions at nearly quantitative yield with no byproducts. It was attempted to improve yields and to simplify the purification process. Unfortunately, the standard Cu(I) catalyzed reaction using a terminal alkyne bearing lipid was never successful. Instead, a Cu(I)-free click route was attempted using a lipid bearing the common strained cyclooctyne moiety. This reaction proceeded in high yield. However, no binding was detected using this motif.

It was decided that the large size of the strained cyclooctyne moiety, which is on the same size scale of the mannotriose itself, was hindering the binding interaction. With the Huisgen based click reaction routes exhausted, a simple amidation reaction was used to couple an amine-bearing α-3,6-mannotriose with a carboxylic acid functionalized lipid. While the reaction runs in lower yields and requires some purification, the amide linker produced is quite small and not likely to interfere with the binding interaction. The SPR binding experiments are shown in **Figure 3.7**. Once again, no binding was detectable via SPR.

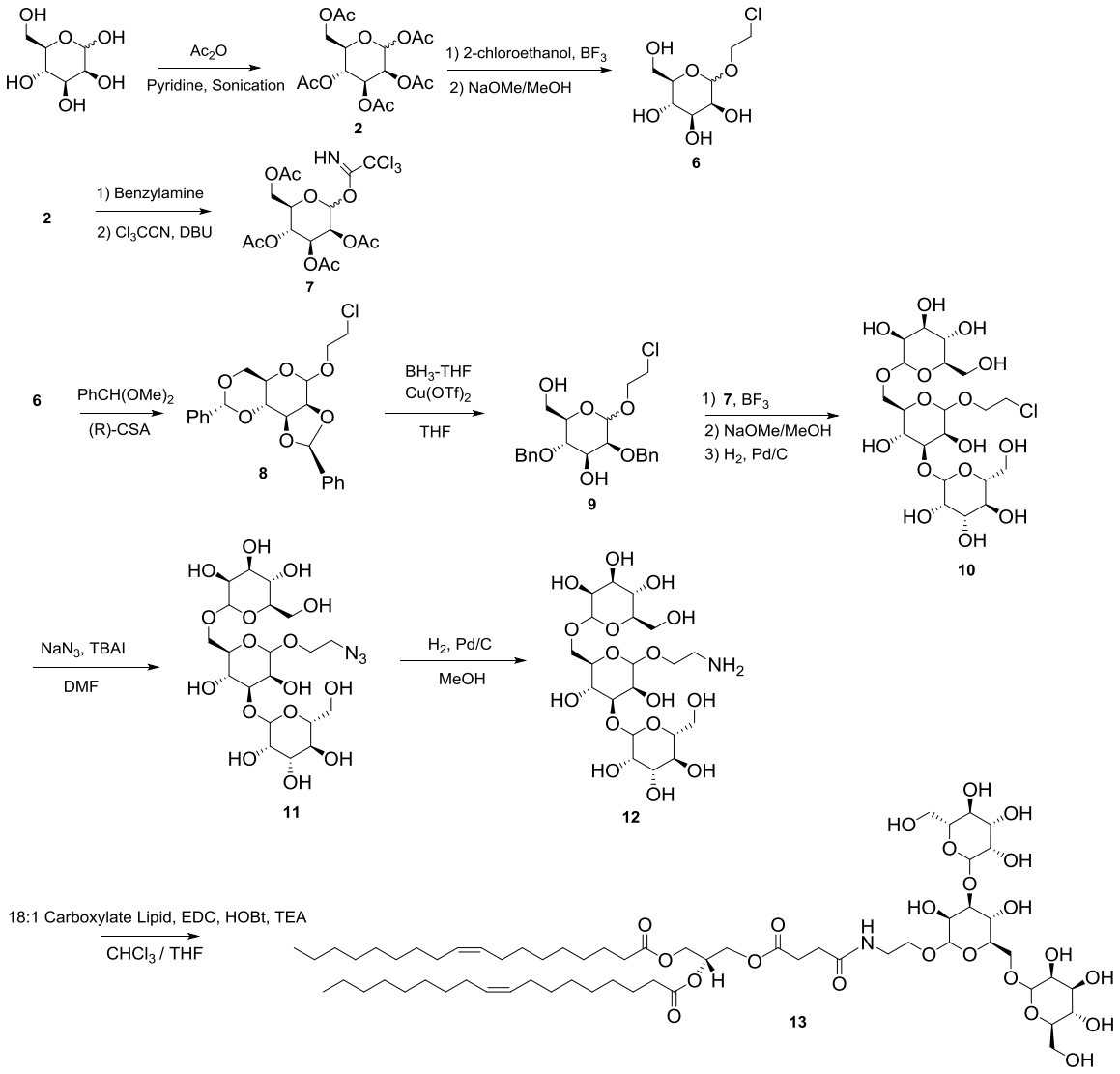

Scheme 3.2. *Synthesis of α-3,6-mannotriose lipid conjugate*.

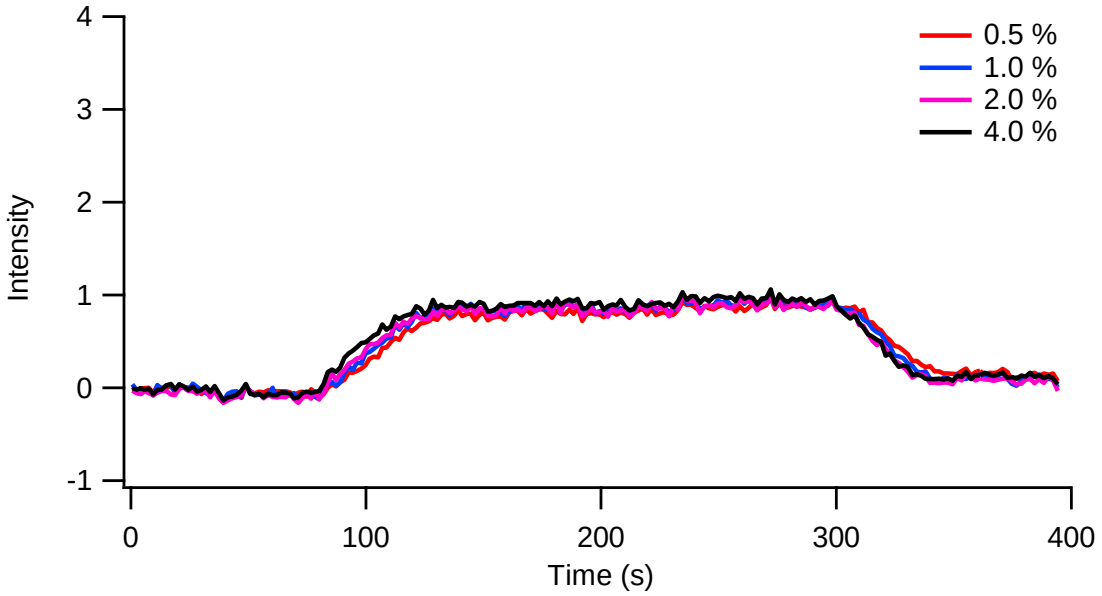

Figure 3.7. *Binding of DC-SIGN to mannotriose functionalized lipid bilayer*. DC-SIGN concentration was 200nM. Mannotriose-lipid concentrations are shown as percent composition of the bilayer.

This was unexpected since a common method of binding DC-SIGN involves using BSA functionalized with α-3,6-mannotriose. What may be the case is that the local concentrations of mannose on mannosyl-BSA covered surfaces are much higher than the ligand density in the lipid bilayer. It may also be the case that impurities not removed by the HPLC are interfering with the binding process. A more complex high density mannose ligand will need to be synthesized to overcome this limitation. Improved purification of product must also be achieved.

3.3.4 Synthesis of High-Mannose Lipids

The high density mannose ligands commonly referred to as Man-6 and Man-9 are currently in the process of being synthesized. The completed steps of the synthesis are detailed in **Scheme 3.3**. This synthetic route has significant overlap with the synthesis of

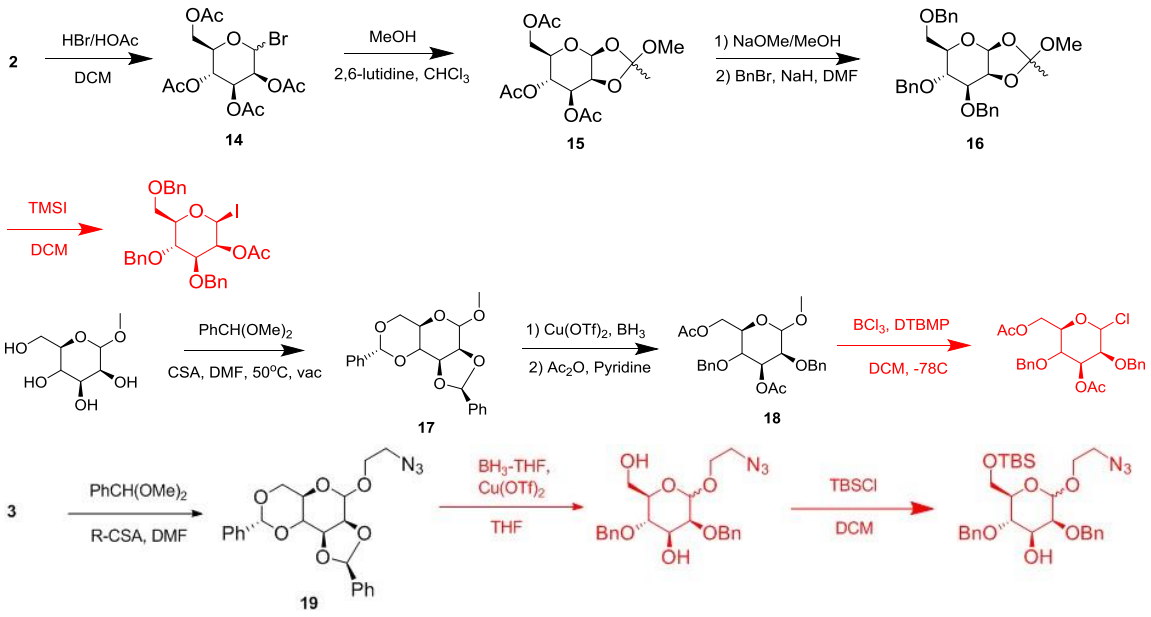

Scheme 3.3. *Synthesis of Man6 and Man9 to date. Uncompleted steps are shown in red.*

α-3,6-mannotriose, so much of the same starting materials and products can be used. The glycosyl donors which have not yet been synthesized are unstable and must be used soon after they are synthesized.

3.4. Conclusions and Future Directions

With this work we have demonstrated that the lipid microarray system developed works as intended. The lipid bilayer formed is stable under the conditions used and is fully capable of quantitative assessment of binding kinetics between lectins and their respective glycan receptors. Recruitment of mannose residues was not effective enough in establishing a significant binding interaction with DC-SIGN.

Future work will include the joining of the monomeric mannose units together to form the high-mannose sugars Man-6 (**Scheme 3.4**) and Man-9 (**Scheme 3.5**) with amine functionality. These functionalized ligands must then be coupled to the carboxylic acid bearing lipid to complete the glycolipid. SPR experiments on the binding of DC-SIGN to

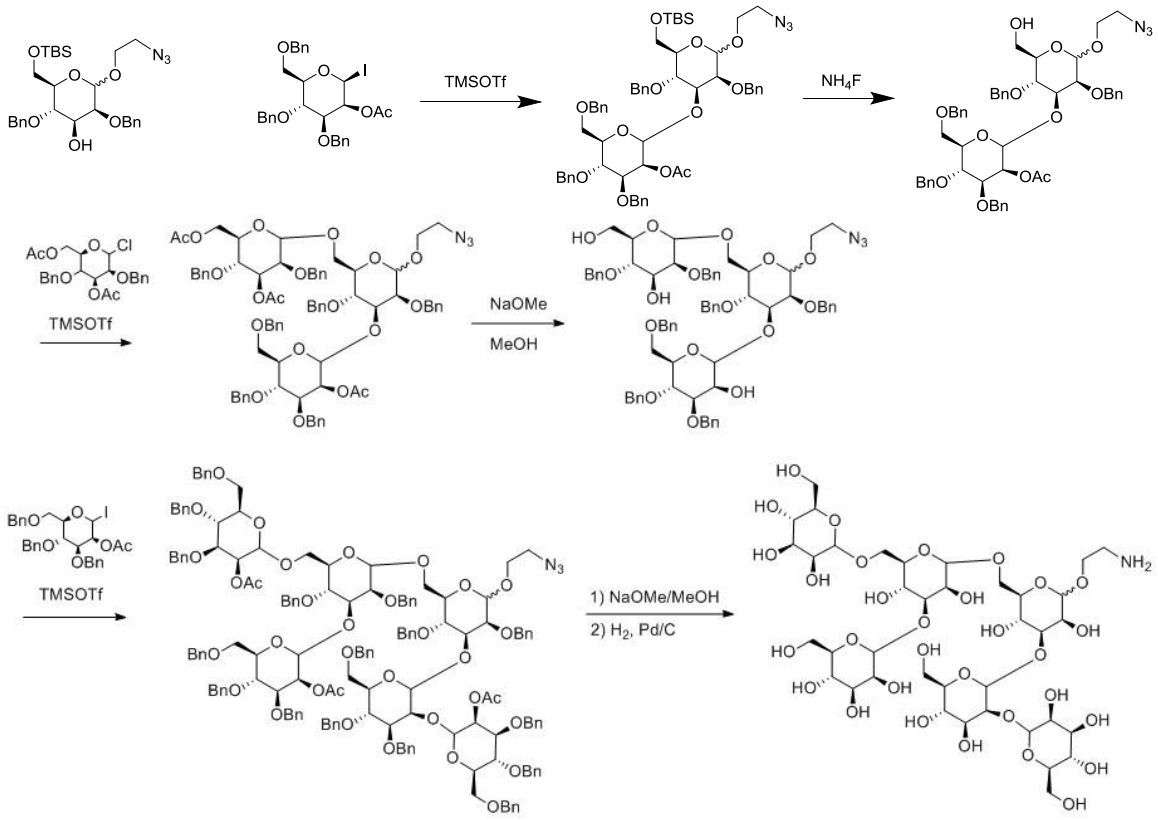

Scheme 3.4. *Proposed synthesis of Man6*.

the synthetic glycolipids in lipid bilayers will then be performed. Should the binding prove to be undetectable using the current method, it may be necessary to use more sensitive SPR equipment. It may be necessary to use more sensitive techniques involving fluorescent labeling such as TIRF to observe the potentially weak interaction.

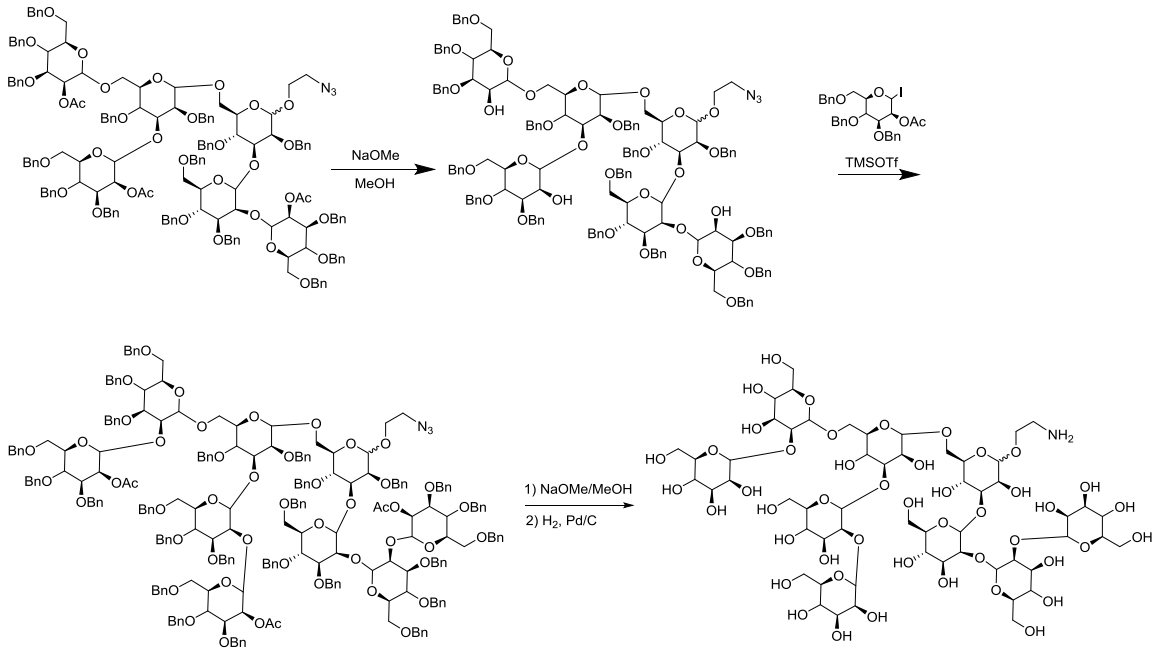

Scheme 3.5. *Proposed synthesis of Man9*.

3.5. MATERIALS AND METHODS

CTB was purchased from Sigma Aldrich and used as received. GM1 functionalized lipid, egg phosphatidylcholine, 18:1 (product 870314) and 16:0 (product 870225) carboxylic acid terminated lipids were purchased from Avanti Polar Lipids and were used as received. All other reagents were purchased from Sigma Aldrich or Acros Chemicals unless indicated otherwise.

XPS

All XPS spectra were recorded using a PHI 5700 ESCA XPS using an aluminum electrode.

SPR

All SPR spectra were recorded on a SPRimagerII (GWC Technologies Inc.) spectrometer at room temperature (23 ^{o}C). Initially, the sample substrate was equilibrated

in the PBS buffer (pH 7.4) at a flow rate of 3 mL/s. Once a stable background was obtained, protein PBS buffer solution was injected into the cell at the same flow rate. The SPR signals for 16 parts (0.5 × 0.5 mm^2 each) on the sample substrate (18 × 18 mm^2) were measured and averaged as a function of time until they reached a plateau. Then, the original PBS buffer solution was injected to replace the protein solution and to wash away the weakly bound proteins. From the value change of the SPR baseline, the absorption amount of objects can be calculated.

HPLC

HPLC was run using a Shimadzu HPLC with a Gemini C18 column (250mm x 10mm, 5μm).

NMR

NMR spectra were obtained using a Varian DirectDrive or Varian INOVA NMR spectrometer. NMR solvents were purchased from Cambridge Isotope Laboratories.

MS and LC-MS

Mass spectra were obtained using a Finnigan MAT-VSQ 700 or DSQ spectrometer. ESI mass spectra were obtained using an Agilent 6350 Accurate-Mass Q-TOF LC/MS.

3.6. EXPERIMENTAL INFORMATION

SPR chip synthesis

A high quality glass microscope slide was cut into small squares using a glass cutter of the proper size to fit into the SPR chip holder. The chips were cleaned for at least one hour in a solution of boiling H_2SO_4/30% H_2O_2 in a 4:1 ratio. After rinsing with DI water, isopropanol, and drying with N_2, a 2nm coating of chromium at 0.1 Å/s followed by 50nm of gold at 0.4 Å/s were deposited on the surface by thermal deposition.

Layer by Layer Glassification

LBL glassification was performed according to a modified literature procedure.[115] 3-mercaptopropionic acid was substituted with 11-mercaptoundecanoic acid to improve SAM quality. PAH pH set to 7.6. At pH 8, as suggested by the literature, a precipitate would form in solution during the deposition process.

ICP/CVD

SPR chips were coated with a 1nm layer of chromium to improve adhesion of the SiO_2 before deposition. Silane gas and NO_2 were introduced into the chamber. Formation of the plasma was sustained for 20 seconds creating a film of approximately 5nm thick as determined by ellipsometry. Si and O content were confirmed by XPS.

Array Fabrication

Glassified SPR chips were spin coated with S1818 positive photoresist polymer at 2000 rpm for 50 seconds. The photoresist coated chips were cured at 100°C for 2 minutes. Chips were developed by UV exposure in a Suss MA6 mask aligner using a photomask designed to shade 2mm diameter circular regions on the photoresist. Developed film was washed with M319 surfactant to remove developed photoresist. Chips were treated with O_2 plasma for 60 seconds to remove residual photoresist. 10nm of chromium were deposited at 0.2Å/s via thermal deposition.. Remaining photoresist was removed by rinsing with acetone. Exposed films were treated with O_2 plasma for 60 seconds to remove residual photoresist.

Lipid Bilayer Preparation

A mixture of functionalized lipid with Egg phosphatidylcholine in chloroform was evaporated w/ N_2. Lipids were dissolved in Tris buffer (50mM Tris + 25mM NaCl, pH 7.8) to a total concentration of 1mg/mL. Solution was passed through a 0.05μm membrane filter 11 times. Solutions were spotted onto the glass surface and incubated in

a humidity controlled chamber at RT for 45 minutes. Chips were then placed into an SPR flow cell and rinsed for 1hr with Tris buffer. The array was then exposed to a 2mg/mL BSA solution to block any area on the chip not covered by the lipid bilayer.

FRAP

A lipid bilayer composed of 0.2% Texas Red® DHPE with Egg PC was prepared as previously described. The chips were removed from the SPR flow cell. Chips were dried on the back side and additional buffer was added to the functionalized side forming a meniscus. Chips were placed onto a microscope slide and a coverslip was placed onto the meniscus. Bilayers were bleached with a Melles Griot Krypton/Argon laser for 10 seconds. Images were taken at regular intervals using a Micros fluorescence microscope equipped with a SPOT RT3 model 25.1 2Mp monochrome camera. Diffusion coefficients were calculated using IGOR Pro curve fitting software.

3.5.1. Synthesis

2-azidoethanol[136] and compounds **2**[137], **3**[138], **7**[136], **14**[139], **15**[136], **16**[136], **17**[140], and **18**[141] were synthesized according to literature procedures. Characterization data matched with literature results.

Mannosamine-Lipid (**1**)

Mannosamine (11 mg, 0.45 mmol) was dissolved in 1.5 mL of anhydrous MeOH. Triethylamine (7.5 μL) was added. 16:0 carboxylate lipid (40 mg, 0.05 mmol) were added to the solution. HOBt (4 mg, 0.03 mmol) were added. EDC (5 mg, 0.03 mmol) was dissolved in $CHCl_3$ (200 μL) and added to the solution. A rice stirbar was added. Solution was stirred at room temperature for 24 h. Solvents were removed by evaporation under N_2. Solids were dissolved in DCM and washed 3x with H_2O. Organics were dried with Na_2SO_4 and concentrated in vacuo.

LRMS (m/z): [M+Cl^-] calcd. For $C_{45}H_{83}NO_{12}Cl$ 864.6; Found 864.2. [M-OH^-] calcd. for $C_{45}H_{82}NO_{11}$ 812.6; Found 812.2

1-(2-aminoethyl)-α-D-mannopyranoside (**4**)

Compound **3** (52 mg, 0.21 mmol) was dissolved in EtOH (1.75 mL) and added to a roundbottom flask. 10% Pd/C (13 mg) was added with a stirbar. System was purged 3x with H_2. System was left with H_2 balloon attached stirring at room temperature 24 h. Catalyst was removed by centrifugation. Solvent was removed in vacuo. Product was acquired in quantitative yield.

^{1}H NMR (400MHz, CD3OD) δ: 1.01-1.05 (t, 2H, J=7.1), 3.16-3.17 (m, 2H), 3.38-3.43 (m, 1H), 3.45-3.51 (m, 2H), 3.53-3.64 (m, 2H), 3.70 (m, 1H), 3.76 (m, 1H), 3.80-3.84 (m, 1H), 4.69 (d, 1H, J = 1.2Hz).

^{13}C NMR (133 MHz, CD_3OD) δ: 16.97, 39.16, 61.27, 67.05, 70.24, 70.83, 73.58, 100.51

Mannose-Lipid (**5**)

Compound **4** (47 mg, 0.21 mmol) was dissolved in MeOH (2 mL) in a roundbottom flask with stirbar. 18:1 carboxylate lipid (50 mg @ 25 mg/mL in $CHCl_3$, 0.07 mmol) were added. TEA (10 μL) was added. HOAt (18 mg, 0.06 mmol) was added. EDC (20 mg, 0.13 mmol) was added. Solution was stirred at room temperature overnight. Solution was washed 3x with DI H_2O. Organics were dried with Na_2SO_4 and concentrated in vacuo.

^{1}H NMR (400 MHz, $CDCl_3$) δ : 0.88 (s, 6H), 1.27-1.30 (m, 40H), 1.61 (s, 4H), 2.01 (m, 8H), 2.29-2.34 (m, 5H), 2.50 (s, 2H), 2.65 (s, 2H), 3.42-3.54 (m, 3H), 3.77-

3.92 (m, 5H), 4.11-4.17 (m, 2H), 4.26-4.34 (m, 2H), 4.81 (s, 1H), 5.25-5.28 (m, 1H), 5.33-5.36 (m, 4H),

^{13}C NMR (133 MHz, $CDCl_3$) δ: 14.09, 22.66, 24.80, 24.82, 24.86, 27.14, 27.19, 28.71, 28.85, 29.02, 29.06, 29.09, 29.15, 29.20, 29.29, 29.50, 29.69, 29.71, 29.74, 31.87, 33.98, 34.12, 34.17, 51.87, 61.97, 62.55, 68.70, 68.77, 129.62, 129.64, 129.65, 129.67, 129.97,

LRMS (m/z): [M+Cl^-] calcd. for $C_{51}H_{91}NO_{13}Cl$ 960.6; Found 959.5. [M+Na^+] calcd. for $C_{51}H_{91}NO_{13}Na$ 948.6; Found 948.0

1-(2-chloroethyl)-α-D-mannopyranoside (**6**)

Compound **2** (5.31 g, 13.6 mmol) was dissolved in DCM (22 mL). 2-chloroethanol (2.9 mL, 2.42 g, 27 mmol) was added. BF_3 etherate (5.9 mL, 48%) was added dropwise with stirring via syringe. Solution was stirred at RT overnight. Solution was transferred to a separatory funnel and washed with sat'd $NaHCO_3$ solution and water. Organics were dried w/ Na_2SO_4 and concentrated in vacuo. 5.70 g of crude product were isolated. Product was dissolved in MeOH (90 mL). NaOMe (3.761 g, 70 mmol) were added. Solution was stirred at room temperature for 2 h. Solution was neutralized with HCl/MeOH.

^{1}H NMR (400 MHz, D_2O) δ : 3.44-3.87 (m, 10H), 4.76 (d, 1H, J = 1.75)

^{13}C NMR (133 MHz, D_2O) δ: 43.2, 60.8, 66.6, 67.6, 69.8, 70.4, 72.8, 99.7

1-(2-chloroethyl)-2,3:4,6-di-O-benzylidene-α-D-mannopyranoside (**8**)

Compound **6** (1.026 g, 4.2 mmol) was combined with anhydrous DMF (16 mL) in a roundbottom flask. R-camphorsulfonic acid (69 mg, 0.30 mmol) was dissolved in anhydrous DMF (3 mL) and added to the mixture. Benzaldehyde dimethylacetal (1.6 mL,

10.4 mmol) was added to the solution. Solution was heated to 50 °C and degassed with stirring under high vacuum. After 30 min, the starting material had fully dissolved. Solution was stirred at 50 °C with periodic introduction of vacuum for 24 h. Additional benzaldehyde dimethylacetal (3.2 mL, 20.8 mmol) was added via syringe and the reaction continued an additional 24 h. Solution was concentrated in vacuo. Solids were dissolved in DCM and washed 2x with $NaHCO_3$. Organics were dried with Na_2SO_4 and concentrated in vacuo. 1.218 g of crude product were isolated (69% yield). Product was recrystallized in isopropanol/ethyl acetate. The crystals were found to be ~88% *endo* product.

^{1}H NMR (400 MHz, $CDCl_3$) δ Endo: 3.63-4.00 (m, 7H), 4.28-4.32 (dd, 1H), 3.35 (d, 1H), 4.51 (m, 1H), 5.24 (s, 1H), 5.53 (s, 1H), 5.97 (s, 1H), 7.33-7.38 (m, 3H), 7.39-7.44 (m, 3H), 7.48-7.51 (m, 2H), 7.53-7.55 (m, 2H).

^{13}C NMR (133 MHz, $CDCl_3$) δ: 60.90, 68.24, 68.32, 73.85, 75.68, 78.35, 80.57, 98.12, 101.95, 104.31, 126.27, 126.43, 126.47, 126.72, 128.40, 128.45, 128.61, 128.68, 129.27, 129.68, 137.11, 137.33

1-(2-chloroethyl)-2,4-di-O-benzyl-α-D-mannopyranoside (**9**)

Compound **8** (241 mg, 0.58 mmol) were transferred to an oven dried vial w/ stirbar. Sample was dissolved in 1M BH_3/THF (5.9 mL) at 0 °C. $Cu(OTf)_2$ in THF (2.6 mL at 69 mM, 0.18 mmol) at 0 °C was added dropwise to this solution. Solution was stirred at 0 °C for 30 min. The reaction vessel was removed from the ice bath and allowed to warm to room temperature with stirring for 70 min. Reagents were then neutralized by dropwise addition of NEt_3/MeOH. Solvent was removed in vacuo and the residues were dissolved in DCM. Organics were washed 3x with H_2O, dried with Na_2SO_4, and concentrated in vacuo.

H^1 NMR (400 MHz, $CDCl_3$) δ: 3.61-3.73 (m, 3H), 3.78 (d, 1H, *J*=2.7), 3.84-3.90 (m, 2H), 4.00-4.03 (dd, 1H, J_1=3.5, J_2=8.7), 4.62-4.71 (m, 3H), 4.85-4.90 (m, 2H), 7.26-7.39 (m, 10H)

^{13}C NMR (133 MHz, $CDCl_3$) δ: 62.17, 67.81, 71.65, 71.98, 73.44, 74.99, 76.21, 78.36, 97.77, 127.91, 127.97, 128.05, 128.08, 128.16, 128.23, 128.55, 128.60, 128.64, 128.72, 137.71, 138.39

LRMS (m/z): [$M+Na^+$] calcd. For $C_{22}H_{27}ClO_6Na$ 445.1; Found 445.0. [$M+Cl^-$] calcd.457.6; Found 457.9

2-chloroethyl O-α-D-mannopyranosyl(1→3)[O-α-Dmannopyranosyl(1→6)]-α-D-mannopyranoside (**10**)

Compound **9** (93 mg, 0.22 mmol) was combined with compound **7** (501 mg, 1.02 mmol) in an oven dried 22mL vial. 4 Å molecular sieves were added. Anhydrous DCM (10 mL) was added as well as a stirbar. The solution was stirred in an ice bath for 20 min. BF_3 etherate (200 μL, 48%) of were added. Solution was allowed to warm to room temperature overnight with stirring. Solution was neutralized with $NaHCO_3$. Organics were dried with Na_2SO_4 and concentrated in vacuo. Solids were dissolved in KOMe/MeOH (6 mL, 2.5 %w/v) and left to react overnight. Solution was neutralized with HCl/MeOH. Solution was concentrated in vacuo and redissolved in H_2O. Aqueous solution was washed with DCM. Aqueous layer was separated, purified via HPLC, and concentrated in vacuo. Solids were dissolved in MeOH (3 mL). 10% Pd/C (6 mg) was added. Solution was degassed and backfilled with N_2. The system was purged 3x with H_2. System was left with an H_2 balloon attached stirring at room temperature 48 h. System was recharged with fresh H_2 and additional 10% Pd/C (5 mg) after 24 h. Catalyst was

removed via centrifugation and solvent was removed in vacuo. 45 mg of product were isolated (36% yield).

^{1}H NMR (400 MHz, D_2O) δ: 3.61-4.14 (m, 22H), 4.05 (dd, 1H, J_1=1.7, J_2=3.4), 4.13 (dd, 1H, J_1=1.9, J_2=2.9), 4.88 (dd, 2H, J_1=1.9, J_2=2.9), 5.09 (d, 1H, J=1.7)

^{13}C NMR (133 MHz, D_2O) δ: 43.29, 60.82, 60.89, 65.12, 65.56, 66.58, 66.65, 68.01, 69.42, 69.81, 69.93, 70.23, 70.47, 71.11, 72.58, 73.22, 78.31,99.20, 99.94, 102.26

HRMS (m/z): [M+Na^+] calcd. For $C_{20}H_{35}ClO_{16}Na$ 589.1514; Found 589.1509.

2-azidoethyl O-α-D-mannopyranosyl(1–~~3~~)[O-α-Dmannopyranosyl(1–~~6~~)]-α-D-mannopyranoside (**11**)

NaN_3 (16 mg, 0.25 mmol), TBAI (2 mg, 0.0054 mmol) and compound **10 (**40 mg, 0.071 mmol) of were added to a glass vial. Solids were dissolved in DMF (1 mL) w/ stirbar. Solution was stirred at 50 °C overnight. Solvent was removed in vacuo. Product was obtained in quantitative yield.

^{1}H NMR (400 MHz, CD_3OD) δ: 3.73-3.464 (m, 2H), 3.54-3.70 (m, 10H), 3.73-3.85 (m, 8H), 3.89-3.90 (dd, 1H, J_1=1.5, J_2=3.4), 3.9-3.93 (m, 2H), 3.94-3.97 (dd, 1H, J_1=1.6, J_2=3.4), 4.03-4.04 (dd, 1H, J_1=1.0, J_2=2.9), 4.79 (d, 1H, J=1.8), 4.81 (d, 1H, J=1.7), 5.01 (d, 1H, J=1.7)

HRMS (m/z): [M+Na^+] calcd. For $C_{20}H_{35}N_3O_{16}Na$ 596.1917; Found 596.1914.

2-aminoethyl O-α-D-mannopyranosyl(1–~~3~~)[O-α-Dmannopyranosyl(1–~~6~~)]-α-D-mannopyranoside (**12**)

Compound **11** (80 mg, 0.14 mmol) was dissolved in MeOH (2 mL). 10% Pd/C (8 mg) was added with stirbar. Solution was degassed under vacuum and backfilled with H_2 twice. System was left stirring with H_2 balloon attached at 45 °C for 48 h. H_2 balloon was

refilled and old catalyst was removed by centrifugation and replaced with fresh 10% Pd/C (7 mg) after 24 h. Catalyst was removed by centrifugation. Solvent was removed in vacuo. Product was obtained in quantitative yield. NMR was found to agree with literature results.[142]

^{1}H NMR (400 MHz, CD_3OD) δ: 3.26 (m, 2H), 3.62-3.84 (m, 11H), 3.87-3.97 (m, 6H), 3.98-3.99 (m, 1H) , 4.00 (d, 1H, J=4.2) 4.03 (d, 1H, J=4.2), 4.07 (m, 1H),, 4.15 (m, 1H), 4.86 (s, 1H) 4.90 (s, 1H), 5.10 (m, 1H),

HRMS (m/z): [M+H$^+$] calcd. For $C_{20}H_{37}NO_{16}$ 548.211; Found 548.218. [M+Na$^+$] calcd. 570.201; Found 570.201

Mannotriose-Lipid (**13**)

Compound **12** and carboxylate lipid were joined by amidation to form **13**. Synthesis was performed by Lei Shen of Columbia University.

1-(2-azidoethyl)-2,3:4,6-di-O-benzylidene-α-D-mannopyranoside (**19**)

Compound **3** (272 mg, 1.09 mmol) was combined with R-camphorsulfonic acid (16 mg, 0.069 mmol) and benzaldehyde dimethylacetal (480 μL, 487 mg, 3.20 mmol) in a glass vial with stirbar. Anhydrous DMF (6 mL) was added. Solution was stirred at 45 °C with periodic degassing for 48 h. After 24h had passed, additional benzaldehyde dimethyl acetal (1 mL) was added. DMF was removed via genevac (3 h at 50 °C). Residues were dissolved in EtOAc and washed DI H_2O followed by 3x with $NaHCO_3$. Organics were dried with Na_2SO_4 and concentrated in vacuo. NMR suggests a mixture of ~1.4:1 in favor of the *endo* product.

^{1}H NMR (400 MHz, $CDCl_3$) δ Endo: 3.24-3.35 (m, 2H), 3.46-3.59 (m, 1H), 3.64-3.90 (m, 4H), 4.24-4.32 (m, 2H), 4.44-4.48 (dd, 1H, J_1=6.3, J_2=7.5), 5.17 (s, 1H), 5.48 (s, 1H), 5.91 (s, 1H), 7.27-7.38 (m, 6H), 7.43-7.53 (m, 4H)

^{13}C NMR (133 MHz, $CDCl_3$) δ: 60.59, 66.57, 68.63, 73.88, 76.91, 78.08, 80.37, 97.72, 101.66, 104.11, 126.06, 126.23, 126.27, 126.51, 128.13, 128.17, 128.37, 128.42, 129.11, 129.43, 136.94, 137.18

LRMS (m/z): [$M+H^-$] calcd. for $C_{22}H_{24}N_3O_6$ 426.2; Found 426.0

Appendix A: NOESY and COSY NMR for Mannotrioses

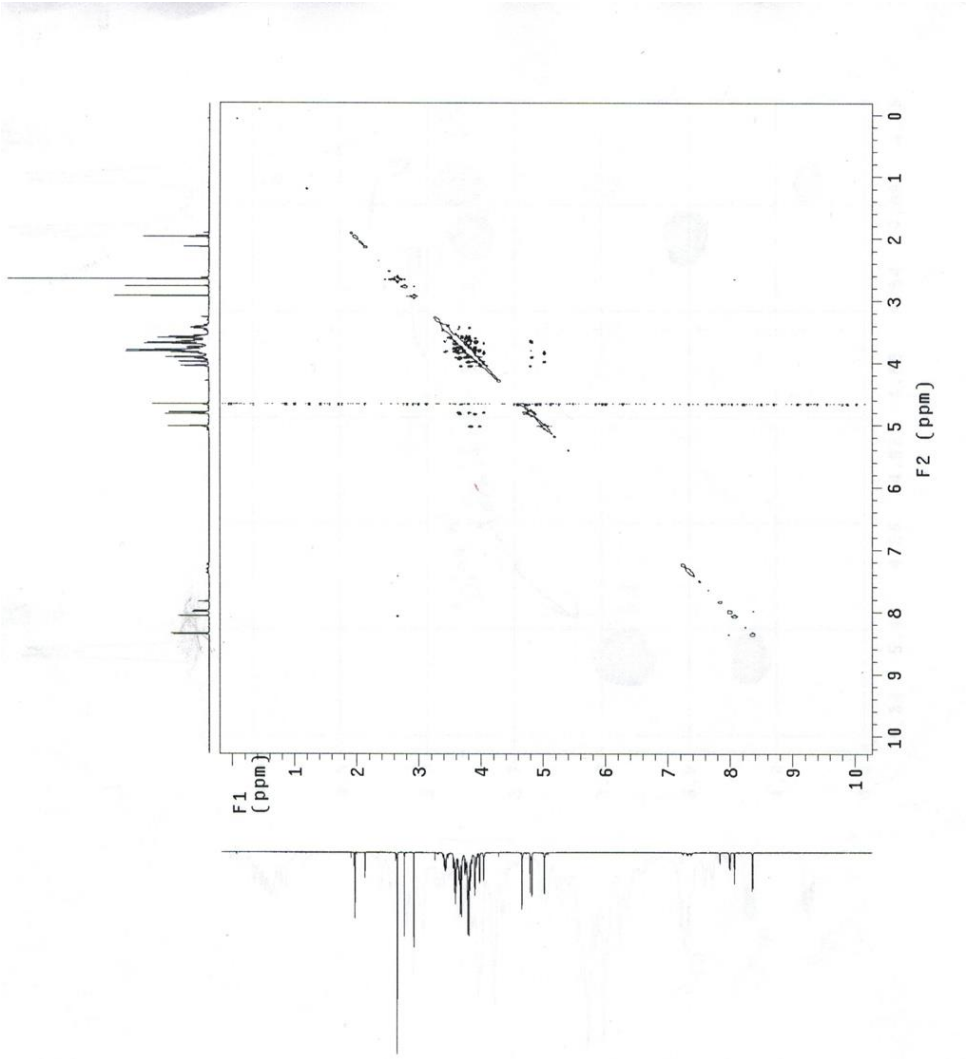

Figure A.1. 500MHz NOESY for azido-α-3,6-mannotriose in D_2O

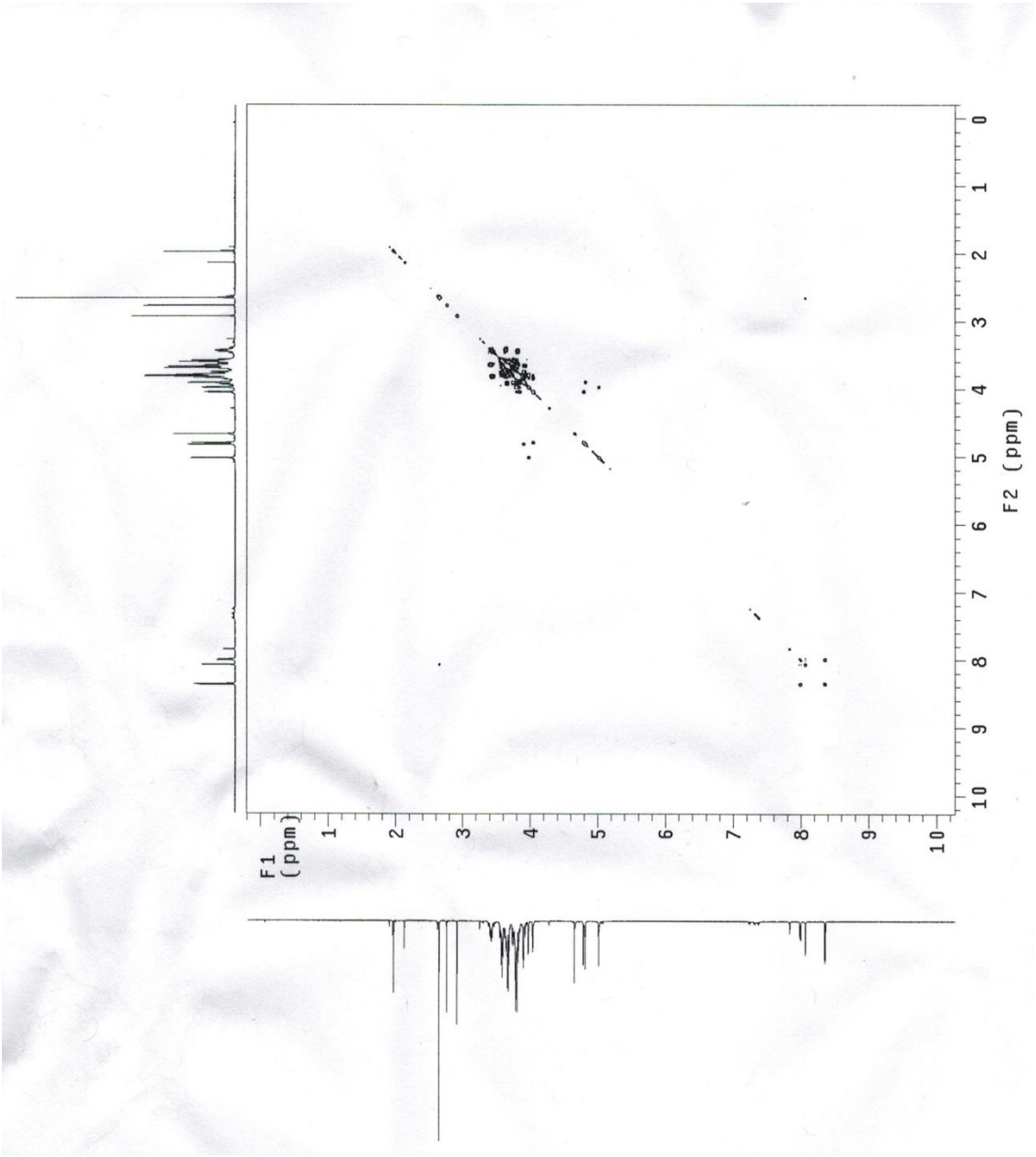

Figure A.2. 500MHz COSY for amino-α-3,6-mannotriose in D_2O

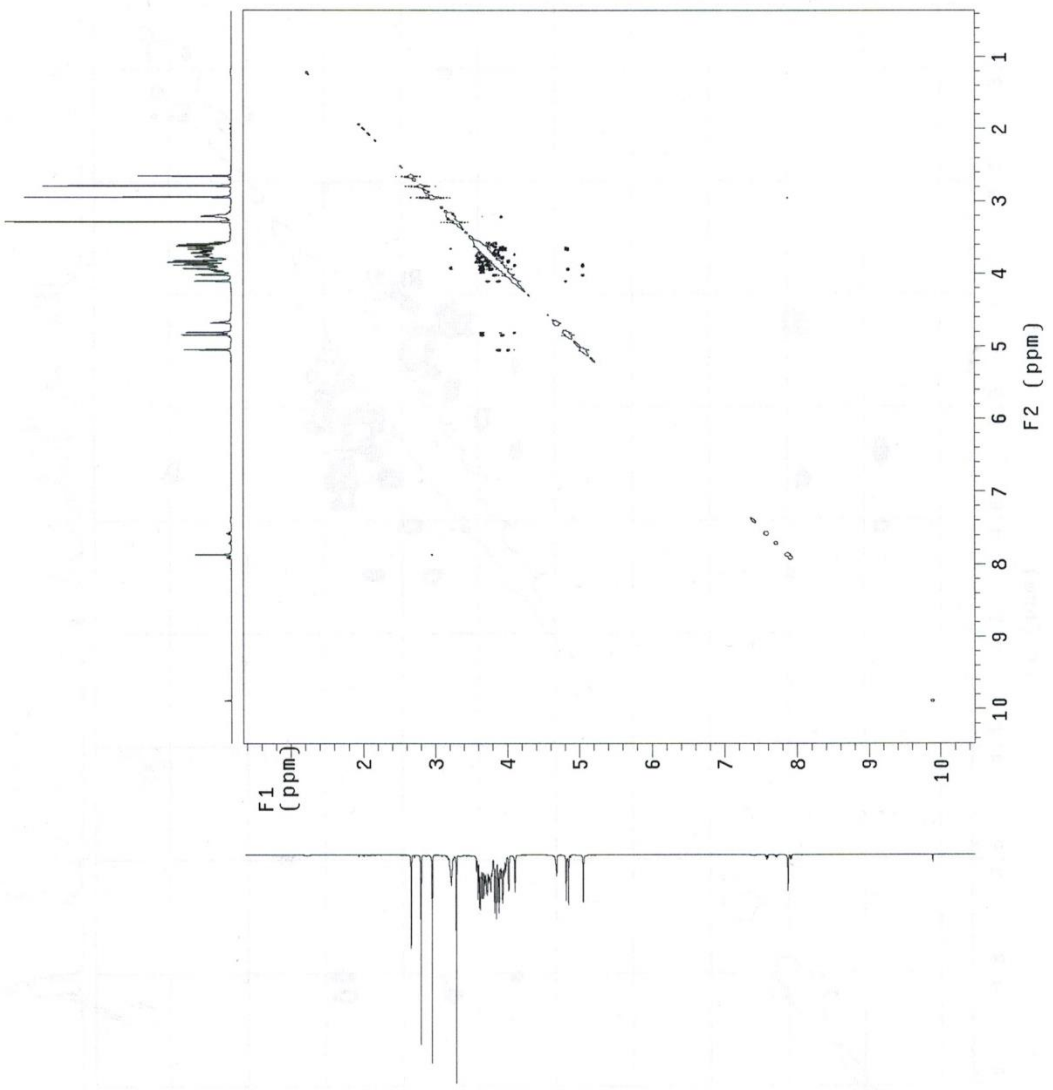

Figure A.3. 500MHz NOESY of amino-α-3,6-mannotriose in D_2O

Appendix B: Raw Data for CTB-GMI Binding Experiment

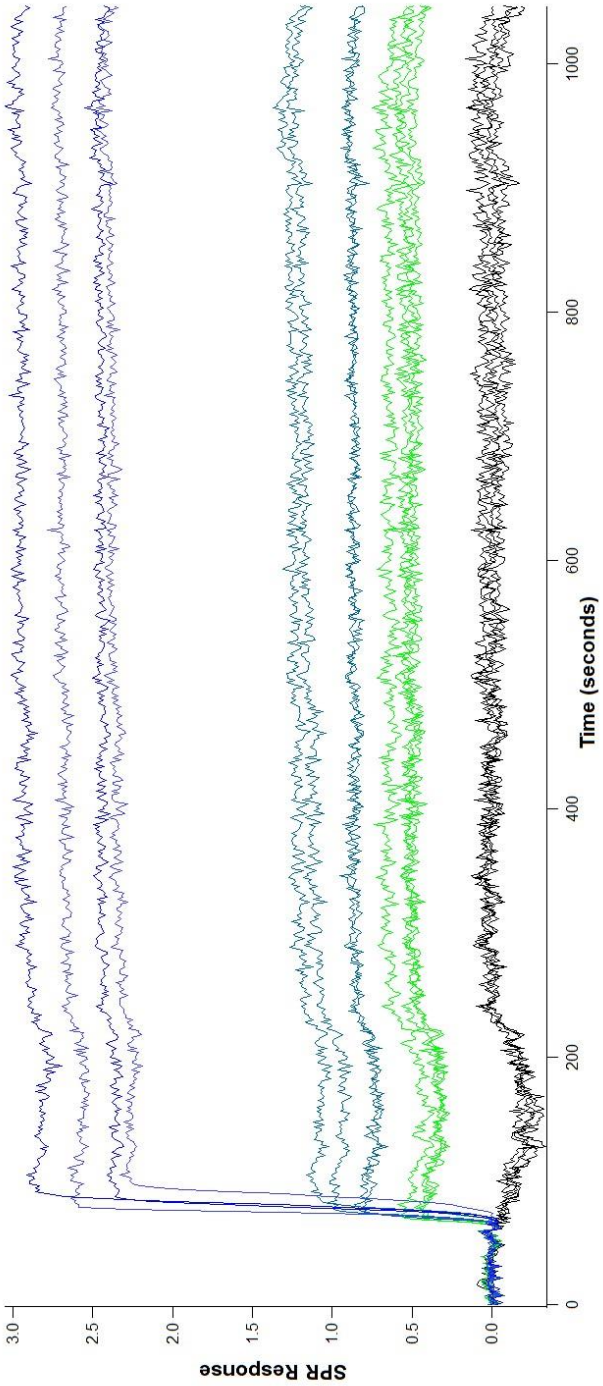

Bibliography

[1] D. G. Castner, B. D. Ratner, Biomedical surface science: foundation to frontiers. *Surf. Sci.* 500 (2002) 28-60.

[2] M. Tirrell, E. Kokkoli, M. Biesalski, The role of surface science in bioengineered materials. *Surf. Sci.* 500 (2002) 61-83.

[3] B. Kasemo, Biological surface science. *Surf. Sci.* 500 (2002) 656-677.

[4] Kisliuk, P., The sticking probabilities of gases chemisorbed on the surfaces of solids. *J. Phys. Chem. Solids* **1957,** *3* (1–2), 95-101.

[5] A. W. Adamson, A. P. Gast. Physical chemistry of surfaces, 6th edition (John-Wiley & Sons, New York, 1997).

[6] M.P. Goertz, J. E. Houston, X.-Y. Zhu, Hydrophilicity and the viscosity of interfacial water. *Langmuir* 23 (2007) 5491-5497.

[7] S. H. Khan, G. Matei, S. Patil, P. M. Hoffmann, Dynamic solidification in nanoconfined water films. *Phys. Rev. Lett.* 105 (2010) 106101.

[8] S. Granick, S. C. Bae, S. Kumar, C. Yu, Confined Liquid Controversies Near Closure? *Physics* 3 (2010) 73.

[9] H. I. Kim, et al. Viscous "Interphase" Water Adjacent to Oligo(ethylene glycol)-terminated monolayers. *Langmuir* 19 (2003) 9271-9275.

[10] L. Shen, Athena Guo, X.-Y. Zhu, Tween surfactants: adsorption, self-organization, and protein resistance. *Surf. Sci.* 605 (2011) 494–499.

[11] Voller, A.; Bartlett, A.; Bidwell, D. E., Enzyme immunoassays with special reference to ELISA techniques. *Journal of Clinical Pathology* **1978,** *31* (6), 507-520.

[12] Wertz, C. F.; Santore, M. M., Fibrinogen Adsorption on Hydrophilic and Hydrophobic Surfaces: Geometrical and Energetic Aspects of Interfacial Relaxations. *Langmuir* **2001,** *18* (3), 706-715.

[13] P.G. de Gennes, Polymer solutions near an interface. Adsorption and depletion layers. *Macromolecules* 14 (1981) 1637-1644.

[14] M. A. C. Stuart, G. J. Fleer, Adsorbed polymer layers in nonequilibrium situations. *Annu. Rev. Mater. Sci.* 26 (1996) 463-500.

[15] Y. Shin, J. E. Roberts, M. M. Santore, Influence of charge density and coverage on bound fraction for a weakly cationic polyelectrolyte adsorbing onto silica. *Macromolecules* 35 (2002) 4090-4095.

[16] A.V. Dobrynin, A. Deshkovsky, M. Rubinstein, Adsorption of polyelectrolytes at an oppositely charged surface. *Macromolecules* 34 (2001) 3421-3436.

[17] M. A. C Stuart, *Polyelectrolytes on solid surfaces* Editions Frontières (1995) pp. 3-12.

[18] M.C.P. van Eijk, M. A. C. Stuart. Polymer adsorption kinetics: effects of supply rate. *Langmuir* 13 (1997) 5447-5450.

[19] D. Hall. Use of optical biosensors for the study of mechanistically concerted surface adsorption processes. *Anal. Biochem.* 288 (2001) 109-125.

[20] C. M. Ruggiero, et al. Protein-surface interactions. *Cell Biochem. Biophys.* 43 (2005) 407-417.

[21] R.A. Latour. Biomaterials: protein–surface ionteractions. *Encyclopedia of Biomaterials and Biomedical Engineering*. G. E. Wnek, G. L. Bowlin, edt. Page 1 – 15 (Informa Healthcare, USA, Inc. New York, 2005).

[22] H.G.W. Lensen, Competitive adsorption of plasma proteins at solid--liquid interfaces. *J. Chromatography B: Biomed. Sci. Appl.* 376 (1986) 191-198.

[23] Cuypers, P. A.; Corsel, J. W.; Janssen, M. P.; Kop, J. M.; Hermens, W. T.; Hemker, H. C., The adsorption of prothrombin to phosphatidylserine multilayers quantitated by ellipsometry. *Journal of Biological Chemistry* **1983,** *258* (4), 2426-31.

[24] Bruckenstein, S.; Shay, M., Experimental aspects of use of the quartz crystal microbalance in solution. *Electrochimica Acta* **1985,** *30* (10), 1295-1300.

[25] M. Andersson, et al. Quartz crystal microbalance-with dissipation monitoring (QCM-D) for real time measurements of blood coagulation density and immune complement activation on artificial surfaces. *Biosensors & Bioelectronics* 21 (2005) 79-86.

[26] G. Steiner. Surface plasmon resonance imaging. *Anal. Bioanal. Chem.* 379 (2004) 328-331.

[27] C. T. Campbell, G. Kim, SPR microscopy and its applications to high-throughput analyses of biomolecular binding events and their kinetics. *Biomaterials* **28**(15) (2007) 2380-2392.

[28] M. A. Brusatori, et al. Protein adsorption kinetics under an applied electric field: an optical waveguide lightmode spectroscopy study. *Langmuir* 19 (2003) 5089-5097.

[29] H. J. Griesser, S.L. McArthur, M.S. Wagner, P. Kingshott, K.M. McLean and D.G. Castner, XPS, ToF-SIMS and MALDI-MS for characterizing adsorbed protein films. *Biopolymers at Interfaces*, 2nd Edition, Ed. M. Malmsten (Marcel Dekker, New York, 2003) page 641-669.

[30] P. Roach, Interpretation of Protein Adsorption: Surface-Induced Conformational Changes. *J. Am. Chem. Soc.* 127 (2005) 8168-8173.

[31] X. Chen, et al. Recognition of Protein Adsorption onto Polymer Surfaces by Scanning Force Microscopy and Probe−Surface Adhesion Measurements with Protein-Coated Probes. *Langmuir* 13 (1997) 4106-4111.

[32] H.J. Butt, B. Cappella, M. Kappl, Force measurements with the atomic force microscope: Technique, interpretation and applications. *Surf. Sci. Rep.* 59 (2005) 1-152.

[33] J. Hemmerlé, Direct observation of the anchoring process during the adsorption of fibrinogen on a solid surface by force-spectroscopy mode atomic force microscopy. *Proc. Nat. Acad. Sci. USA* 96 (1999) 6705-6710.

[34] H. Noh, E. A. Vogler. Volumetric interpretation of protein adsorption: Partition coefficients, interphase volumes, and free energies of adsorption to hydrophobic surfaces. *Biomater.* 27 (2006) 5780-5793.

[35] C. F. Wertz, M. M. Santore. Adsorption and Reorientation Kinetics of Lysozyme on Hydrophobic Surfaces. *Langmuir* 18 (2002) 1190-1199.

[36] G.B., Sigal, et al. Effect of surface wettability on the adsorption of proteins and detergents. *J. Am. Chem. Soc.*120 (1998) 3464-3473.

[37] W. Feng, et al. Adsorption of fibrinogen and lysozyme on silicon grafted with poly(2-methacryloyloxyethyl phosphorylcholine) via surface-initiated atom transfer radical polymerization. *Langmuir* 21 (2005) 5980-5987.

[38] Y. L. Jeyachandran, Quantitative and qualitative evaluation of adsorption/desorption of bovine serum albumin on hydrophilic and hydrophobic surfaces. *Langmuir* 25 (2009) 11614-11620.

[39] S. Herrwerth, et al. Factors that determine the protein resistance of oligoether self-assembled monolayers − internal hydrophilicity, terminal hydrophilicity, and lateral packing density. *J. Am. Chem. Soc.* 125 (2003) 9359-9366.

[40] Harder, P.; Grunze, M.; Dahint, R.; Whitesides, G. M.; Laibinis, P. E., Molecular conformation in oligo(ethylene glycol)-terminated self-assembled monolayers on gold and silver surfaces determines their ability to resist protein adsorption. *J. Phys. Chem. B* **1998,** *102* (2), 426-436.

[41] R. A. Latour, Thermodynamic perspectives on the molecular mechanisms providing protein adsorption resistance that include protein-surface interactions. *J. Biomed. Mater. Res. A* 78A (2006) 843-854.

[42] S. Kalasin, M. M. Santore, Non-specific adhesion on biomaterial surfaces driven by small amounts of protein adsorption. *Colloids and Surfaces B: Biointerfaces* 73 (2009) 229-236.

[43] Gon, S.; Santore, M. M., Single Component and Selective Competitive Protein Adsorption in a Patchy Polymer Brush: Opposition between Steric Repulsions and Electrostatic Attractions†. *Langmuir* **2011,** *27* (4), 1487-1493.

[44] Gon, S.; Bendersky, M.; Ross, J. L.; Santore, M. M., Manipulating Protein Adsorption using a Patchy Protein-Resistant Brush. *Langmuir* **2010,** *26* (14), 12147-12154.

[45] M Morra, C. Cassinelli, Surface field of forces and protein adsorption behavior of

poly(hydroxyethylmethacrylate) films deposited from plasma. *J. Biomed. Mater. Res.* 29 (1995) 39-45.

[46] A.P. Ngankam, et al. Fibronectin Adsorption onto Polyelectrolyte Multilayer Films. *Langmuir* 20 (2004) 3362-3370.

[47] K Nakanishi, et al. On the adsorption of proteins on solid surfaces, a common but very complicated phenomenon. *J. Biosci. Bioengin.* 91 (2001) 233-244.

[48] E. Ostuni, et al. A survey of structure−property relationships of surfaces that resist the adsorption of protein. *Langmuir* 17 (2001) 5605-5620.

[49] S. H. Baxamusa, K. K. Gleason. Random copolymer films with molecular-scale compositional heterogeneities that interfere with protein adsorption. *Adv. Funct. Mater.* 19 (2009) 3489-3496.

[50] D. Hobara, et al. Preferential adsorption of horse heart cytochrome c on nanometer-scale domains of a phase-separated binary self-assembled monolayer of 3-mercaptopropionic acid and 1-hexadecanethiol on Au(111). *Nano Lett.* 2 (2002) 1021-1025.

[51] L. Shen, X. Y. Zhu, Evidence of a mobile precursor state in nonspecific protein adsorption. *Langmuir* 27 (2011) 7059-7064.

[52] P. Roach, et al. Surface tailoring for controlled protein adsorption: effect of topography at the nanometer scale and chemistry. *J. Am. Chem. Soc.* 128 (2006) 3939-3945.

[53] Y. H. Tan, et al. A nanoengineering approach for investigation and regulation of protein immobilization. *ACS Nano* 2 (2008) 2374-2384.

[54] M. Matsusaki, et al. Protein nanoarrays on a highly-oriented lamellar surface. *Chem. Commun.* 46 (2010) 1911-1913.

[55] K. Rechendorff, et al. Enhancement of protein adsorption induced by surface roughness. *Langmuir* 22 (2006) 10885-10888.

[56] P. Billsten, et al. Conformation of human carbonic anhydrase ii variants adsorbed to silica nanoparticles. *Langmuir* 15 (1999) 6395-6399.

[57] M. Karlsson, et al. Adsorption of human carbonic anhydrase ii variants to silica nanoparticles occur stepwise: binding is followed by successive conformational changes to a molten-globule-like state. *Langmuir* 16 (2000) 8470-8479.

[58] T. Arnebrant, et al. Adsorption of [alpha]-lactalbumin and [beta]-lactoglobulin on metal surfaces versus temperature. *J. Colloid. Interface Sci.* 119 (1987) 383-390.

[59] H. Sota, et al. Detection of conformational changes in an immobilized protein using surface plasmon resonance. *Anal. Chem.* 70 (1998) 2019-2024.

[60] J. Buijs, V. Hlady. Adsorption kinetics, conformation, and mobility of the growth hormone and lysozyme on solid surfaces, studied with TIRF. *J. Colloid. Interface Sci.* 190 (1997) 171-181

[61] M. Holmberg, X. Hou, Competitive Protein Adsorption of Albumin and Immunoglobulin G from Human Serum onto Polymer Surfaces. *Langmuir* 26 (2009) 938-942.

[62] S.M. Daly, et al. Coverage-dependent orientation of lysozyme adsorbed on silica. *Langmuir* 19 (2003) 3848-3857.

[63] A. Guo, X.-Y. Zhu, Surface chemistry for protein microarrays. *Int. J. Nanosci.* 6 (2007) 109-116.

[64] E. Pefferkorn, A. Elaissari. Adsorption--desorption processes in charged polymer/colloid systems; structural relaxation of adsorbed macromolecules. *J. Colloid. Interface Sci.* 138 (1990) 187-194.

[65] A. Agnihotri, C. A. Siedlecki, Time-dependent conformational changes in fibrinogen measured by atomic force microscopy. *Langmuir* 20 (2004) 8846-8852.

[66] Tie, Y.; Calonder, C.; Van Tassel, P. R., Protein adsorption: Kinetics and history dependence. *J. Colloid Interface Sci.* **2003,** *268* (1), 1-11.

[67] Calonder, C.; Tie, Y.; Van Tassel, P. R., History dependence of protein adsorption kinetics. *Proceedings of the National Academy of Sciences* **2001,** *98* (19), 10664-10669.

[68] M. M. Santore, C. F. Wertz. Protein spreading kinetics at liquid−solid interfaces via an adsorption probe method. *Langmuir* 21 (2005) 10172-10178.

[69] M. van der Veen, et al. Spreading of proteins and its effect on adsorption and desorption kinetics. *Colloids and Surfaces B: Biointerfaces* 54 (2007) 136-142.

[70] Tilton, R. D.; Robertson, C. R.; Gast, A. P., Lateral diffusion of bovine serum albumin adsorbed at the solid-liquid interface. *J. Colloid Interface Sci.* **1990,** *137* (1), 192-203.

[71] Burghardt, T. P.; Axelrod, D., Total internal reflection/fluorescence photobleaching recovery study of serum albumin adsorption dynamics. *Biophysical journal* **1981,** *33* (3), 455-467.

[72] Vieira, E. P.; Rocha, S.; Pereira, M. C.; Mohwald, H.; Coelho, M. A. N., Adsorption and Diffusion of Plasma Proteins on Hydrophilic and Hydrophobic Surfaces: Effect of Trifluoroethanol on Protein Structure. *Langmuir* **2009,** *25* (17), 9879-9886.

[73] Kastantin, M.; Langdon, B. B.; Chang, E. L.; Schwartz, D. K., Single-Molecule Resolution of Interfacial Fibrinogen Behavior: Effects of Oligomer Populations and Surface Chemistry. *J. Am. Chem. Soc.* **2011,** *133* (13), 4975-4983.

[74] M. J. Saxton, Lateral diffusion in an archipelago - the effect of mobile obstacles. *Biophys. J.* 52 (1987) 989-997.

[75] R.D. Tilton, et al. Surface diffusion of interacting proteins. Effect of concentration on the lateral mobility of adsorbed bovine serum albumin. *Biophys. J.* 58 (1990) 1321-1326.

[76] Zhu, X.; Shen, L., A Mobile Precursor Determines Amyloid-β Peptide Fibril Formation at the Liquid-Solid Interface. *Biophys. J.* **2012,** *102* (3, Supplement 1), 257a.

[77] M. Wahlgren, et al. The adsorption of lysozyme to hydrophilic silicon oxide surfaces: comparison between experimental data and models for adsorption kinetics. *J. Colloid Interface Sci.* 175 (1995) 506-514.

[78] L Vroman, A. L. Adams, Identification of rapid changes at plasma–solid interfaces. *J. Biomed. Mater. Res.* 3 (1969) 43-67.

[79] C. F. Wertz, M. M. Santore, Adsorption and relaxation kinetics of albumin and fibrinogen on hydrophobic surfaces: single-species and competitive behavior. *Langmuir* 15 (1999) 8884-8894.

[80] S.-Y. Jung, et al. The Vroman effect: a molecular level description of fibrinogen displacement. *J. Am. Chem. Soc.* 125 (2003) 12782-12786.

[81] H. Noh, E. A. Vogler. Volumetric interpretation of protein adsorption: competition from mixtures and the Vroman effect. *Biomater.* 28 (2007) 405-422.

[82] E.A. Vogler, C. A. Siedlecki. Contact activation of blood-plasma coagulation. *Biomater.* 30 (2009) 1857-1869.

[83] M. Rabe, et al. Understanding protein adsorption phenomena at solid surfaces. *Adv. Colloid Interf. Sci.* 162 (2011) 87-106.

[84] C.S. Lee, G. Belfort. Changing activity of ribonuclease A during adsorption: a molecular explanation. *Proc. Nat. Acad. Sci. USA* 86 (1989) 8392-8396.

[85] X.-L. Sun, et al. Carbohydrate and protein immobilization onto solid surfaces by sequential diels−alder and azide−alkyne cycloadditions. *Bioconj. Chem.* 17 (2005) 52-57.

[86] T.-W. Cha, A. Guo, X.-Y. Zhu, Enzymatic activity on a chip: the critical role of protein orientation. *Proteomics* 5 (2005) 416-419.

[87] B. Holtz, et al. Denaturing and refolding of protein molecules on surfaces." *Proteomics* 7 (2007) 1771-1774.

[88] J. Masek, et al. Immobilization of histidine-tagged proteins on monodisperse metallochelation liposomes: Preparation and study of their structure. *Anal. Chem.* 408 (2011) 95-104.

[89] Choi, Y. S.; Lee, C.-S., Generation of protein and cell microarrays on functionalized surfaces. *Methods Mol Biol* **2011,** *671*, 207-17.

[90] A. Pulsipher, M. N. Yousaf. A renewable, chemoselective, and quantitative ligand density microarray for the study of biospecific interactions. *Chem. Commun.* 47 (2011) 523-525.

[91] A.M.W. Reed, S. J. Metallo, Oriented protein adsorption to gold nanoparticles through a genetically encodable binding motif. *Langmuir* 26 (2010) (24) 18945-18950.

[92] Vörös, J.; Blättler, T.; Textor, M. Bioactive patterns at the 100 nm scale produced via multifunctional physisorbed adlayers. *MRS Bulletin* **2005**, *30*, 202-206.

[93] Lee, K. B.; Kim, E. Y.; Mirkin, C. A; Wolinsky, S. M. The use of nanoarrays for highly sensitive and selective detection of human immunodeficiency virus type 1 in plasma. *Nano. Lett.* **2004**, *4*, 1869–1872.
[94] Vogel, V.; Sheetz, M. Local force and geometry sensing regulate cell functions. *Nature Rev.Mol. Cell Biol.* **2006**, *7*, 265–275.
[95] Théry, M. Micropatterning as a tool to decipher cell morphogenesis and functions. J. *Cell Sci*. **2010**, *123*, 4201–4213.
[96] Lee, K.-B.; Park, S.-J.; Mirkin, C. A.; Smith, J. C.; Mrksich, M. Protein nanoarrays generated by dip-pen nanolithography. *Science* **2002**, *295*, 1702-1705.
[97] Tan, Y. H.; Liu, M.; Nolting, B.; Go, J.G.; Gervay-Hague, J.; Liu, G.-Y. A nanoengineering approach for investigation and regulation of protein immobilization. *ACS Nano* **2008**, *2*, 2374-2384.
[98] Chai, J.; Wong, L. S.; Giam, L.; Mirkin, C. A. Single-molecule protein arrays enabled by scanning probe block copolymer lithography. *PNAS* **2011**, *108*, 19521–19525.
[99] Bates, F. S.; Fredrickson, G. H. Block co-polymer thermodynamics: theory and experiment. *Annu. Rev. Phys. Chem.* **1990**, *41*, 525.
[100] Wang, J.-Y.; Chen, W.; Russell, T. P. Patterning with block copolymers. Unconventional Nanopatterning Techniques and Applications. Rogers, J. A.; Lee. H. H.; Hoboken, N. J. etd. (John Wiley and Sons, New York, **2009**) page 233-290.
[101] a) Kumar, N.; Hahm, J. Nanoscale protein patterning using self-assembled diblock copolymers. *Langmuir* **2005**, *21*, 6652-6655;
b) Kumar, N.; Parajuli, O.; Dorfman, A.; Kipp, D.; Hahm, J. Activity study of selfassembled proteins on nanoscale diblock copolymer templates. *Langmuir* **2007**, *23*, 7416- 7422;
c) Kumar, N.; Parajuli, O.; Gupta, A.; Hahm, J. Elucidation of protein adsorption behavior on polymeric surfaces: toward high-density, high-payload protein templates. *Langmuir* **2008**, *24*, 2688-2694.
[102] a) Lau, K. H. A.; Bang, J.; Kim, D. H.; Knoll, W. Self-assembly of protein nanoarrays on block copolymer templates. *Adv. Funct. Mater.* **2008**, *18*, 3148-3157; b) Lau, K. H. A.; Bang, J.; Hawker, C. J.; Kim, D. H.; Knoll, W. Modulation of protein−surface interactions on nanopatterned polymer films. *Biomacromolecules* **2009**, *10*, 1061-1066.
[103] Liu, D.; Wang, T.; Keddie, J. L. Protein nanopatterning on self-organized poly(styrene-b-isoprene) thin film templates. *Langmuir* **2009**, *25*, 4526-4534.
[104] Li, L.; Hitchcock, A. P.; Robar, N.; Cornelius, R.; Brash, J. L.; Scholl, A.; Doran, A. X ray microscopy studies of protein adsorption on a phase-segregated polystyrene/polymethyl methacrylate surface. 1. concentration and exposure-time dependence for albumin adsorption. *J. Phys. Chem. B* **2006**, *110*, 16763-16773.
[105] Zemla, J.; Lekka, M.; Raczkowska, J.; Bernasik, A.; Rysz, J.; Budkowski, A. Selective protein adsorption on polymer patterns formed by self-organization and soft lithography. *Biomacromolecules* **2009**, *10*, 2101-2109.

[106] Neto, C. A novel approach to the micropatterning of proteins using dewetting of polymer bilayers. *Phys. Chem. Chem. Phys.* **2007**, *9*, 149-155.
[107] Hucknall, A.; Rangarajan, S.; Chilkoti, A. In pursuit of zero: polymer brushes that resist the adsorption of proteins, advanced materials. *Adv. Mater.* **2009**, *21*, 2441-2446.
[108] Shen, L.; Zhu, X.-Y. Evidence for mobile precursor states in nonspecific protein adsorption. *Langmuir* **2011**, 27, 7059–7064.
[109] Hartl, F. U.; Hayer-Hartl, M., Molecular Chaperones in the Cytosol: from Nascent Chain to Folded Protein. *Science* **2002,** *295* (5561), 1852-1858
[110] Tanzi, R. E.; Bertram, L., Twenty Years of the Alzheimer's Disease Amyloid Hypothesis: A Genetic Perspective. *Cell 120* (4), 545-555
[111] Rambaran, R. N.; Serpell, L. C., Amyloid fibrils: Abnormal protein assembly. *Prion* **2008,** *2* (3), 112-117
[112] Kim, Y. E.; Hipp, M. S.; Bracher, A.; Hayer-Hartl, M.; Ulrich Hartl, F., Molecular Chaperone Functions in Protein Folding and Proteostasis. *Annu. Rev. Biochem* **2013,** *82* (1), 323-355.
[113] Carroll, G. T.; Sojka, M. E.; Lei, X.; Turro, N. J.; Koberstein, J. T., Photoactive Additives for Cross-Linking Polymer Films: Inhibition of Dewetting in Thin Polymer Films. *Langmuir* **2006,** *22* (18), 7748-7754.
[114] Nguyen, D. P.; Lusic, H.; Neumann, H.; Kapadnis, P. B.; Deiters, A.; Chin, J. W., Genetic Encoding and Labeling of Aliphatic Azides and Alkynes in Recombinant Proteins via a Pyrrolysyl-tRNA Synthetase/tRNACUA Pair and Click Chemistry. *J. Am. Chem. Soc.* **2009,** *131* (25), 8720-8721.

[115] Kolb, H. C.; Finn, M. G.; Sharpless, K. B. Click Chemistry: Diverse Chemical Function from a Few Good Reactions. *Angew. Chem. Int. Ed*. **2001**, *40*, 2004–2021.
[116] Porath, J.; Carlsson, J. A. N.; Olsson, I.; Belfrage, G., Metal chelate affinity chromatography, a new approach to protein fractionation. *Nature* **1975,** *258* (5536), 598-599

[117] Deegan, R. D.; Bakajin, O.; Dupont, T. F.; Huber, G.; Nagel, S. R.; Witten, T. A., Capillary flow as the cause of ring stains from dried liquid drops. *Nature* **1997,** *389* (6653), 827-829.
[118] Hoffman, W. L.; Jump, A. A., Tween 20 removes antibodies and other proteins from nitrocellulose. *Journal of Immunological Methods* **1986,** *94* (1–2), 191-196.

[119] Goddard-Borger, E. D.; Stick, R. V. An efficient, inexpensive, and shelf-stable diazotransfer reagent: imidazole-1-sulfonyl azide hydrochloride. *Org. Lett.* **2007**, *9*, 3797-3800.
[120] van Dongen, S. F. M.; Teeuwen, R. L. M.; Nallani, M.; van Berkel, S. S.; Cornelissen, J. J. L. M.; Nolte, R. J. M.; van Hest, J. C. M. Single step azide introduction in protein via an aqueous diazo transfer. *Bioconjug. Chem*. **2009**, *20*, 20-23.

[121] Hart, G. W., Thematic Minireview Series on Glycobiology and Extracellular Matrices: Glycan Functions Pervade Biology at All Levels. *J. Biol. Chem.* **2013,** *288* (10), 6903.

[122] Feinberg, H.; Castelli, R.; Drickamer, K.; Seeberger, P. H.; Weis, W. I., *J. Biol. Chem.* **2007,** *282* (null), 4202.

[123] van Liempt, E.; Bank, C. M. C.; Mehta, P.; Garcı´a-Vallejo, J. J.; Kawar, Z. S.; Geyer, R.; Alvarez, R. A.; Cummings, R. D.; Kooyk, Y. v.; van Die, I., Specificity of DC-SIGN for mannose- and fucose-containing glycans. *FEBS Letters* **2006,** *580* (26), 6123-6131

[124] Hijazi, K.; Wang, Y.; Scala, C.; Jeffs, S.; Longstaff, C.; Stieh, D.; Haggarty, B.; Vanham, G.; Schols, D.; Balzarini, J.; Jones, I. M.; Hoxie, J.; Shattock, R.; Kelly, C. G., DC-SIGN Increases the Affinity of HIV-1 Envelope Glycoprotein Interaction with CD4. *PLoS ONE* **2011,** *6* (12), e28307.

[125] Godula, K.; Bertozzi, C. R., Density Variant Glycan Microarray for Evaluating Cross-Linking of Mucin-like Glycoconjugates by Lectins. *J. Am. Chem. Soc.* **2012,** *134* (38), 15732-15742.

[126] Borrok, M. J.; Kiessling, L. L., Non-carbohydrate Inhibitors of the Lectin DC-SIGN. *J. Am. Chem. Soc.* **2007,** *129* (42), 12780-12785.

[127] Han, X.; Critchley, K.; Zhang, L.; Pradeep, S. N. D.; Bushby, R. J.; Evans, S. D., A Novel Method To Fabricate Patterned Bilayer Lipid Membranes. *Langmuir* **2006,** *23* (3), 1354-1358.

[128] Kienle, S.; Lingler, S.; Kraas, W.; Offenhausser, A.; Knoll, W.; Jung, G., *Biosens. Bioelectron.* **1997,** *12*, 779.

[129] Mani, G.; Johnson, D. M.; Marton, D.; Dougherty, V. L.; Feldman, M. D.; Patel, D.; Ayon, A. A.; Agrawal, C. M., Stability of Self-Assembled Monolayers on Titanium and Gold. *Langmuir* **2008,** *24* (13), 6774-6784.

[130] Phillips, K. S.; Han, J.-H.; Martinez, M.; Wang, Z.; Carter, D.; Cheng, Q., Nanoscale Glassification of Gold Substrates for Surface Plasmon Resonance Analysis of Protein Toxins with Supported Lipid Membranes. *Anal. Chem.* **2005,** *78* (2), 596-603.

[131] Chen, T.; Ishihara, R.; Beenakker, K., High Quality SiO2 Deposited at 80 ° C by Inductively Coupled Plasma Enhanced CVD for Flexible Display Application. *Electrochem. Solid-State Lett.* **2010,** *13* (8), J89-J91.

[132] Tsai, S. Y.; Lu, Y. M.; Hon, M. H., Study on the low leakage current of an MIS structure fabricated by ICP-CVD. *Journal of Physics: Conference Series* **2008,** *100* (4), 042030.

[133] Miller, L. W., *Probes and Tags to Study Biomolecular Function: For Proteins, RNA, and Membranes*. Wiley: 2008

[134] Mitchell, D. A.; Fadden, A. J.; Drickamer, K., A novel mechanism of carbohydrate recognition by the C-type lectins DC-SIGN and DC-SIGNR: Subunit organisation and binding to multivalent ligands. *J. Biol. Chem.* **2001**.

[135] Appelmelk, B. J.; van Die, I.; van Vliet, S. J.; Vandenbroucke-Grauls, C. M. J. E.; Geijtenbeek, T. B. H.; van Kooyk, Y., Cutting Edge: Carbohydrate Profiling Identifies New Pathogens That Interact with Dendritic Cell-Specific ICAM-3-Grabbing Nonintegrin on Dendritic Cells. *The Journal of Immunology* **2003,** *170* (4), 1635-1639

[136] del Barrio, J.; Oriol, L.; Alcalá, R.; Sánchez, C., Azobenzene-Containing Linear−Dendritic Diblock Copolymers by Click Chemistry: Synthesis, Characterization, Morphological Study, and Photoinduction of Optical Anisotropy. *Macromolecules* **2009,** *42* (15), 5752-5760

[137] Patel, M. K.; Vijayakrishnan, B.; Koeppe, J. R.; Chalker, J. M.; Doores, K. J.; Davis, B. G., Analysis of the dispersity in carbohydrate loading of synthetic glycoproteins using MALDI-TOF mass spectrometry. *Chem. Commun.* **2010,** *46* (48), 9119-9121

[138] Kaya, E.; Gutsmiedl, K.; Vrabel, M.; Müller, M.; Thumbs, P.; Carell, T., Synthesis of Threefold Glycosylated Proteins using Click Chemistry and Genetically Encoded Unnatural Amino Acids. *ChemBioChem* **2009,** *10* (18), 2858-2861

[139] Beignet, J.; Tiernan, J.; Woo, C. H.; Kariuki, B. M.; Cox, L. R., Stereoselective Synthesis of Allyl-C-mannosyl Compounds: Use of a Temporary Silicon Connection in Intramolecular Allylation Strategies with Allylsilanes. *The Journal of Organic Chemistry* **2004,** *69* (19), 6341-6356.

[140] Tanaka, N.; Ogawa, I.; Yoshigase, S.; Nokami, J., Regioselective ring opening of benzylidene acetal protecting group(s) of hexopyranoside derivatives by DIBAL-H. *Carbohydr. Res.* **2008,** *343* (15), 2675-2679

[141] Szurmai, Z.; Balatoni, L.; Lipták, A., Synthesis of some partially substituted methyl α-d- and phenyl 1-thio-α-d-mannopyranosides for the preparation of manno-oligosaccharides. *Carbohydr. Res.* **1994,** *254* (0), 301-309

[142] Reina, J. J.; Diaz, I.; Nieto, P. M.; Campillo, N. E.; Paez, J. A.; Tabarani, G.; Fieschi, F.; Rojo, J., Docking, synthesis, and NMR studies of mannosyl trisaccharide ligands for DC-SIGN lectin. *Organic & Biomolecular Chemistry* **2008,** *6* (15), 2743-2754